AUGUST 2023

Ph.D. in Mechanical Engineering

MAHMUT TANDOĞAN

REPUBLIC OF TÜRKİYE

GAZİANTEP UNIVERSITY

GRADUATE SCHOOL OF NATURAL & APPLIED SCIENCES

EVALUATION OF PROCESS PARAMETERS OF MULTIPOINT SHEET METAL FORMING

Ph.D. THESIS

IN

MECHANICAL ENGINEERING

BY

MAHMUT TANDOĞAN

AUGUST 2023

EVALUATION OF PROCESS PARAMETERS OF MULTIPOINT SHEET METAL FORMING

Ph.D. Thesis

in

Mechanical Engineering

Gaziantep University

Supervisor

Prof. Dr. Ömer EYERCİOĞLU

Co-Supervisor

Asst. Prof. Dr. Mustafa DÜLGER

by

Mahmut TANDOĞAN

August 2023

EVALUATION OF PROCESS PARAMETERS OF MULTIPOINT SHEET METAL FORMING

submitted by **Mahmut TANDOĞAN** in partial fulfillment of the requirements for the degree of Doctor of Philosophy in **Mechanical Engineering, Gaziantep University** is approved by,

Prof. Dr. Mehmet İshak YÜCE
Director of the Graduate School of Natural and Applied Sciences ………..............

Prof. Dr. M. Sait SÖYLEMEZ
Head of the Department of Mechanical Engineering ………..............

Prof. Dr. Ömer EYERCİOĞLU
Supervisor ………..............

Asst. Prof. Dr. Mustafa DÜLGER
Co-Supervisor, Mechanical Engineering
İstanbul University-Cerrahpaşa ………..............

Exam Date: 23.08.2023

Examining Committee Members:

Prof. Dr. Abdul Kadir EKŞİ
Çukurova University ………..............

Prof. Dr. Necip Fazıl YILMAZ
Gaziantep University ………..............

Prof. Dr. Ömer EYERCİOĞLU
Gaziantep University ………..............

Prof. Dr. Metin KÖK
Kahramanmaras Sütçü İmam University ………..............

Prof. Dr. A. Tolga BOZDANA
Gaziantep University ………..............

I hereby declare that all information in this document has been obtained and presented in accordance with academic rules and ethical conduct. I also declare that, as required by these rules and conduct, I have fully cited and referenced all material and results that are not original to this work.

Mahmut TANDOĞAN

ABSTRACT

EVALUATION OF PROCESS PARAMETERS OF MULTIPOINT SHEET METAL FORMING

TANDOĞAN, Mahmut
Ph.D. in Mechanical Engineering
Supervisor: Prof. Dr. Ömer EYERCİOĞLU
Co-Supervisor: Asst. Prof. Mustafa DÜLGER
August 2023
83 pages

Sheet metal forming is a method that is frequently used to produce 3D parts in several industries, such as automotive and aviation. One of the most popular sheet metal forming techniques is stamping. However, traditional forming methods created for mass production are inflexible and expensive. For this reason, it makes them economically unsuitable for small-batch and prototype production. Flexible forming techniques, such as multi-point forming (MPF), which have recently been developed, are more suitable for small-batch and prototype manufacturing. Traditional solid stamping equipment could be replaced by a set of discrete dies containing pin boxes.

The damage factor, effective stress distribution, and required forming loads of aluminium 1100 parts with a thickness of 0.5 mm were examined in this study using relative fixation and active punch adjustment methods. Finite element simulations were carried out using 10 mm, 12 mm, and 14 mm diameter pins for V-shaped (F1), wavy-shaped (F2), and 3D free-form surface (F3) components. Furthermore, experiments of relative fixation for the 12 mm diameter pin were performed, and the simulations were compared with the forming loads and the thinning contact points of the pin and formed sheet metal sections. In conclusion, it was discovered that the MPF process is significantly affected by pin diameter. Higher stresses and sheet metal tearing were caused by larger diameter pins. Also, it was seen that the active punch adjustment method is better than the relative fixation method for all shapes.

Key Words: Multi-point forming, Sheet metal, Simulation

ÖZET

ÇOK NOKTALI SAC METAL ŞEKİLLENDİRMEDE PROSES PARAMETRELERİNİN İNCELENMESİ

TANDOĞAN, Mahmut
Doktora Tezi, Makine Mühendisliği
Danışman: Prof. Dr. Ömer EYERCİOĞLU
İkinci Danışman: Dr. Öğr. Üyesi Mustafa DÜLGER
Ağustos 2023
83 sayfa

Sac metal şekillendirme, otomotiv ve havacılık gibi birçok endüstride 3 boyutlu parçalar üretmek için sıklıkla kullanılan bir yöntemdir. En popüler sac şekillendirme tekniklerinden biri sabit kalıplı şekillendirmedir. Ancak seri üretim için oluşturulan geleneksel şekillendirme teknikleri esnek olmamakla birlikte pahalıdır. Bu durum onları küçük ölçekli ve prototip üretimi için ekonomik olarak uygunsuz hale getirir. Son zamanlarda geliştirilen çok noktalı şekillendirme (ÇNŞ) gibi esnek şekillendirme teknikleri, küçük parti ve prototip üretimi için daha uygundur. Geleneksel katı damgalama ekipmanı, pim kutuları içeren bir dizi ayrı kalıpla değiştirilmiştir.

Bu çalışmada, 0,5 mm kalınlığındaki alüminyum 1100 parçalarının hasar faktörü, etkin gerilme dağılımı ve gerekli şekillendirme yükleri, göreli sabitleme ve aktif zımba ayarlama yöntemleri kullanılarak incelenmiştir. V-biçimli (F1), dalgalı-biçimli (F2) ve 3B serbest biçimli yüzey (F3) bileşenler için 10 mm, 12 mm ve 14 mm çapında pimler kullanılarak sonlu eleman simülasyonları gerçekleştirilmiştir. Ayrıca, 12 mm çapındaki pim için bağıl sabitleme deneyleri gerçekleştirilmiş ve simülasyonlar, pimin ve şekillendirilmiş sac levha bölümlerinin şekillendirme yükleri ve inceltme temas noktaları ile karşılaştırılmıştır. Sonuç olarak, ÇNŞ işleminin pim çapından önemli ölçüde etkilendiği keşfedildi. Daha büyük çaplı pimler daha yüksek gerilimlere ve sac metal yırtılmasına neden oldu. Ayrıca aktif zımba ayarlama yönteminin tüm şekiller için göreli tespit yöntemine göre daha iyi olduğu görülmüştür.

Anahtar Kelimeler: Çok noktalı şekillendirme, Sac metal, Simülasyon

"Dedicated to my family"

ACKNOWLEDGEMENTS

I would like to thank my supervisor, Prof. Dr. Ömer EYERCİOĞLU and co-supervisor, Asst. Prof. Dr. Mustafa DÜLGER for their guidance and supports throughout the study. I am thankful for their encouragements and motivations.

Deep appreciation and thanks are due to Prof. Dr. Abdul Kadir EKŞİ, Prof. Dr. Necip Fazıl YILMAZ, Prof. Dr. Ömer EYERCİOĞLU, Prof. Dr. Metin KÖK and Prof. Dr. A. Tolga BOZDANA for serving on the committee and their valuable suggestions.

I would like to thank colleagues and friends Asst. Prof. Dr. Hakan ÇANDAR, Asst. Prof. Dr. Kaan Emre ENGİN and Mechanical Engineer, MSc, Abdullah Gazi FIRAT for continuous helps.

My endless love and loyalty to my family (My wife, Özlem and daughter Zeynep Ece), whom I will forever be indebted to for their ever-extending love, support trust, and willingness to endure with me the challenges of my endeavours.

TABLE OF CONTENTS

LIST OF TABLES

Page

LIST OF FIGURES

Page

LIST OF SYMBOLS

C	Critical Value of Damage Factor
$\boldsymbol{\varepsilon^{-f}}$	Fracture Strain
$\boldsymbol{\sigma^{*}}$	Maximum Principal Tensile Stress
$\boldsymbol{\bar{\sigma}}$	Effective Stress
$\boldsymbol{\bar{\varepsilon}}$	Effective Strain

LIST OFABBREVIATIONS

MPF	Multi-Point Forming
RF	Relative Fixation Forming
AP	Active Punch Adjustment Forming
F1	V-Shaped Part
F2	Wavy-Shaped Part
F3	3D Free-Form Surface Part
FEM	Finite Element Method
FEA	Finite Element Analysis
Dof	Degree of Freedom
CCS	Computer Control Subsystem
CAD	Computer Aided Drawing
CADS	Computer Aided Drawing Subsystem
CMM	Coordinate Measuring Machine
MPDF	Multi-Point Die Forming
MPSD	Multi-Point Stretch Die
MPSF	Multi-Point Stretch Forming
FBH	Flexible Blank Holder
NBH	No Blank Holder
EBL	Egg-Box-Like
MSPF	Multi-Square Punch Forming
SMPF	Sparse Multi-Point Flexible
CAF	Creep Age Forming
BAHPs	Brazed Aluminium Honeycomb Panels
MPF-ICFD	Multipoint Forming, Individually Controlled Force-Displacement
MPhD	Multipoint Half-Die
ASTM	American Society for Testing and Materials

CHAPTER 1
INTRODUCTION

One of the primary production methods is metal forming. The shape of metal workpieces is altered through plastic deformation. Utilizing a tool, generally referred to as a die in metal forming, allows for the desired deformation. Die-applied stresses are passed across the metal workpiece's yield strength. Metal therefore takes form to adopt the shape established by the die's geometry. Bulk deformation and sheet metal forming methods are the two basic categories into which metal forming may be separated [1].

The significant quantity of plastic deformation is caused by bulk deformation mechanisms. The cross-section area to volume ratio is rather tiny. Bulk refers to workpieces with a low area to volume ratio. These procedures improve the initial geometry's mechanical qualities and offer economic value while also improving the geometry's beginning geometry [1].

Metal sheets, strips, and coils are used in the process known as sheet metal forming, sometimes known as sheet metal working. The cross-section area to volume ratio of the initial sheet metal is high. Since this is the primary distinction, it makes sense to distinguish between sheet metal working and bulk deformation techniques [1]. The two primary types of sheet metal forming methods are conventional and unconventional. The type of dies used in the operation makes the difference between an unconventional forming technique and conventional forming [1].

The production process and industrial level have improved with the advancement of science and technology. Since the beginning, when sheet metal components were shaped with hand tools, through the industrial revolution, and into the era of mass manufacturing employing presses and metal dies. With the least amount of material, sheet metal pieces may be produced in complicated three-dimensional forms using sheet metal forming. The conventional forming uses a set of matching solid dies to create a cavity into which the sheet is inserted.

Different shaped pieces in this procedure will call for various dies. Sometimes many sets of dies are required to manufacture a complex sheet metal item. Die design and production are expensive processes that rely on employees' and designers' prior experience. Furthermore, traditional sheet forming die tools need a lot of manufacturing time and space for storage when not in use during production.

In unconventional forming includes the flexible forming methods. Flexible forming techniques, such the one called multi-point forming (MPF), have recently been developed and are more suitable for small-batch and prototype manufacturing. To replace conventional solid forming tools, a pair of opposing reconfigurable tools with pin matrices may be used. With this method, sheet metal forming tools may be manufactured quickly and with greater flexibility.

The automobile and aviation sectors are the principal users of sheet metal components with 3D forms. The sheet metal forming method is used to create this kind of sheet metal. However, these industries need the development of several die sets for sheet metal parts throughout the design process. The price of manufacture per part goes up as a result. Multi-point forming (MPF) reduces the cost of component design and prototyping because it allows the die's shape to be changed by using adjustable pins.

The study of the multi-point forming process is the subject of this thesis. This study's primary objective is to investigate the effects of forming pin diameter, relative fixation adjustment forming (RF), and active pin adjustment forming (AP) on multi-point forming. Experimental investigations which based of relative fixation were carried out to validate the numerical analysis after a numerical model of the multi-point forming process was developed. On a multi-point sheet metal forming, the pin's diameter is the primary focused parameter. For V-shaped (F1), wavy-shaped (F2), and 3D free-form surface (F3) components in finite element simulations for all forming arrangements, 10 mm, 12 mm, and 14 mm pins were used. For the purposes of the investigation, 12 mm was employed to collect experimental data for all forms in their relative fixation arrangement. Using the finite element approach, examinations into fractures, stress distribution, and thinning distribution were conducted. In order to compare the experimentally obtained load-stroke curves to the load-stroke curves from the finite element analysis, experimental study was conducted.

This thesis addresses the following topics: introduction, literature review, overview of multi-point forming, modelling with finite elements and experimental study, results and discussion, and conclusion. The scope and purpose of the research are outlined in Chapter 1 along with a brief description of the research field. The literature and prior research on some parameters that affected multi-point forming, as well as experimental and numerical investigations, were each provided in depth in Chapter 2. A brief explanation of multi-point forming, and its potential applications is provided in Chapter 3. In chapter 4, the steps of finite element modelling with Deform 3D were presented together with the experimental setup and workpiece. Results obtained finite element analysis and experimental studies are compared and discussed in chapter 5. The study's results and recommendations for more research were presented in chapter 6.

CHAPTER 2
LITERATURE REVIEW

2.1 Introduction

The literature review is important to understand the situation in the world of the subject to be studied. Understanding what has been done and what can be done in the study to be done both guides researchers and saves time. In this section, studies related to multi-point forming are given below.

2.2 Studies on Multi-Point Forming

For the purpose of forming sheet metal, Walczyk et al. [2] (1998) studied the creation and evaluation of variable separate die forming. In this study, discrete die designing ideas were developed and put into practice. Both tightly packed pins and an arrangement of separated pins are examples of reconfigurable die design. In discrete die forming, tightly packed pin designs were employed to support the heavy forming loads. Locking of edge, locking of single pushing wall, wall of pin-clamping and friction of pins, as well as other mechanisms, were all studied in order to create the tightly packed pins formation. It was claimed that increasing the forming load capacity of discrete dies involved using backing pressure supplied by an array row divider and a fluid-filled bladder that was permanently mounted to the die frame. In this article, a few cases were also looked at. The conclusion included a summary of general designing guidelines for discrete die.

Li et al. [3] (1999) investigated the three-dimensional sheet metal multi-point forming process. This technique was given in its simplest form. Deformation properties and forming principles were explored in relation to punch shape. Another study looked at the developing faults of pin buckling and dimple creation. There are four primary varieties of multi-point forming: multipoint die, multipoint half die, multipoint press, and multipoint press with half a die. By using multi-point press forming and repeated forming techniques, springback condition was decreased. By matching the pin and contact sites between sheet metal and pins, dimple development and buckling on pins were minimized.

Cai et al. [4] (2002) examined three primary issues connected with practical finite element modelling methodologies and regulation of multi-point forming processes. These issues were identified as being the determination of the multi-point die's three-dimensional surface, the prediction of the starting sheet blank, and the design of the best forming route from the initial blank to the desired shape. Using an 18-dof high precision triangular numerical modelling approach, the three-dimensional surface of a multi-point die was determined for the surface of the final form. A positive, defined functional design for the blank is suggested since volume is constant during the shaping process. By using an iterative FEM strategy to solve the changing problem, the first sheet blank design for the required objective form was established. To get optimum forming outcomes that can reach the finished form without forming faults, an optimal forming path is also required. Due to the flexible nature of multi-point shaping, any shape may be formed. Membrane finite elements were used to design an ideal path for formation, and the issue was resolved. Finite element examples show how simple and quick to utilize the approach is.

Li et al. [5] (2002) focused on identifying and reducing forming imperfections, varying the deformation path, and sectional forming in multi-point. The primary faults of the MPF method were acquired as dimples or wrinkles. The uniqueness of MPF is its dimples. On sheet metal, this flaw was caused by a localized load. The elimination of the dimple problem was attributed to elastic pads. Another MPF issue was wrinkles. Flexible blank holders might be helpful in removing this issue. This application distorted the sheet while actively controlling the punches during multi-point shaping. Multi-point forming with changing deformation route was the name given to this procedure. Through the use of this sort of multi-point forming, wrinkles were also removed. In MPF, sheet metal pieces were also produced section by section. The production of large sheet products is possible with a small MPF press. As a result, sectional forming of MPF allows for the creation of large components. Flexible blank holders were used to shape sheet metal while achieving high levels of accuracy and quality and applying various deformation paths helped to eliminate faults.

Cai et al [6] 2005 examined the material theory of elastic-plastic for the updated Lagrangian formulation-based progressive relocation approach and finite element modelling of the multi-point sheet manufacturing process. For the combination of stresses, a successful method was described. By using the penalty approach and the Coulomb nonclassical friction law of elastic-plastic formalism, discontinuous contact between the punch and the sheet was modelled. The results showed a good degree of general agreement with the findings of the experiments and explicit/elastoplastic analyses described in the literature. Two illustrative instances of the algorithm's use in MPF are used to introduce its applicability.

Liu et al. [7] (2006) conducted research on the methods and ideas of sheet metal's MPF. MPF was described as two primary groups in multi-point forming principles: multi-point die forming and multi-point press forming. The forming capabilities of MPF was then examined. Process components and operating principles are described in the apparatus section. The components of multi-point die forming include the upper and lower element groups, the hydraulic press, the computer control subsystem (CCS), the CAD integrated software subsystem (CADS), and CMM. In the conclusion, adjustment modes and design concepts were listed. To produce the necessary part, a rapid forming procedure was carried out in accordance with CAD data that showed how quickly the shape of the die changes. In addition, by using unique MPDF techniques, such as the flexible blank holder technique for thin sheet metal forming, sectional MPDF for large-size sheet forming, and closed loop MPDF for high precision forming, components of unique shapes that are hard to form using traditional methods have been produced.

The effects of two different methods of MPF, MSF, and SF, on the formation of the dish head, were examined by Qian et al. [8] (2007). On the stress distribution and strain, the forming concepts and features of various approaches were compared. Experimental research and numerical simulations were conducted. The dramatic shape shift between the formed area and the unformed region was therefore removed in sectional multi point formation. In the transition zone, a decent forming region was also attained. As a consequence, multi-step forming was able to improve forming quality, eliminate wrinkling and dimples, and optimize the deformation route. Numerical simulation results also lined up with experimental findings.

Karayel et al. [9] (2008) have investigated on the finite element simulation of multi-point formation made use of ABAQUS finite element software. They have digital control and die systems as part of their multi-point forming process. The die, which is made up of two punch matrices, was created for the rail bus's front panel. The multi-point forming control system and orientation controlling system models were applied using MatLab. As a consequence, finite element analysis demonstrates that this technology is suitable for sheet metal pieces with 3D shapes.

Zhang et al. [10] (2008) have provided the findings of a study into the impact of workpiece and tool component dimensions and workpiece qualities on the features of the generated part shapes. Plane strain deformation is employed, and the bottom die surface was selected to have a cylindrical shape in order to make it easier to show the impact of tool and process parameters. The studies employed two different types of rubber and three different types of metal sheet. According to experimental findings, the thickness of the sheet has an impact on the forming force and dimple size for the die sheet. Dimples form on the surface of workpieces made of 1 mm thick LF21 aluminium sheet, however they don't form on workpieces made of 2 mm thick Q235B and ST12 steel sheet. The precision of the final form depends on how stiff the interpolator is. Additionally, when lubrication is utilized on a workpiece's surfaces, the forming force of the piece is reduced, and shape accuracy is increased.

By using dynamic explicit finite element analysis, Cai et al. [11] (2009) performed comprehensive finite element simulations of the processes for stretching parabolic cylinder, toroidal saddle, and spherical portions. Comparing multi-point die forming outcomes to conventional die forming results was done. The employing of an elastic pad to prevent part dimpling brought on by discrete punch components was examined, and its impact on part form correctness was discussed. Analysis was done on how the shape of the MPSD and the size of the punch element affected the precision of the manufactured components' shapes. The findings might be helpful in deciding on MPSF specifications and simplifying MPSF manufacturing procedures.

Utilizing an initial blank with dimensions of 800 mm in length, 600 mm in width, and 2 mm in thickness, Quan et al. [12] (2011) carried out finite element model of the bending process with multi-point in the case of various elastic cushion geometry to produce the desired final form as a cylindrical surface with curvature radius and centre angle. Four evaluation indicators—components of stress, energy of plastic dissipation, error form, and ductile damage with maximum—are presented and examined in order to determine the ideal thickness of the elastic cushion. As a consequence, the four assessing indicators' individual values is lowered, and by using the elastic cushion, their distributions on the distorted blank become more uniform. As a result, it can be concluded that the elastic pad using can increase the formability of the magnesium alloy AZ31B, and that a 4 mm-thick elastic pad is ideal for multi-point bending of 2 mm thick AZ31B sheets.

In Liu et al. [13] (2016) work, flexible blank holder (FBH) and no blank holder (NBH) numerical analysis models were constructed. Spherical shaped surface portions with various FBH were simulated with finite element software, and the best FBH was subsequently acquired. According to the findings, the sheet metal movement is more homogeneous, the strain and stress are reduced and spread more evenly, the distribution of thickness is more tolerable, and wrinkling flaws can be successfully avoided by FBH forming technology. Finally, to confirm the feasibility and adaptability of the FBH device, a series of 1060 and 08Al tests with varied thicknesses was completed in MPF dies.

Abebe et al. [14] (2016), through multi-objective optimization, seek to reduce both dimpling and wrinkling by modifying variables including punch speed, punch pressure, and elastic pad thickness. The computational efficiency of conventional Kriging is advantageous for the evaluation of dimpling and wrinkles under modification in these three MPF parameters. The dimpling and wrinkling measures' Pareto fronts are calculated using a genetic algorithm for multi-objective optimization, and the best option among the Pareto optima is found using the TOPSIS approach for ordering desires by proximity to ideal solution. The TOPSIS solution is then numerically checked against the outcomes of a full model simulation and experimentally confirmed by its application to a produced product. This results in a dimpling and wrinkle-free TOPSIS solution.

Abosaf et al. [15] (2017) examined the effects of variables on the caliber of components produced by a flexible multi-point stamping die, including thickness of elastic pad, friction coefficient, size of pin, and curvature radius. The best values for those parameters had to be ascertained. The multi-point formation of hemispherical sections was simulated using numerical modelling. The response surface approach was used to examine how process factors affected wrinkling, departure from the desired form, and variation of thickness. The process parameters that produced the highest product quality features were then identified. According to the findings, size of pin and curvature radius have a considerable impact on thickness variation whereas friction coefficient, size of pin, and curvature radius have a significant impact on wrinkling and divergence between produced and target forms.

The effectiveness of a multi-point die with pins in a square matrix and an appropriate blank holder has been studied by Abaas et al. [16] (2018). With respect to the spring stiffness and the height of the die, each pin in the punch holder may be significantly changed. The results demonstrate a reduction in setting time of (90%) compared to the conventional single point incremental forming process, as well as how the interpolator's distortion throughout the forming procedure can cause a shape error in the formed workpiece and how the blank holder can minimize or dimples elimination that can occasionally appear in the workpiece. The load generated by the multi-point die when the forming process is complete is 30.8 kN, which caused the die to move 32.8 mm at the minimum applied force of 28.556 kN.

Liang et al. [17] (2018) have investigated the multi-point cylindrical bend-forming process of the bi-directional trapezoidal sandwich panel using finite element modelling, analytical technique, and forming tests. Early on, analysis was done on the sandwich panel's forming flaws, regularity, and deformation properties. Then, using a semi-analytical technique in conjunction with the finite element method (FEM), the core layer's comparable elastic constants were identified. Based on this knowledge, a mathematical model was created to calculate bending moments and predict springback throughout the shaped range. According to the outcomes, there was a clear difference in the face sheet stress in the welded and suspended areas. The main distortion of the core cell was caused by changing the relationship among the inclined surface and the platform, the core cell was mostly distorted, and the cell layer was primarily deformed at the transition surface region. The most frequent forming flaws that occur during the bending process are the dimple and straight plane effects. Face sheet thickness and bending radius are the major variables that influence the forming problems.

Cai et al. [18] (2018) have looked at the mechanical viability of converting a sandwich plate that was initially flat into a double curved panel. According to experimental data from (MPF) and finite element calculations, the formability of egg-box-like (EBL) sandwich panels cores is predominantly influenced by the failure types of plastic wrinkling and plastic dimpling of face sheet, and core cell fracture. The essential stress for dimpling and the limit bending radius for wrinkles were established as factors of the geometric dimensions and material characteristics of sandwich plates, and analytical models for forecasting face sheet buckling were created. For the purpose of predicting core cell fracture, we put forth the stress-based fracture boundary graph and associated theoretical formulations. Experimental testing and finite element simulations have been used to validate the analytical models that have been constructed. Finally, multi-point forming tests were conducted to show that it is possible to build sandwich panels with EBL cores utilizing plastic forming techniques.

Shen et al. [19] (2018) have studied the hull structures and offshore structures forming process. Such curved plates have traditionally been manufactured via flame bending. However, because of the uncontrollable process and residual distortion, it is challenging to precisely attain the appropriate shape. A new way of creating 3D ship hull plates is the multi-point forming mechanism with square press heads. However, the main issues with the cold-forming process are spring-back and residual stress. The current research ignores the impact of residual stress on cold forming in favour of focusing on springback. The residual stress distribution in the multi-point formation is examined in this paper using both theoretical derivation methods and numerical investigation. The theoretical model's estimated maximum residual stresses are in good agreement with the numerical outcomes.

Zhu et al. [20] (2019) purposed to identify the physical basis for the deformation of elasto-plastic and springback properties in the multi-square punch forming (MSPF) process and to generate suitable mathematical interpretations. With the help of the 3D CNC hull plate forming machine, a few strip-forming experiments were conducted. In addition, theoretical equations are established that take into consideration the follower load with variable boundary conditions throughout the forming process to analyze the forming process and springback characteristics of the strip. Validation with experimental data demonstrates the accuracy of these equations. The provided formula may be used to properly characterize the profile of the strip under various loading situations during the forming process, indicating the characteristic spectrum of the panel (for example, the panel's thickness) that can be produced on a certain MSPF machine. The strip's springback ratio is found to increase when the tool's thickness and curvature both grow, according to parametric study.

Li et al. [21] (2019) employed a sparse multi-point flexible (SMPF) tool for the creep age forming (CAF) operation to investigate the effect of the placement of the forming pins on the accuracy of the formed shape. For blanks provided by the SMPF tool with different pin configurations, an analytical approach has been developed to forecast the form, strain, and stress distributions. The resultant geometries after loading and CAF have been statistically evaluated utilizing tests and numerical models of the loading and CAF operations using the SMPF tool based on several pin number/interval scenarios. The results show that adding pins to the SMPF tool decreases stress changes and form inaccuracies in the loaded blank, resulting in less deflection of the formed blank following CAF. The resulting shape becomes more resemblant to the shape produced by the corresponding surface tool as the quantity of pins rises. For single curved tool forms made of aluminium alloy 6082, the form rate of errors in loaded blanks after CAF with SMPF tool significantly rises, going from 3% to greater than 20%, and the detailed figure varies depending on the tool shape. The stresses in loaded blanks have been determined to be the first to have the identical stress divergence degree among loaded blanks with SMPF tool and corresponding surface tool to obtain a specific form accuracy after CAF with various tool shapes. Shapes produced by CAF are directly impacted by stresses in loaded blanks. It is recommended that the pin position design criterion in the SMPF tool for the CAF process be specifically and more effectively determined by the stress differential factor for loaded blanks. Additionally, an axis-symmetric pin layout has been suggested, and its usefulness for the CAF process has been investigated and tested. This pattern decreases the number of pins in the SMPF tool by half while increasing efficiency.

Three alternative methods of forming, using a fixed-punch machine, an elastic pad made of polyurethane, and a unit that swings a punch, have been the subject of Erhu et al.'s [22] (2019) numerical experimental studies of the forming processes. An R500-radius sphere was selected as the target surface. Three different forming methods—using a fixed-punch machine, an elastic pad composed of polyurethane, and a unit that swings a punch—were examined using finite element models and experimental methodologies. Mechanical design, forming procedure, and forming basis were all covered for the three forming methods. The impacts of the three forming techniques on the sheet metal's forming quality and accuracy were carefully investigated in terms of curvature distribution, quality of surface, thickness of material, and springback. The study's findings suggest that using a s fixed-punch machine can reduce springback, increase plastic deformation of the sheet, and effectively manage dimple and wrinkle faults.

Peng et al. [23] (2019) have studied the geometry of the interaction between the objective surface and the multi-point punch components in multi-point warm press forming process. Punch height computation and punch positioning modification were done using the multi-point CAD/CAM program. In a series of multi-point warm press forming experiments, the impact of the process temperature, elastic pad, and load of forming on the accuracy of the forming was investigated. Next, it was examined how accurately the experimental and objective components' shapes matched up. Corian sheets were then formed into spherical and saddle-shaped components using optimal forming parameters using a multi-point heated press forming procedure. At 165 °C and 100 kN of forming force, the excellent quality of the surface and form accuracy of both saddle-shaped and spherical pieces were achieved. It demonstrates the viability of the MPWP forming method for producing Corian sheets.

By using theoretical calculations and finite element modelling, Su et al. [24] (2020) investigated the controlling of quick springback compensation of a two-dimensional hull plate. The entire elastic-plastic bending moment is calculated for the cylindrical shell employing the bending forming theory of medium and thick plates, and the curvature change before and after springback is inferred. The exact finite element simulation technology establishes the curvature correction coefficient. A cold bending experiment is also used to confirm the method's validity. Owing to the curvature gradient of its geometric portion line, the variable-curvature shell is split into a number of cylindrical surfaces. The springback curvature of a cylindrical plate correction compensation algorithm produces the compensation curvature array, and a computer model is used to validate the technique. Results indicate that the strategy comes extremely near to producing the desired outcomes. As a result, the efficiency and accuracy of forming will be increased, and the groundwork for digitizing sheet metal forming is formed.

In order to decrease the sheet's forming problems and the time it takes for the lower and upper dies to align, Moheen et al. [25] (2020) utilized a polyurethane buffer between the sheet and the die. The investigation into forming the DC05 steel workpiece under varied punch load conditions employed a variable thickness for waffle-shaped elastic pad. The thickness of the elastic pad, the base radius of the cutout, and the profile radius of the cutout were shown to be the three most crucial factors. The ideal values were found to be 3.01 mm, 2.37 mm, and 10 mm, respectively, for, cut-out profile radius, cut-out base radius and the thickness of pad.

Huang et al. [26] (2021) have researched the reciprocating bending-based multi-point flexible straightening technique. The process is specifically examined in terms of the deformation mechanism and supported by finite element simulations and experiments that straighten a variety of metal profiles made of various materials and beginning forms. Additionally, the distribution of residual stress upon straightening is examined along with the connection between the bending radius and the number of repetitions of reciprocating bending necessary to unify the curvature. The results obtained demonstrate that the process of reciprocating bending may eliminate the variation in starting curvature and make the curvature of each section trend toward uniformity; the length of time required for reciprocating bending to achieve uniform curvature reduces with the reduction in bending radius. This approach is quite feasible, as evidenced by the straightness of the straightened profile that was produced from the experiment and simulation, which is less than 0.2%.

The numerical modelling of electromagnetic incremental forming using a multi-point die has been investigated by Feng et al. [27] (2021). A new forming technique called multi-point die electromagnetic incremental forming combines multi-point die with electromagnetic incremental forming and is intended for large-sized sheet metal forming. At the beginning of the coil's first discharge, the deformation of massive workpieces is mentioned. Explained is the impact of multistep forming on the sheet metal's forming quality. Overall, the simulation and experimental results are in agreement. Through an experiment called multi-point electromagnetic incremental formation, the viability of this method is demonstrated.

Wang et al [28] (2022) have provided an easy-to-use, universal approach for elastoplastic equivalents in sandwich panels based on the Hill'48 yield requirement.

By numerically simulating the mesoscopic sandwich model under uniaxial tensile and pure shear conditions while using a user-defined material subroutine, obtaining the comparable sandwich model's elastoplastic constants was done swiftly. In this method, the sandwich panel's core was equivalent to an orthotropic homogeneous panel. According to comparisons with calculations of analytical and analyses of the outcomes of numeric simulations, the comparable elastoplastic characteristics of brazed aluminium honeycomb panels (BAHPs) with core heights of 9 mm and 12 mm were found. The usefulness of the elastoplastic equivalent technique was then further proven by contrasting the outcomes of the simulation of (MPF) for the equivalent numerical model of BAHPs and mesoscopic model. In the end, cylindrical BAHP MPF tests with various target formation radii were conducted. The outcomes demonstrated that the plastic forming of sandwich panels may be successfully accomplished using the elastoplastic equivalent approach.

In the study by Li et al. [29] (2022), the multi-point plastic forming of sheets of 2024-O aluminium alloy is the research subject. Ultrasonic vibration-assisted forming is used in the stamping process. A novel concept and technique for multi-point forming of sheet metal have been developed as a result of the springback of the material and effects of ultrasonic vibration on the plastic deformation. The fundamental theory of multi-point stamping and ultrasonic vibration-assisted metal sheet plastic forming is covered in this paper, along with a comparison of the technique's material properties when using and without ultrasonic vibration, the impact of various periods on the results, variations in parameters like stress and strain at different frequencies, and the springback effect will also be discussed.

Tolipov et al. [30] (2022) have described the optimization research of a unconventional hole-type rubber punch that would replace the top pin matrix of multipoint incremental forming to decrease the complexity and time involved in setting up and aligning pins. In order to determine how different hole-type rubber punch configurations, such as compression ratio and size and type of hole, affect wrinkling, variation of thickness, and form deviation, finite element modelling and design of experiments were employed. According to this study, the hole size was the key process variable across all replies. It was discovered that wrinkling and form deviation were unaffected by the material's compression ratio. The size of hole that 9 mm, type of hole circular, and ratio of compression of 75% were discovered to be the criteria for hole-type rubber punches. In an experiment, this reduced the amount of time and money required to set up and align the pin arrays while improving components wrinkling by 80% as compared to using a solid rubber punch.

The innovative multipoint forming, individually controlled force-displacement (MPF-ICFD) and standard multipoint forming (MPF) have been compared by Jia et al. [31] (2022). Analysing the strain concentration and the dimension of the part's wall finite element modelling and tests, respectively, using the cylindrical surface as the study object. The findings of theoretical analysis are confirmed by experiments and computational modelling, and they are utilized to compute the MPF-ICFD process' creating window. The results show that, when used with MPF-ICFD, the springback of Q295 and 1060 aluminium alloys may be decreased by almost 74% and 45%, respectively, when compared to traditional MPF. The plate's strain homogeneity is low in typical MPF, and the rate of maximum thinning is nearly 4.5%. The strain is extremely uniform and has a rate of maximum thinning of about 0.25 percent. For a sheet of aluminium alloy with walls that are 1.5 to 3 mm thick, the maximum and minimum values of the forming force for a single head are seen to vary linearly from around 6.5–13 kN and from 0.5–1 kN, respectively.

Shao et al. [32] (2023) used theoretical research, finite element analysis, and experiments to study the springback phenomena of hyperbolic component. The introduced springback compensation technique, the resulting springback compensation formula based on surface curvature, and the additional correction and fitting of the compensated die surface are all covered in this article. According to the results, the multi-point forming technique for corrosion-resistant aluminium alloy hyperbolic components may successfully minimize springback error using the springback compensation approach described in this work.

Li et al. [33] (2023) have investigated how the ultrasonic vibration forming method reduces springback. The impact of ultrasonic vibration on minimizing springback is investigated using the finite element program ANSYS/ABAQUS and ultrasonic vibration forming experiments of common materials. The theoretically derived and numerically simulated springback agrees with the findings of the experiment.

2.3 Place of This Study in Literature

It is clear from the literature that MPF was often used for the components to take advantage of process flexibility. Some process variables, such as pin diameter and comparison between relative fixation and active pin arrangements, have not yet been studied. With the use of finite element modelling and experimental research, the goal of this thesis is to analyse these MPF parameters. This research may fill a gap in the literature.

CHAPTER 3

OVERVIEW OF MULTI-POINT FORMING

3.1 Introduction

Many various manufacturing techniques are used to turn raw materials into final goods, additionally metal forming is a crucial one thanks to its benefits, which include process flexibility, resource savings, and potential properties of material enhancement.

Depending on the size and shape of the metal workpiece, metal forming is classified into two major categories: bulk deformation and sheet metal deformation as shown in Figure 3.1.

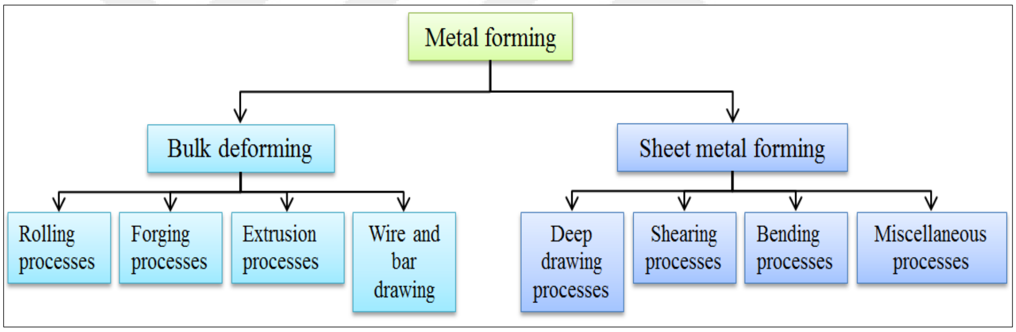

Figure 3.1 Metal forming classification diagram [1]

The processes can also be separated based on how hot the workpieces were when it was being formed. As indicated in Figure 3.2, there are three types of forming based on temperature: cold, warm, and hot. In Figure 3.2, T_A represents the ambient temperature and T_M represents the workpiece melting temperature.

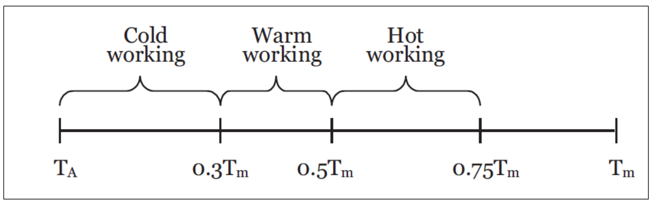

Figure 3.2 Temperatures in metal forming [1]

In this study, sheet metal forming is the main focused area. The process of sheet metal forming involves shaping a metal sheet (metal blank) into the desired shape. The forming tools used in sheet metal forming processes typically consist of rigid pieces. Figure 3.3 shows the main components of sheet metal forming processes. Additionally, there is no need to retain the sheet in some metal sheet formation techniques.

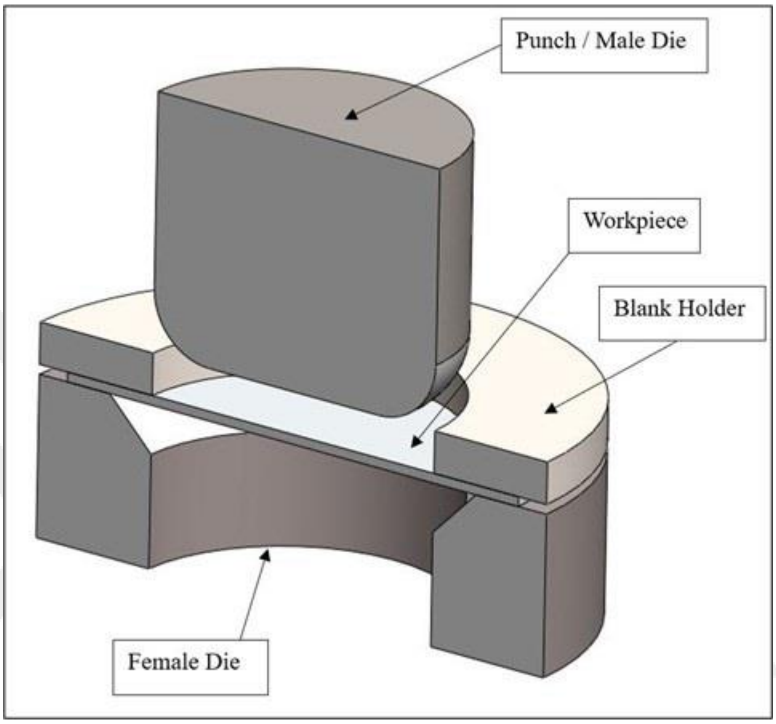

Figure 3.3 Main components of sheet metal forming

Stamping is the typical method that is most frequently used to create three-dimensional shaped parts. The tools used in mass manufacturing are made precisely for each desired form, but they are also highly expensive and huge, making this method impractical for creating small quantities of goods [34]. This led to the creation of a novel forming technique [35] that forms three-dimensional surfaces using changeable discrete dies. Process that uses the changeable die is called as multi-point forming process.

3.2 Overview of Multi-Point Forming

In order to lower the cost of die design, adjustable tooling, or die forming for variable forms, has long been considered interesting because it would provide rapid and nearly cost-free design changes. Researchers have up to this point offered several temporary concepts for changeable tooling. The multipoint forming (MPF) technique for panels that made of sheet metal has advanced thanks to Li et al. [36, 37]. The fundamental concept behind MPF is the substitution of a solid die for a collection of punch pieces that form the tool's surface. Due to the controllability of each element, the shaped tool face may therefore be changed at any time. Steel structures like the Bird's Nest Stadium (home of the Beijing Olympics), high-speed train bodies, skins for aerospace panels, and facades of buildings have all been made using MPF. The basic conception of MPF die is shown in Figure 3.4 [3]. As seen in Figure 3.4, the fundamental concept of MPF is to use punch components rather than solid dies to split the curved surface of the conventional die into several distinct pins. By adjusting the position of the punch elements in both the top and bottom sides of the apparatus, it is possible to utilize this MPF device to create a variety of curved surfaces as opposed to utilizing several fixed dies.

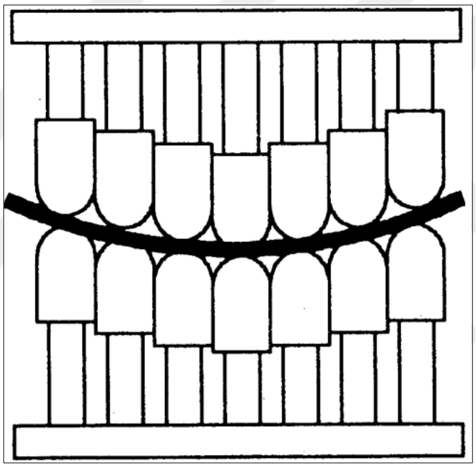

Figure 3.4 Basic conception of MPF die [3]

The sheet blank must be plastically deformed throughout the forming process by applying enough pressure to the punch. Figure 3.5 shows an illustration of the making of sheet metal part by using multi-point forming [38].

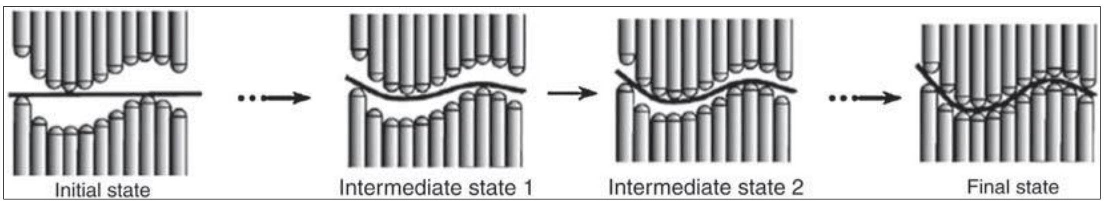

Figure 3.5 Process of MPF for curved geometry [38]

In place of the traditional stamping dies, a set of structures of punches with cylindrical tips is employed. The set of structures of punches may be controlled to resemble a uninterrupted working surface of a die tool by altering the rise of every punch. It is possible to produce sheet metal components in any arbitrary shape using a multi-point die (MPD). It is clear that the accuracy of the surface approximation increases with decreasing spacing between punches.

3.2.1 Various Punch Adjustment Methods

The punches' height may be changed to form various curved surfaces, which is the key characteristic of MPF [3]. As seen in Figure 3.6, there are different ways to alter the punch height.

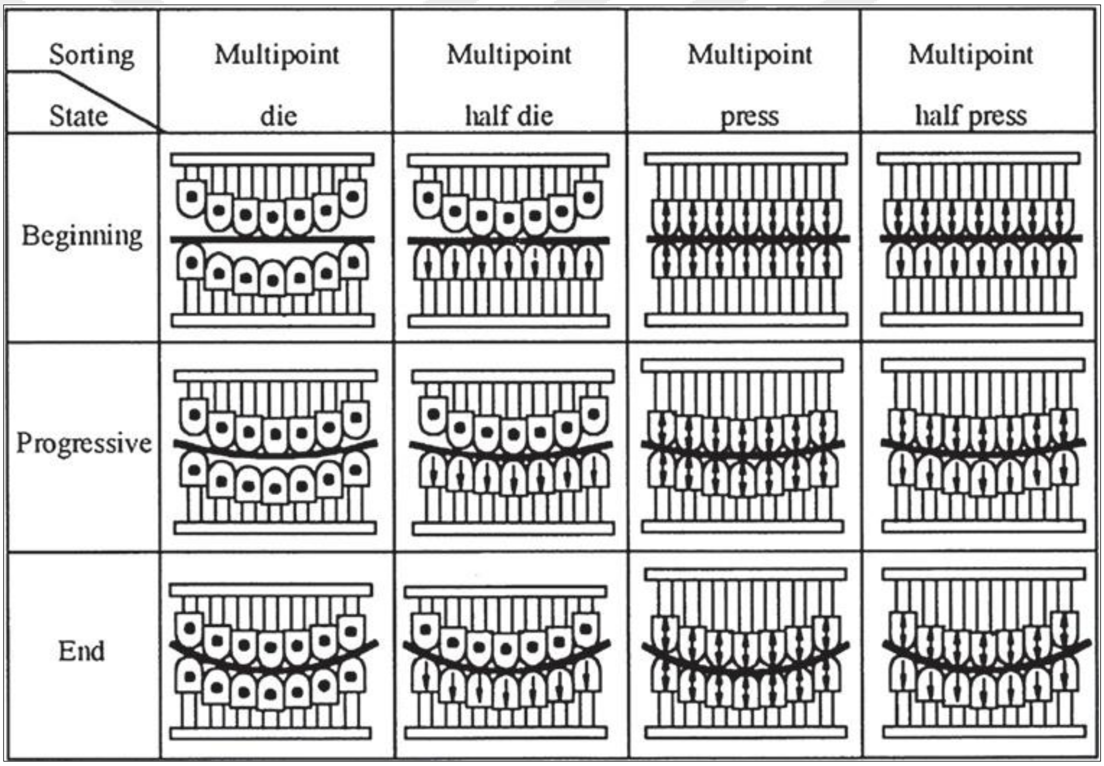

Figure 3.6 Different ways of MPF [3]

Six different forming procedures are available depending on the composition of the punch adjustment, four of those that are attractive and functional. Beginning with technique is known as multipoint die formation (consisting solely of unmoving punches), The following method is known as multipoint half-die (MPhD) formation (it uses both unmoving and inactive punches), multipoint press is the third (consists of all the top and bottom punches that are in motion), moreover, the fourth multipoint half press (which incorporates punches throughout the action that are both passive and active).

Relative Fixation: Punches in relative fixing are correctly positioned before shaping and forming the tool face. The punches do not move at all while the shape is being formed. Similar to conventional forming, but with the solid die divided into separate pins. Therefore, MPD forming is a suitable name for this technique.

Passive Adjustment: The MPhD formation, which consists of both unmoving and inactive punches, may make advantage of inactive adjustment. With the other fixed punches, the top punches (or lower punches) are prepared to the required shape prior to forming. During the forming process, the fixed die serves as the top set of punches, while the bottom group moves inactively as a consequence of the upper group until the formation is complete (there is no relative motion between the punches). The number of the regulated elements is noticeably decreased, which is the key characteristic of this strategy.

Active Adjustment: It is possible to apply active adjustment in multipoint press forming. The punches are properly positioned during the process of forming, rather than prior to it, so that the products may be dynamically formed into the required shape. It may be referred to as multipoint press forming process since there is relative motion between the punches and each pair acts as a little press. The loading force state may be best represented using this technique since it completely captures flexible features. Additionally, operators can easily alter the deforming way to get the optimal deformation.

In a multipoint half press, both passive and active adjustment are applicable. While the other passive punches are compelled to move as a result of the active punches bearing down on them, the active punches manage their movement according to necessity.

3.3 Technology of Forming and Deformation Characteristics

3.3.1 Defects in Deformation Process

As in other sheet metal forming processes, some defects occur in multi-point forming. These are dimple formation, wrinkling and tearing and springback.

Dimple Formation: The flexibility of MPF is a noteworthy benefit over classic stamping, however using a discrete-MPD also introduces certain limits since the characteristics of junction in the MPF process are quite dissimilar from those in the classic pressing process. Dimples, which are caused by contacts of point and irregular interactions between the punches and the sheet, are one of the MPF's most visible defects [11, 39]. The issues with MPF that designers must solve are dimples. One of the most glaring drawbacks is the necessity of a pliable pressing medium (i.e., elastic pad) between the punch points and the sheet metal in order to avoid the formation of dimples on the surface of the final geometry.

In order to compare the results of traditional stretching (using solid die) with those of the MPF procedures with absence of elastic pad, the outcomes for pieces were examined. The consequences of elastic pads on dimple suppression were further investigated by numerically analysing the MPF processes with elastic pads of various thicknesses Figure 3.7 depicts the MPF simulation results for saddle-shaped and cylindrical sections with absence of elastic pad [11]. On the surface of the cylindrical component, dimples are visible throughout and emerge where the part makes contact with the punch elements. Additionally, the areas surrounding the corners of the saddle-shaped section show significant dimples.

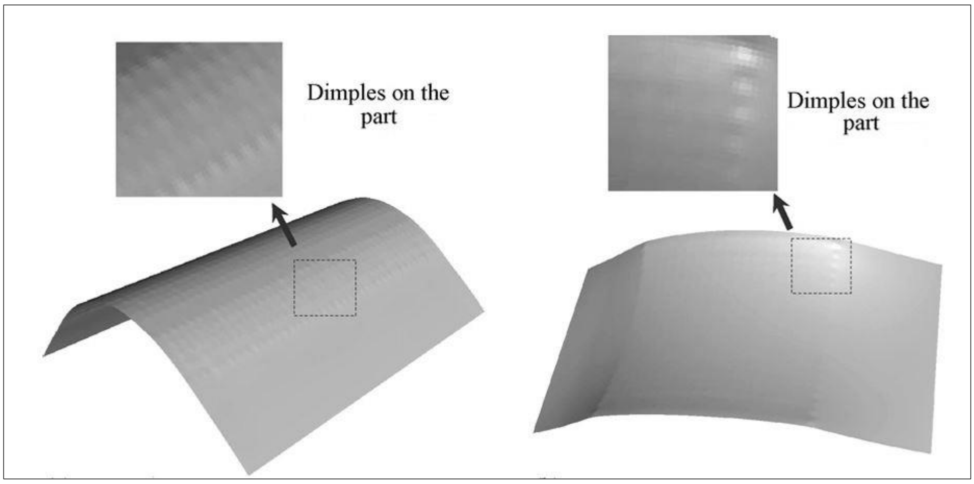

Figure 3.7 Dimples on the parts [11]

Due to the concentrated stresses that the punch elements place on the sheet blank in the absence of an elastic cushion, the sheet workpiece will be dimpled by the tip of the punch element. The surface of the die tool must be smoothed in some way, and elastic medium must be employed in MPF, in order to manufacture a qualified component, in discrete MPD. Utilizing an elastic cushion will reduce MPF dimpling and enhance the contact situation between the discrete die and sheet blank. However, there may be a difference between the shape of a produced component and that of a discrete MPD because to the elastic cushion.

Wrinkling and Tearing: The plane compressive stresses produced when complicated three-dimensional sheet metal components with significant deformation are formed frequently result in wrinkling [5]. A blank holder used in traditional stamping binds the material at the edge to provide an in-plane tensile bias, which suppresses the defects (tearing and wrinkling) [40-44]. The similar method may be used to get rid of these problems in MPF. To create complicated sheet metal components free of tearing and wrinkling errors, an MPF press with a blank holder was built.

Three-dimensional components may be successfully formed using MPF and a blank holder without tearing or wrinkling. It will be highly helpful in the production of intricate sheet metal components, such as car panels. Four steel components made using this method are shown in Figure 3.8 [5].

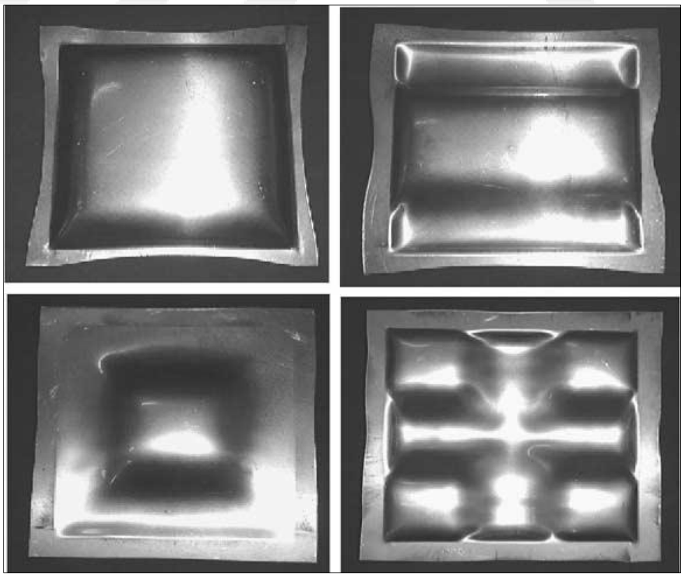

Figure 3.8 Final parts after MPF process [5]

Springback: After the sheet metal is removed from the forming tools, springback is a common occurrence because the inconsistent deformation over the thickness can change the product's shape and size with the stress still within it, particularly when using a large workpiece in cold forming [3, 45-48]. In general, the testing and revision of the die in traditional forming requires substantially more time in preparation. However, by applying the MPF approach and making little modifications to the punches, this issue may be immediately resolved. Additionally, if the MPF technique is applied, taking advantage of its flexible properties, no springback forming may be performed. In MPF, each punch may be actively changed. As can be seen in Figure 3.9 [3], repeated shaping may be easily accomplished by adjusting the height and direction of the punches.

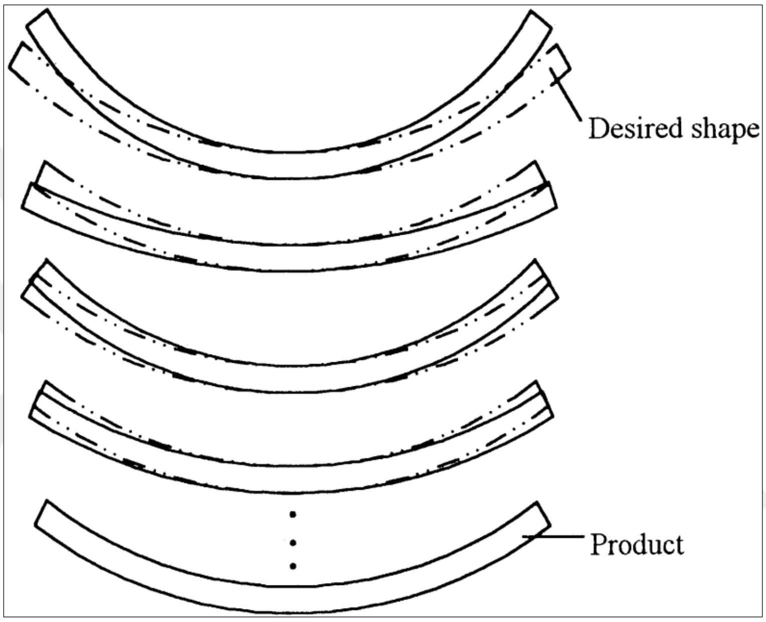

Figure 3.9 Forming with MPF [3]

3.3.2 Technology of Forming

Sectional MPF: Based on the adaptability of MPF, a workpiece may be created section by section using the so-called sectional MPF by altering the form of the MPD [5, 38]. A big size sheet workpiece is split into six parts and manufactured in six phases in Figure 3.10.

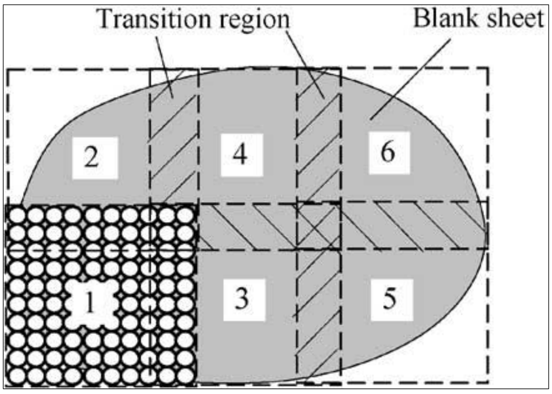

Figure 3.10 Sections of sheet workpice

The sheet metal is divided into three fundamental regions: the transition zone, the undeformed zone, and the deformed zone. Transition zones are the areas that overlap the deformed sections from earlier forming stages and the current step's forming section. They are particularly significant to sectional MPF.

The Ideal Forming Path of MPF: The two failures—tearing and wrinkling—are brought on by the non-uniform distribution of metal deformation during the forming process: too much local stretching strain can cause tensile unsteadiness, which results in tearing, and too much regional in-plane compressive stress can cause compressive unsteadiness, which results in wrinkling. In order to get the most homogeneous strain distributions in the finished products, optimum forming processes are accomplished when material constituents are required to deform along minimal plastic work directions. Therefore, forming metal along "ideal path" is an efficient way to prevent failures while creating sheet metal parts [38, 49].

3.4 Some Examples of Employed MPF

Beijing National Stadium is the most known application of MPF, is shown in Figure 3.11 constructed in the south of the Beijing Olympic Green. The National Stadium is a special-grade oval structure with an intended service life of up to 100 years. It is 333 m in length, 296 m in width, and 69 m in height at its highest point.

Figure 3.11 Beijing national stadium

China produced the whole 110 000 tons of steel used to construct Beijing National Stadium. When employing the conventional solid die, the primary challenge is the shaping of the steel framework employed in the Beijing National Stadium. A matching solid die set is used in the conventional solid process to create a cavity into which the sheet is displaced; however, this step is very expensive due to the length of the development process and the high cost of manufacture.

In typical die forming, the die surfaces create the planned shape of the product, whereas in MPF, the element group's envelope surface creates that shape. In an MPF press, a range of geometrical forms of products may be produced by arbitrarily changing the geometrical form of the forming sheet by adjusting the relative locations of the parts. Thanks to this, using the MPF process will result in considerable savings in terms of time and money spent designing, manufacturing, and adjusting solid dies compared to the traditional solid die forming method. This benefit will also become more obvious the larger the product is.

The CRH380A, a Chinese-built production train that travels at 486.1 km/h, currently holds an international record for the fastest train as shown in Figure 3.12 [50].

Figure 3.12 The CRH380A high speed train

Considering aerodynamics, the panel of high-speed trains has significant effects on these vehicles. The high-speed train's panel was made using conventional solid die technology. The main issue with this method is that it is quite expensive to create these intricate dies due to the expenses of both manufacturing and research. The panel of high-speed trains has been effectively formed using the MPF press to address these issues. Following their creation by the MPF equipment, these various panel forms will be welded. The conventional technology can then be used to build high-speed trains.

Manufacturing of aircraft outer shell panels, aircraft skin, is the industry that uses the MPF technology. Production of the outer skin parts of aircraft frequently use stretch-forming processes [51-53]. However, conventional stretching dies are expensive and large, and they also need a lot of setup time at the forming before production can start. The discrete multipoint stretching die (MPSD), which is made up of matrices of punch pieces with hemispherical ends, has replaced the conventional solid stretching die as a novel technique for stretch forming. MPSD can produce the necessary forms in accordance with the CAD data by modifying the height of punch parts. Stretch-forming is used on the sheet metal over the MPSD. Stretch forming with MPSD, also known as SF-MPSD, is schematically described in Figure 3.13 [11].

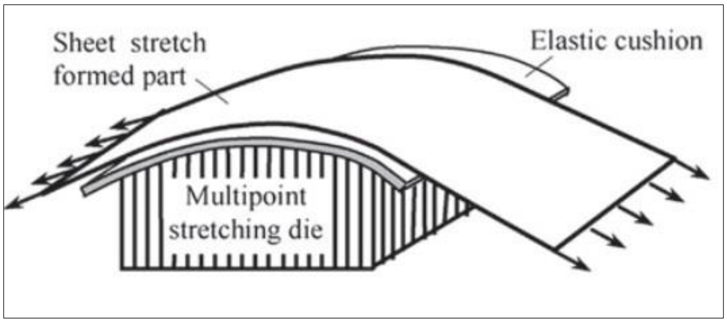

Figure 3.13 Stretch forming with MPSD [11]

MPF is also used in medical engineering, mainly in *Titanium Alloy Cranial Prosthesis*. A typical neurosurgical clinical situation is absenting cranium caused by surgery or wound [54]. There have been several attempts to fix the skull in recent years using materials like silicone glue, polymers, and plexiglas. The materials are often prone to disfigurements, such as subcutaneous effusion, rejection, inflammatory response, and material aging; as a result, application of the materials gradually declines [55, 56].

Because of its innocuity, corrosion resistance, low allergy issues, stable chemistry, and satisfactory biocompatibility, titanium alloy is regarded as a superior biomaterial. It is currently widely employed in medical applications. Titanium alloy retiary sheets are used to create the titanium alloy cranial prosthesis, which is dependent on the size and location of the absenting cranium. Because titanium alloy has poor formability and various missing craniums have diverse forms, conventional forming techniques are difficult to utilize. Therefore, a very precise MPF press with a blank-holder mechanism is used to create the 3D curved surface.

CHAPTER 4

MODELLING WITH FINITE ELEMENTS AND EXPERIMENTAL STUDY

4.1 Introduction

The properties of workpiece, experimental setup and methods, and finite element modelling which was used in multi-point forming are included in this chapter. The experimental study and jobs of measuring were performed in the Laboratories of Department of Mechanical Engineering in both Adiyaman University and Gaziantep University. DEFORM-3D Ver 6.1 finite element software was used to model finite element. The following headlines introduce experimental setup, the mechanical properties of workpiece material and finite element modelling steps.

4.2 Experimental Works

4.2.1 The Properties of Workpiece Material

In this study, aluminium alloy 1100 H14 or ASTM B209 with 0.5 mm thickness sheet was used in experiment and finite element modelling. There is no requirement for heating when using this material for cold shaping. Since Al 1100 has a high strength to weight ratio, low density, high ductile behaviour, toughness, and fatigue resistance, it is frequently utilized as shaped parts in the aerospace and automotive industries. In addition, it is ductile and soft, making this material suitable for sheet metalworking operations. Table 4.1 provides information about the workpiece material's chemical components.

Table 4.1 Chemical components of Al 1100 H14 alloy

Fe	Mn	Cu	Zn	Si	Al
0.09	0.049	0.117	0.72	0.081	Balance

The designation H14 for this aluminium refers to the sheet metal's temper type. The letter H stands for the strain hardening or work hardening temper type. The strength of Al 1100 aluminium alloy sheet is increased through work hardening using cold working techniques like rolling or pressing. Without using the annealing operation, half of the hard is obtained.

Tensile properties of Al 1100 aluminium alloy sheet were acquired from tensile test. Shimadzu AG-X machine manufactured in Shimadzu Corporation, Tokyo, Japan was used to conduct tensile test with ASTM E8 standard. Test speed was selected as 1 mm/min. Figure 4.1 shows the captures of a few specimens following tensile testing.

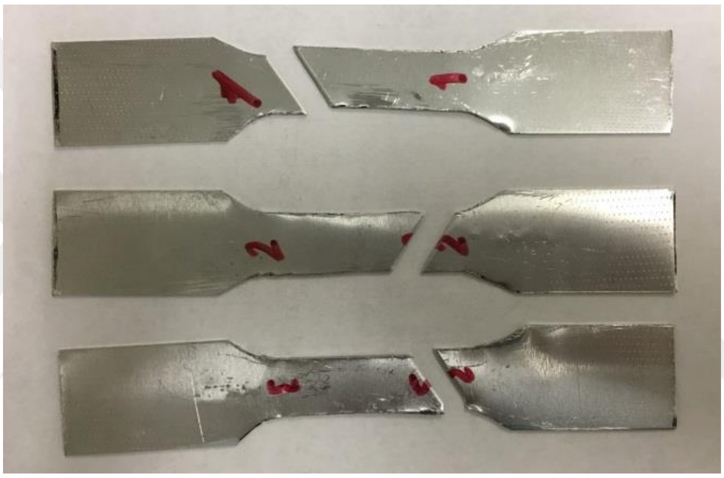

Figure 4.1 Aluminium specimens after tensile test

By applying the offset yield technique, the longitudinal yield strength of 105 MPa was estimated, and the tensile strength of 112 MPa was acquired in Figure 4.2.

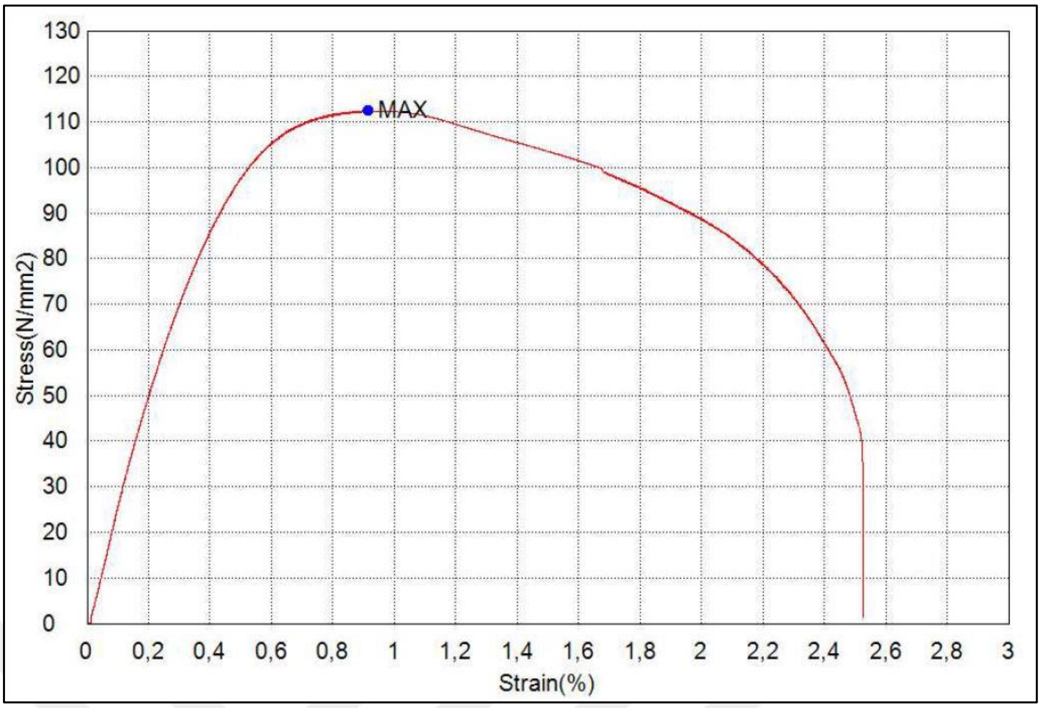

Figure 4.2 Tensile test result from Shimadzu AG-X

4.2.2 Experimental Setup

In order to define some boundary conditions of finite element modelling and verify finite element result carried out in DEFORM-3D Ver 6.1, experimental studies were performed for multi-point forming.

Experimental works were carried out by using a die set for multi-point forming with 7-row × 7-column (likely 7x7 matrices) as schematic representation shown in Figure 4.3. Die setup was constructed as relative fixation manner. This die set has two main component, bottom die section and top die section. Each die section includes 7x7 forming pins. All materials in multi-point forming die set were manufactured from AISI 4140 steel's mechanical characteristics [57]. Top plate and bottom plates have 8x8 M8 thread holes. Center-to-center distance of each hole is 15 mm. These holes were produced with CNC milling machine in mechanical engineering laboratory, Gaziantep University. Guide pins were also manufactured in CNC turning. Figure 4.4 shows the pins and top plate assembly. Pins have 87 mm length and 12 mm diameter. M8 internal hole was also processed with 45 mm length to pins. Additionally, pins have tip of 6 mm radius. Plates and pins were connected to each other with M8 bolt with 10.8 grade value. Figure 4.5 (a), (b) and (c) show the pins dimensions.

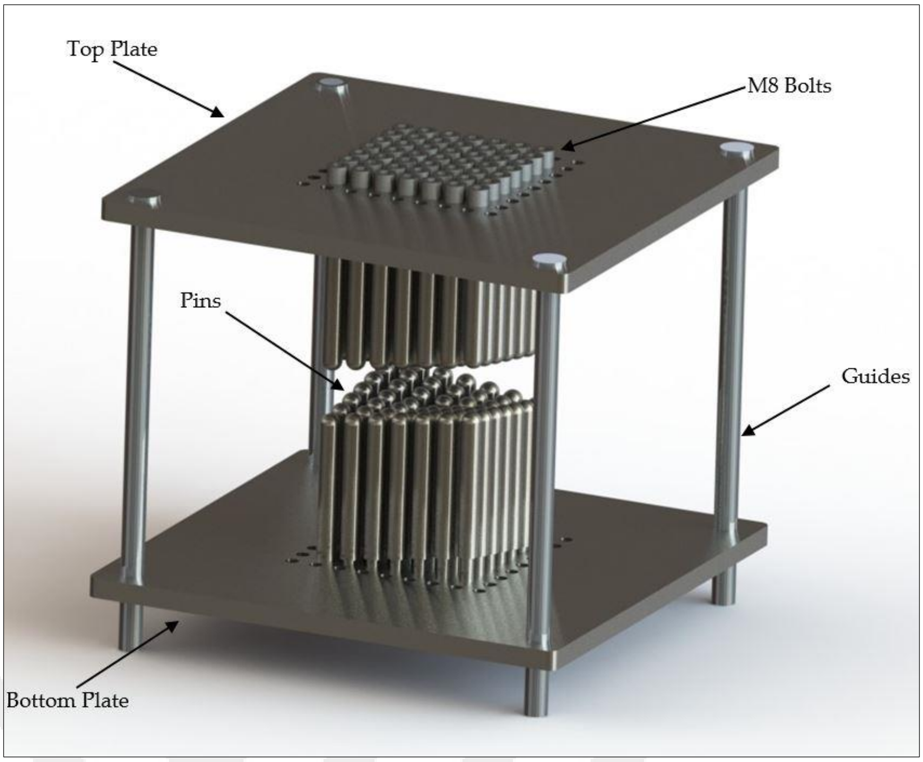

Figure 4.3 Schematic representation of multi-point die set

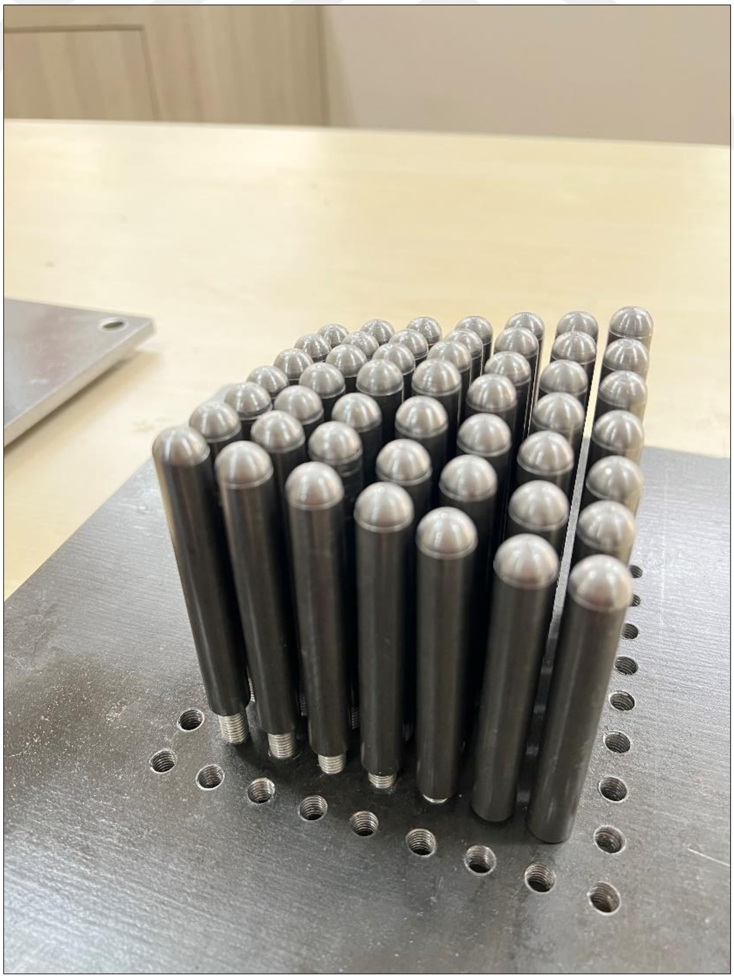

Figure 4.4 The pins and plate assembly

(a)

(b)

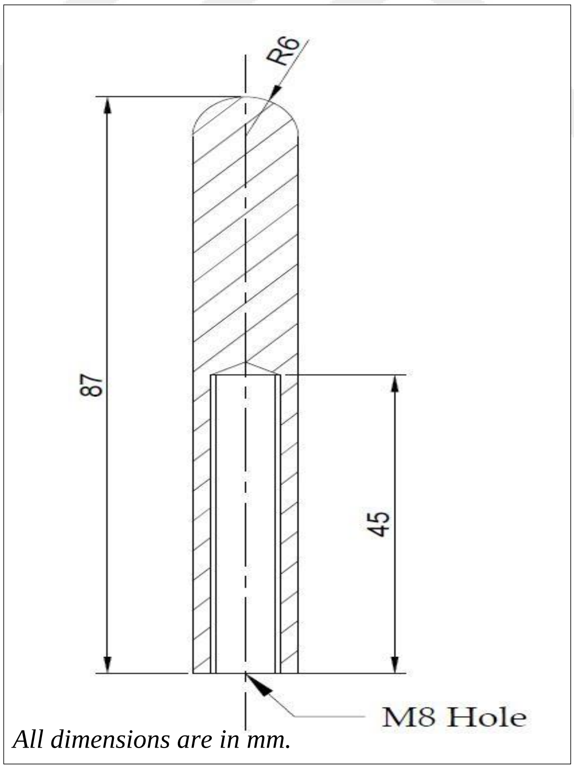

(c)

Figure 4.5 Pin dimension of (a) Length, (b) Diameter and (c) Technical drawing

When doing experimental works and finite element simulations, three types of shapes were utilized in the multi-point forming process. These final shapes were made from a blank sheet of 150 by 150 mm. The last shape of Form 1 (F1) is a V-shape, whereas Form 2 (F2) was a wavy shape, and Form 3 (F3) was a 3D free-form surface. The schematic illustrations and technical drawings in Figure 4.6 (a), (b), and (c) are shown.

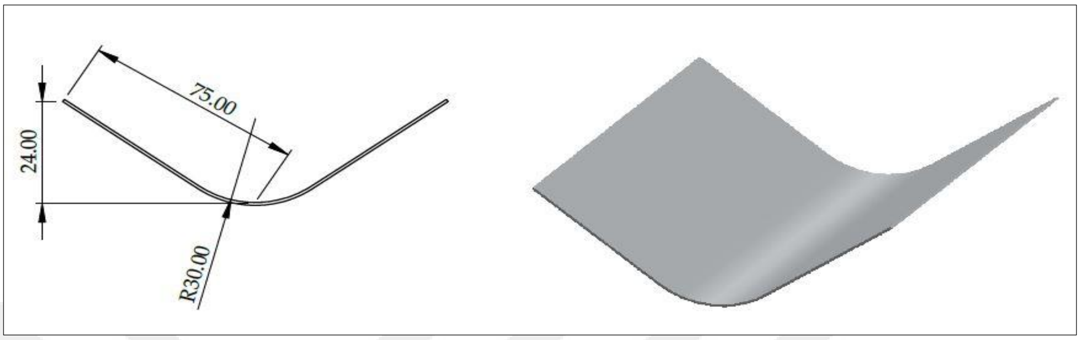

(a)

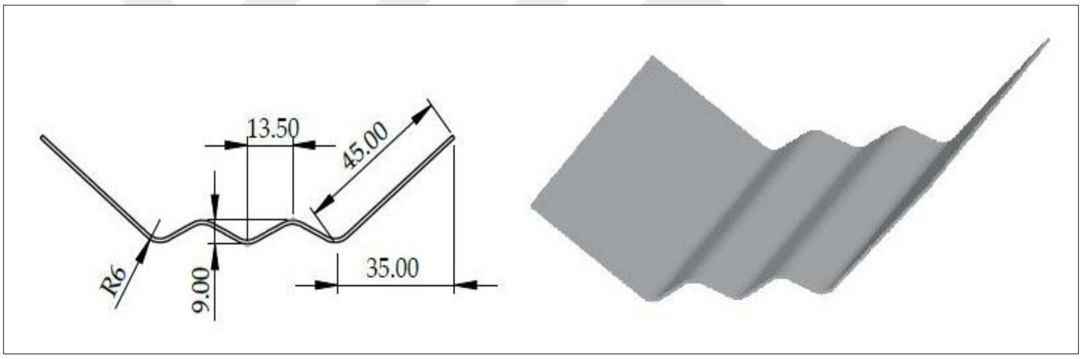

(b)

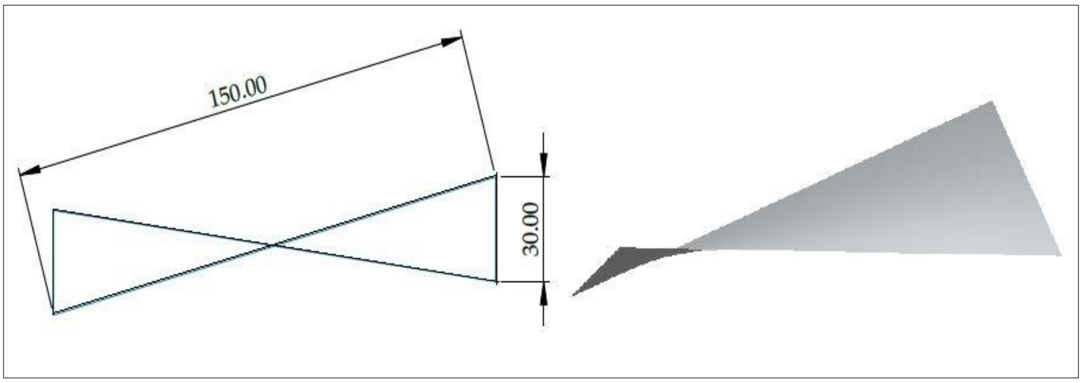

(c)

Figure 4.6 The shape of (a) Form 1 (F1) V-shape, (b) Form 2 (F2) wavy shape and (c) Form 3 (F3) 3D free-form surface

As the press source, a Utest universal testing apparatus with a 20 kN maximum load capacity was employed. Sheet metal was formed at room temperature by the press head moving at a stroke rate of 1 mm/min. The interface between the sheet and the pins was additionally lubricated with SEA 40 oil. The reason for using SEA 40 oil is the ring compression test. The adhesion friction factor may be easily and accurately determined using the ring compression test, which has been widely accepted as a completely suitable method for this purpose. Its approach is based on the application of geometric alterations to the strained ring itself, such as a reduction in thickness and a reduction in bore inner diameter [65]. In numerical analysis, friction factor was defined as 0.1 [61]. Accordingly, an aluminium specimen in the dimensions in Figure 4.7 was used to perform test and friction factor determinates as 0.1. The material of punch plate of test was made from AISI 4140 steel.

This test was also modelled and simulated in finite element analysis by using 0.1 friction and giving reduction in height with 50 %. Then, inner diameter reduction was obtained as nearly -15 %. After obtaining this value, the ring compression test was performed using several different oil types, and the decrease in the inner diameter was measured in the order of -16% in the test using SAE 40 oil. Therefore, the accuracy of SAE 40 oil has been decided for lubrication.

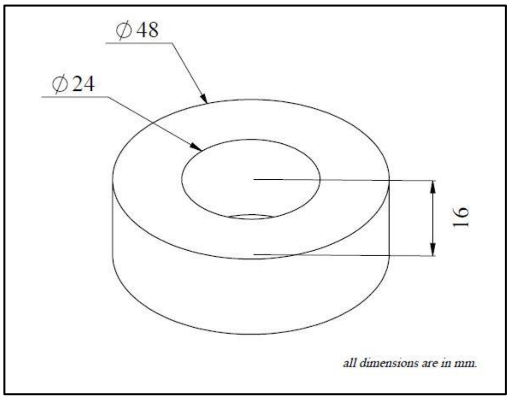

(a) (b)

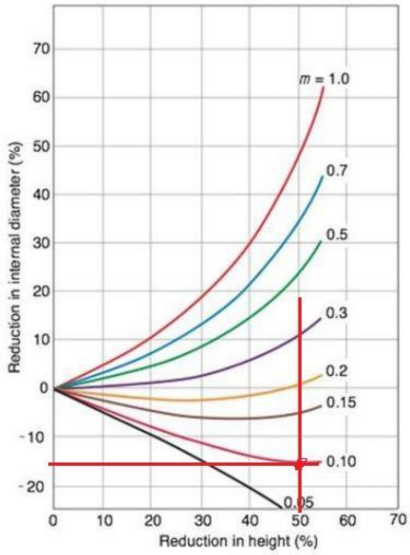

(c) (d)

Figure 4.7 Ring compression test specimen (a) Dimensions, (b) Initial ring, (c) Ring after experiment, and (d) Graph of friction

The testing machine's load was obtained after each 1 mm of movement. Figure 4.8 (a), (b) and (c) indicates the photographs of the die and sheet during the forming process for F1, F2 and F3, respectively. By individually altering the pin height, the geometry of the die set's forming regions was produced. First, the sheet metal's forming area was separated into 7 by 7 matrices, and then CAD data in Solidworks was used to compute the pin heights required.

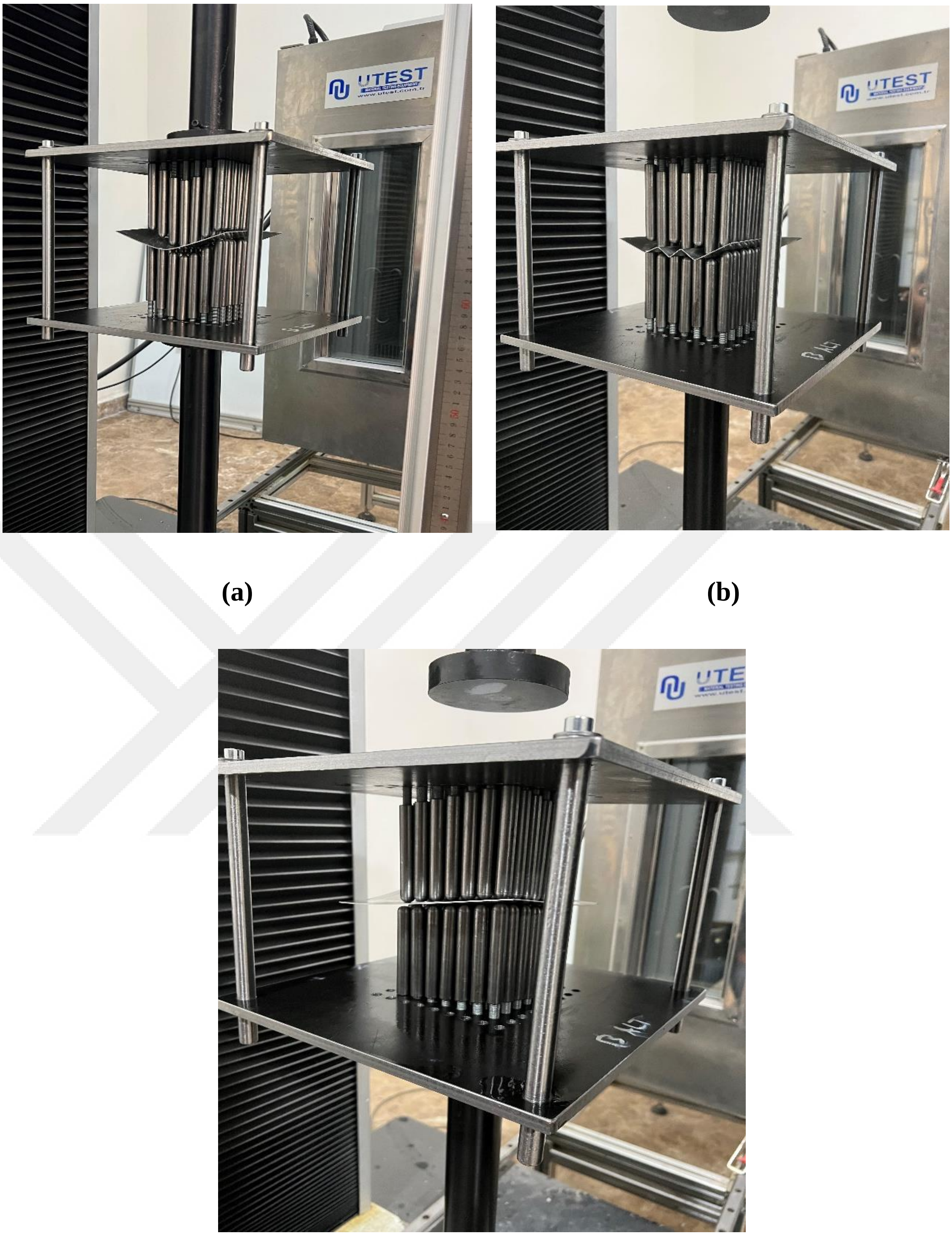

(a) **(b)**

(c)

Figure 4.8 The die and sheet during the forming process for (a) F1, (b) F2 and (c) F3

4.3 Finite Element Modelling

4.3.1 Introduction

FEM, the finite element method, is a practical technique for simulating and predicting the actual behaviour of challenging engineering issues. Software for commercially accessible and got a lot of validation from finite element analysis (FEA) from academics or students at institutions as well as engineers in industry. FEA is vital to cutting down on the time used while creating or modelling an engineering system. A powerful computer method for predicting solutions in a range of actual complicated engineering systems with accurately defined boundary conditions is the FEM. The basis for FEA's operation is the division of an engineering system or domain into a finite number of components, or subdomains, from which a systematic approximation may be created by using variational methods [58].

FEA reduces problem of the engineering system to a limited number of unknowns by dividing this domain into subdomains (components) and describing the role of the field's unknown variable within each element. These functions, which are also known as interpolation functions, are specified in terms of the field variable values at particular nodes, or locations. A certain series of global node numbers is used to present each element, which is expressed with an element number. Every node in a FEM model builds a mesh, which is a grid Figure 4.9 depicts how the mesh, nodes, and elements are related.

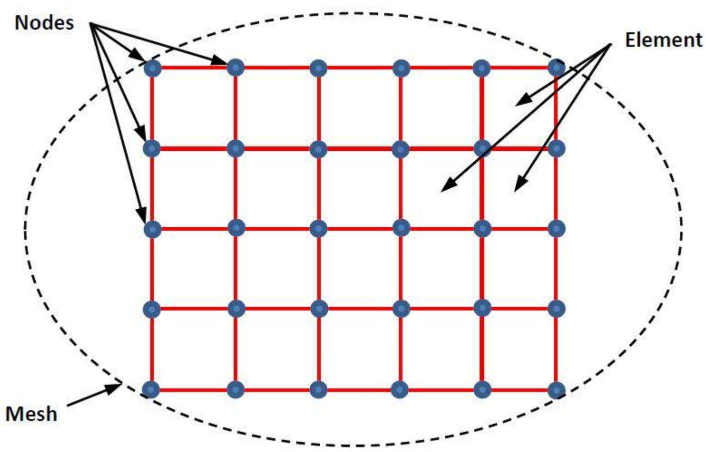

Figure 4.9 Element, nodes, and mesh relation

The mesh must be used to store the geometrical and material features that determine how the body will respond to outside influences.

4.3.2 Finite Element Modelling in DEFORM-3D

In this study, to model the finite element works, the commercial finite element software package DEFORM-3D was employed. Multi-point forming is one of the metal forming processes, as mentioned before. Owing to this, DEFORM-3D was used to simulate the process. The software main interface is illustrated in Figure 4.10.

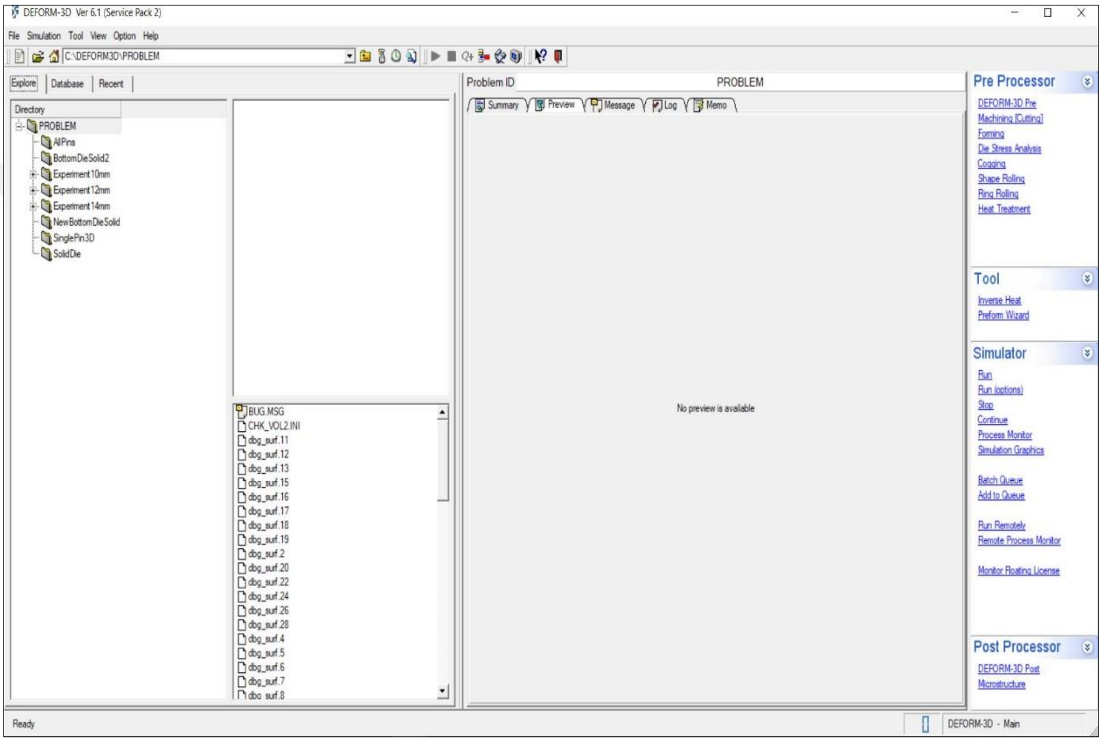

Figure 4.10 The software main interface

Pre Processor, Simulator and Post Processor are the main levels of DEFORM-3D Ver 6.1 as shown in Figure 4.11. In modelling section, all levels have specific job to do. The pre-processor is used to specify the object form, material type, mesh feature, contact type (friction), and simulation control in order to set up the steps and add the boundary conditions for carrying out the simulations [59]. Figure 4.12 shows the general view of Pre Processor section. In simulator section, model occurred in pre processor is run using predetermined characteristics in this area. This section contains visuals for process monitoring and simulation [59].

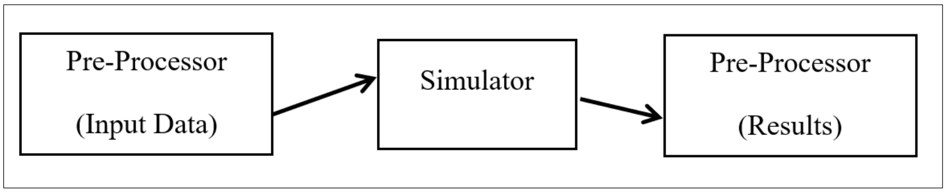

Figure 4.11 DEFORM-3D analysis levels

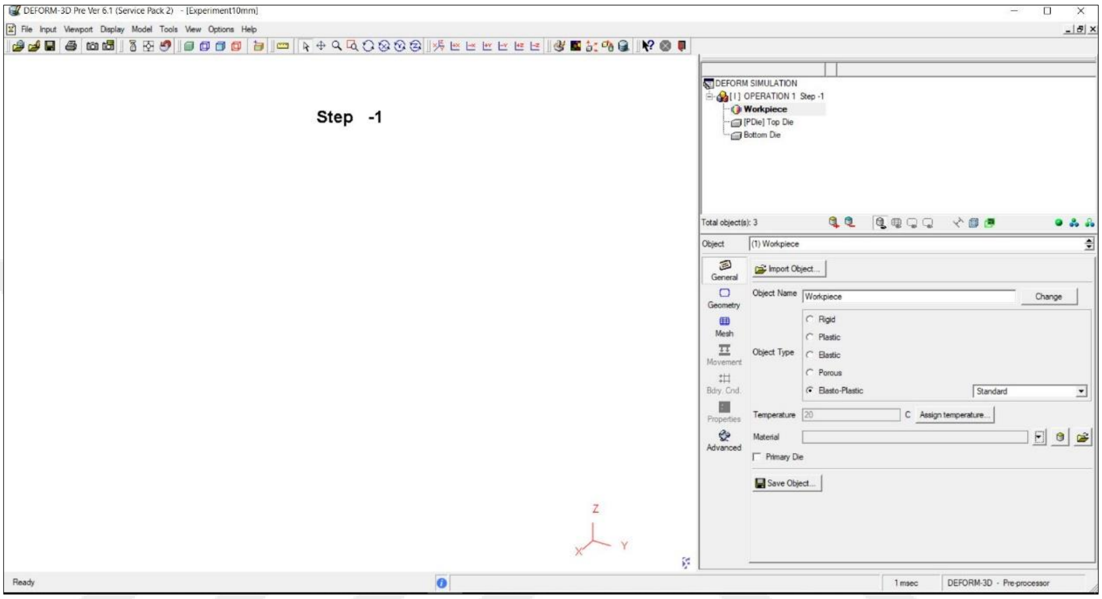

Figure 4.12 Window of pre processor

The Post Processor component of DEFORM is the last section. Data are gathered from a database file of simulations and the results are observed. All simulation steps are preserved as a result of the simulation engine. The Post Processor includes these procedures as well. Applied die motions, deformed mesh and geometry at each stage, contour viewing of any graphical values (such press stroke per load), stress, fracture, and effective strain, and a graph of any state variable between two user-defined locations are all available information in the post-processor [59]. The general view is shown in Figure 4.13.

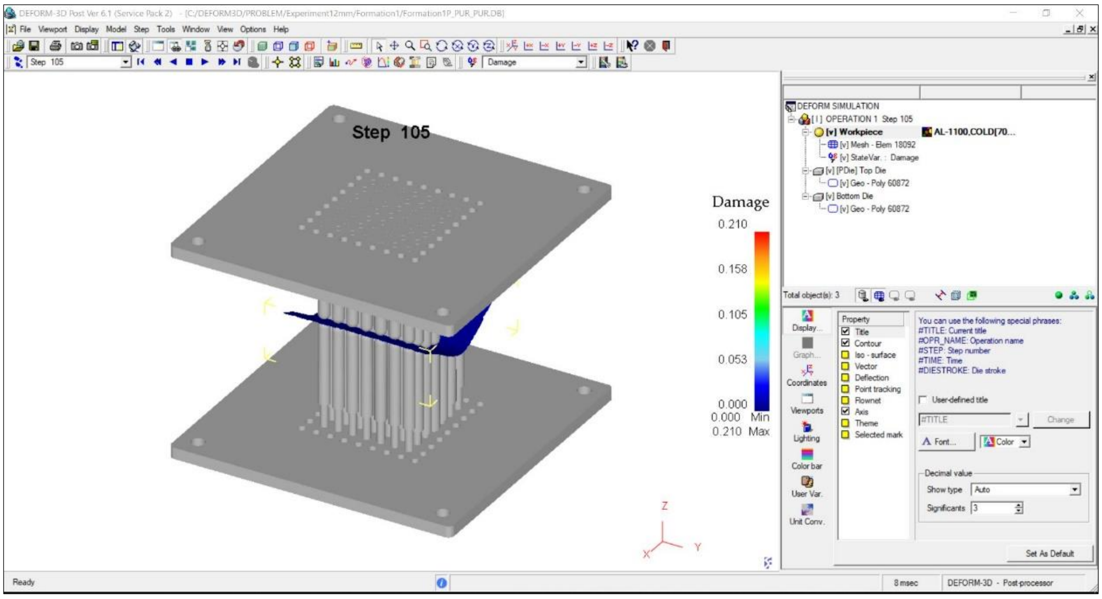

Figure 4.13 DEFORM post-processor window

4.3.3 Finite Element Modelling of Multi-Point Forming

Finite element model (FEM) is constructed for three types of forms, F1, F2, and F3. For both relative fixation and active punch adjustment. For each model, analysis was carried out by the way of pin diameter effect. 10 mm, 12 mm, and 14 mm pins are utilized in FEM. Two types of forming adjustments are used to investigate the effect of forming adjustment. Effective stress-strain distribution, thinning at pin sheet contact area, and maximum required loads are compared each other to examine the parameters. Diameter effect was also compared the experiment to verify and validate the finite element analysis.

In forming process, AL 1100 has lower strength than AISI 4140 steel. Owing to this and to reduce the simulations time, plates, bolts, and pins are modelled as rigid body. In DEFORM 3D, for rigid bodies, no material type was added, and no mesh wasn't created. Elasto-plastic material was used to model the workpiece. The elasto-plastic material characteristics of AL 1100 are included in the DEFORM-3D database for cold forming. Figure 4.14 illustrates the agreement between the calculated flow stress-strain curve from the tensile test and the database flow stress-strain curve for Al 1100. Poisson’s ratio and elastic modulus are 0.33 and 70 GPa, respectively.

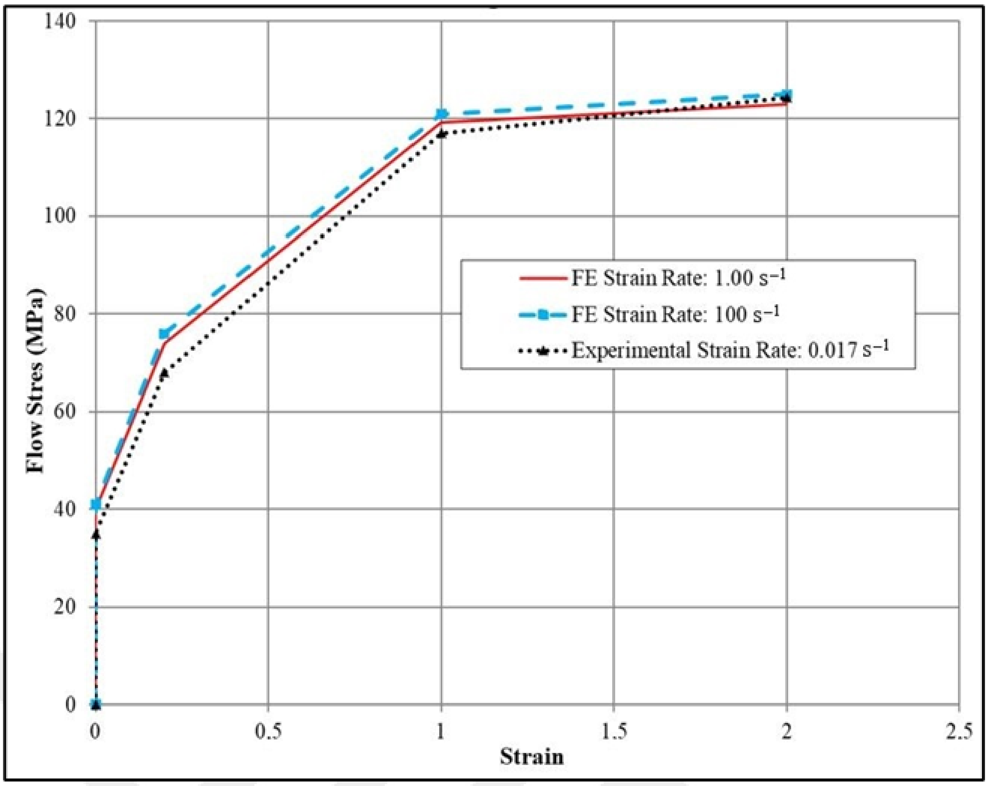

Figure 4.14 Flow stress-strain curve of AL 1100

In finite element analysis, fracture is the one of the main difficulties. To analyse how sheet metal cracks occur, the fracture criteria in DEFORM-3D ver. 6.1 software must be established. Due to the accuracy of strain, the fracture criteria was decided to be the normalized Cockroft & Latham since it is a better criterion for the metal forming process [60]. This criteria states that the fracture occurs when the effective strain is greater than the critical value shown by Equation in:

$$\int_{0}^{\varepsilon^{-f}} \left(\frac{\sigma^*}{\bar{\sigma}}\right) d\bar{\varepsilon} = C \tag{1}$$

Where C is the critical value or damage factor, ε^{-f} is the fracture strain, and σ^* is the maximum principal tensile stress. The $\bar{\sigma}$ and $\bar{\varepsilon}$ are effective stress and effective strain, respectively. A tensile test may be used to assess the critical value C, which is the regardless functioning operation. Based on the results of a tensile test, Al 1100's damage factor was calculated to be 0.34.

The friction that exists between pins and sheet metal has to be identified. According to Coulomb's model, friction was defined to be 0.1 as mentioned before. Mesh is crucial in the part on finite element modelling as well. An automatic mesh generator (AMG) was employed by DEFORM-3D to provide the optimum re-meshing and handle severe deformations throughout the forming process. The element type was designated as a tetrahedral mesh type. The element and node numbers were obtained by choosing a mesh above the point at which the mesh number no longer had an impact on the parameters. Table 4.2 displays the total number of sheet metal nodes and components for all forms of relative fixation and active punch adjustment.

Table 4.2 Element and node numbers

Pin Diameter	Form	Elements Number	Nodes Number
10 mm	F1 F2 F3	18069	6259
12 mm	F1 F2 F3	18069	6259
14 mm	F1 F2 F3	18069	6259

Figure 4.15 (a), (b), and (c) demonstrate the example relative fixation of F1, F2 and F3 shape appeared prior to simulation in the DEFORM-3D. Additionally, Figure 4.16 (a), (b), and (c) shows the active punch adjustment of F1, F2, F3 forms before the simulations.

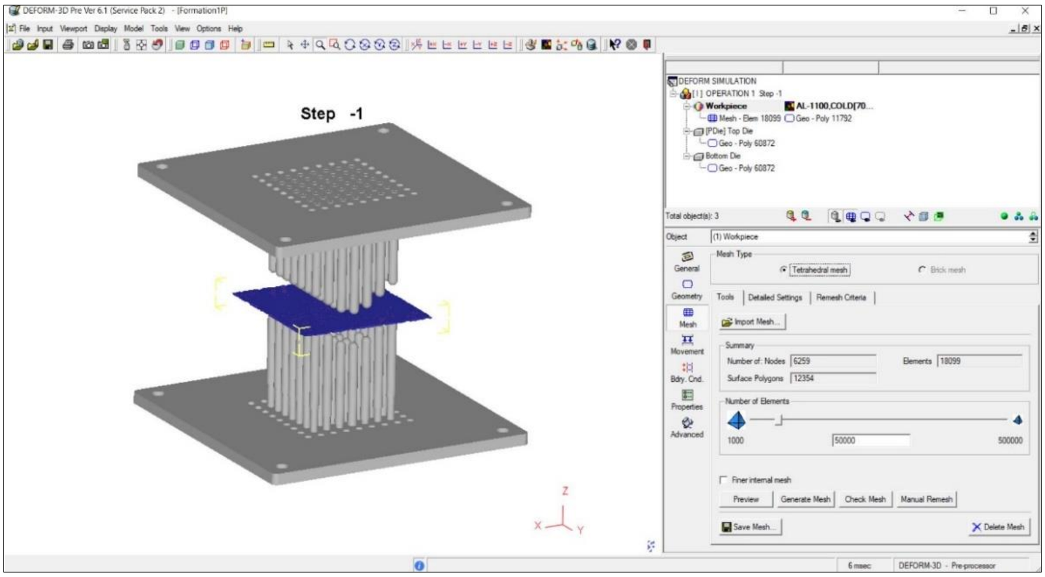

(a)

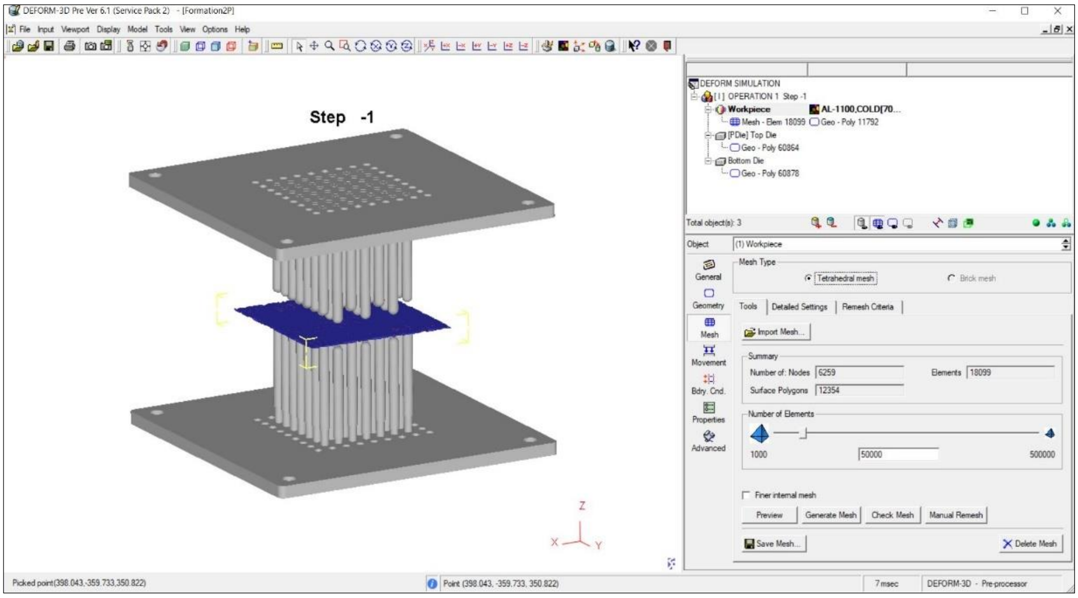

(b)

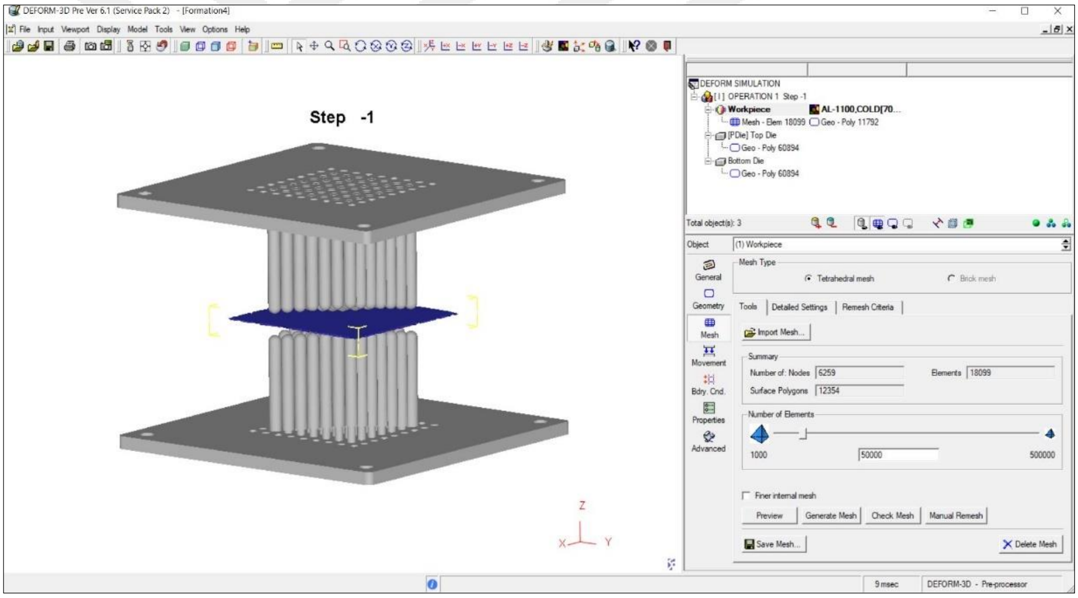

(c)

Figure 4.15 Shapes appeared prior to simulation in the DEFORM-3D of relative fixation adjustment of (a)F1 10 mm pin, (b) F2 10 mm pin and (c) F3 10 mm pin

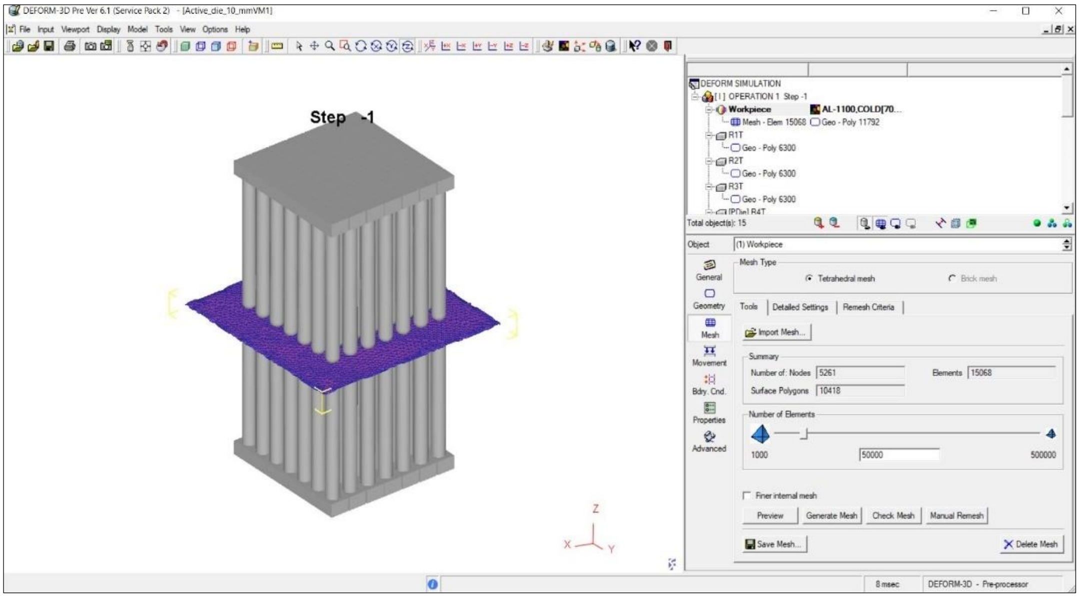
DEFORM-3D Pre Ver 6.1 (Service Pack 2) - [Active_die_10_mmVM1]
File Input Viewport Display Model Tools View Options Help
Step -1
DEFORM SIMULATION
[1] OPERATION 1 Step -1
Workpiece
AL-1100,COLD[70...
Mesh - Elem 15068
Geo - Poly 11792
R1T
Geo - Poly 6300
R2T
Geo - Poly 6300
R3T
Geo - Poly 6300
Total object(s): 15
Object
(1) Workpiece
General
Geometry
Mesh
Movement
Bdry. Cnd.
Properties
Advanced
Mesh Type
Tetrahedral mesh
Brick mesh
Tools
Detailed Settings
Remesh Criteria
Import Mesh...
Summary
Number of: Nodes
5261
Elements
15068
Surface Polygons
10418
Number of Elements
1000
50000
500000
Finer internal mesh
Preview
Generate Mesh
Check Mesh
Manual Remesh
Save Mesh...
Delete Mesh
8 msec
DEFORM-3D - Pre-processor

(a)

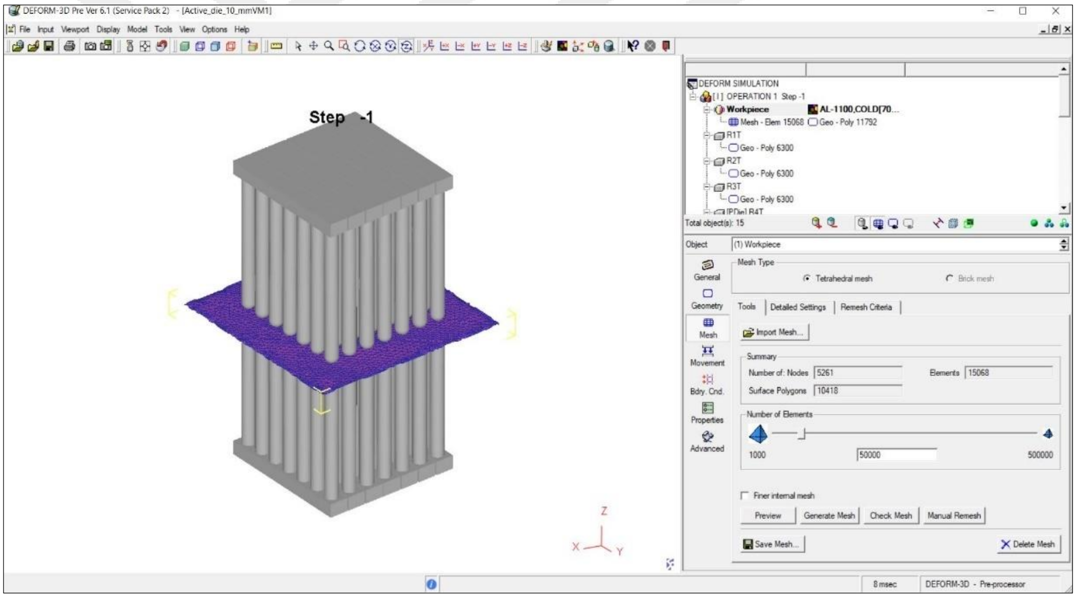
DEFORM-3D Pre Ver 6.1 (Service Pack 2) - [Active_die_10_mmVM1]
File Input Viewport Display Model Tools View Options Help
Step -1
DEFORM SIMULATION
[1] OPERATION 1 Step -1
Workpiece
AL-1100,COLD[70...
Mesh - Elem 15068
Geo - Poly 11792
R1T
Geo - Poly 6300
R2T
Geo - Poly 6300
R3T
Geo - Poly 6300
Total object(s): 15
Object
(1) Workpiece
General
Geometry
Mesh
Movement
Bdry. Cnd.
Properties
Advanced
Mesh Type
Tetrahedral mesh
Brick mesh
Tools
Detailed Settings
Remesh Criteria
Import Mesh...
Summary
Number of: Nodes
5261
Elements
15068
Surface Polygons
10418
Number of Elements
1000
50000
500000
Finer internal mesh
Preview
Generate Mesh
Check Mesh
Manual Remesh
Save Mesh...
Delete Mesh
8 msec
DEFORM-3D - Pre-processor

(b)

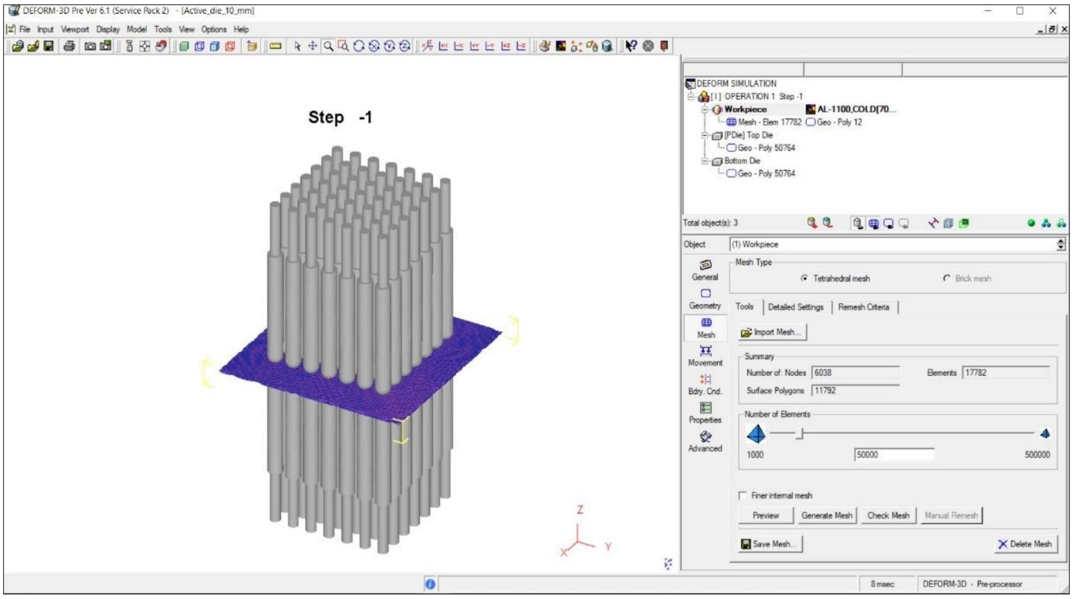

(c)

Figure 4.16 Shapes appeared prior to simulation in the DEFORM-3D of active adjustment of (a)F1 10 mm pin, (b) F2 10 mm pin and (c) F3 10 mm pin

CHAPTER 5
RESULTS AND DISCUSSION

5.1 Introduction

In this study, some multi-point forming parameters were investigated to understand the effect of these parameters on the process. AL 1100 with 0.5 mm thickness sheet metal was employed as workpiece material. The effect of pin diameter in MPF was investigated in both numerical and experimental ways for relative fixation (RF). Numerical simulations were aimed to verify by experiments. After that, the active punch (AP) arrangement of the process was also studied by using the finite element method. Effective stress distributions, thinning at contact points, damage factors, and load-stroke graphs were examined to understand the effects. The load-stroke curves and thinning at contact points of the numerical and experimental data were compared in the section on experimental results with the goal of validating the finite element simulations.

5.2 Finite Element Results and Discussion

5.2.1 Effects of Pin Diameter on Effective Stress Distribution in Relative Fixation

In the first simulations, relative fixation adjustment was carried out for all shapes. In this adjustment, pins were arranged before the forming operation then the loading was applied to the sheet metal.

According to Smith et al. [62], stress during sheet metal forming has a direct impact on the sheet metal's formability. Figure 5.1 displays the effective stress distributions by using finite element analysis, pins with diameters of 10 mm, 12 mm, and 14 mm were placed on F1 sheet metal. With pins of 10 mm and 12 mm diameter, the maximum effective stresses on F1 were obtained as nearly 83.750 MPa and 92.700 MPa, respectively. However, it was discovered that the maximum effective stress for the 14 mm pin-forming process was roughly 120 MPa, which was about 30% higher than the forming for pins with a diameter of 10 mm. Localized stress was encountered as a result of the pins' interaction with the sheet metal during the MPF forming process, as shown in Figure 5.1.

The 14 mm diameter pin's rate of material wrapping around it was higher than the two other pin diameters because of the larger contact area. Because the material could not flow freely to acquire shape, a larger localized stress was the end outcome.

Figure 5.2 shows F2 as having a more complex shape than F1 and having more constricting regions. For pins with a diameter of 10 mm, 12 mm, and 14 mm, respectively, the highest effective stresses computed on F2 were about 109 MPa, 113.220 MPa, and 122.700 MPa. According to calculations, the maximum effective stresses for a pin with a 14 mm diameter are 12.5% and 7.7% greater than that for pins with 10 mm and 12 mm diameters, respectively.

F3 features a 3-D free-form surface, giving it one extra forming dimension than F1 and F2, which both needed to be formed in two dimensions. As mentioned in the literature [2–7], MPF forming is a very adaptable approach for 3-D components. Figure 5.3 depicts the stress distribution for F3. For pin sizes of 10 mm, 12 mm, and 14 mm, nearly 94 MPa, 105 MPa, and 121 MPa were computed as the highest effective stresses, respectively. Additionally, compared to the 10 mm and 12 mm diameter pins, the loads on the pin with a 14 mm diameter were greater by 22.2% and 13.8%, respectively.

The FE simulations demonstrated that higher-level stresses and a reduction in thickness are present at the point where the pin and sheet make contact. A 10 mm diameter pin, on the other hand, produced the least stress distributions and damage factor values associated with tearing. In contrast, the biggest diameter pin (14 mm) produced the highest effective stress values.

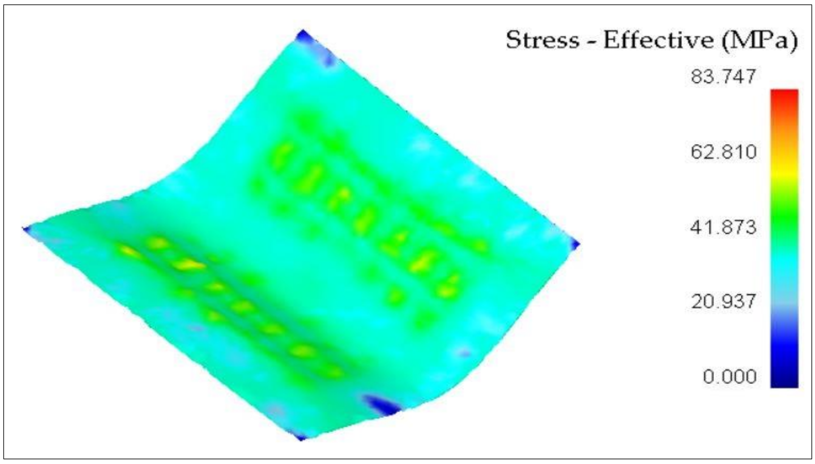

(a)

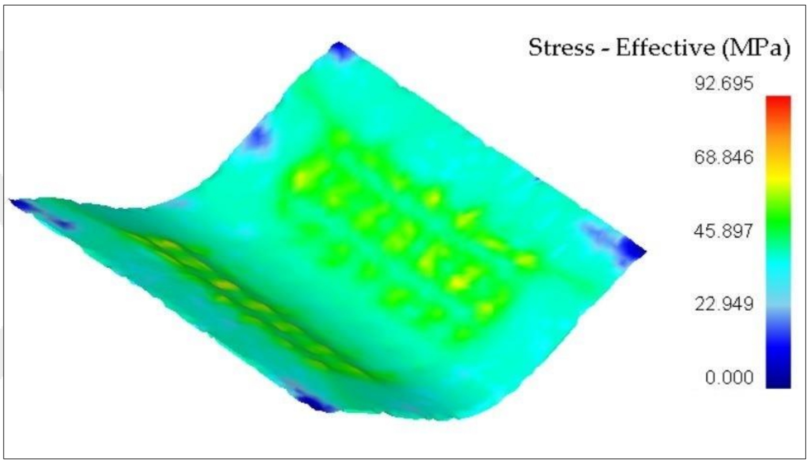

(b)

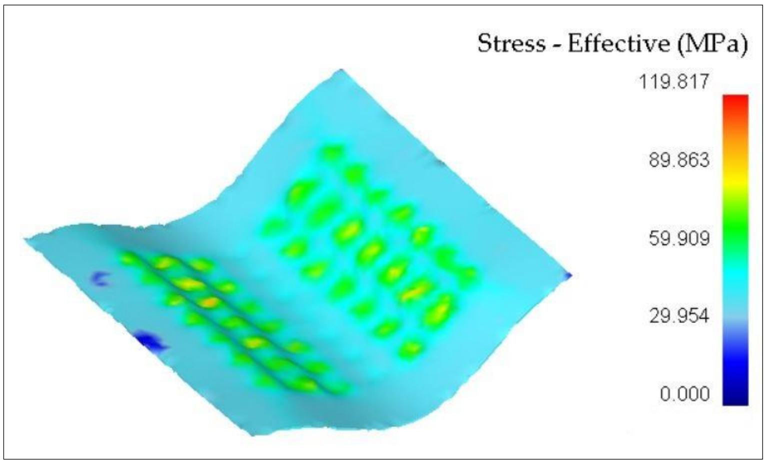

(c)

Figure 5.1 The effective stress distributions of F1 sheet metal (a) 10 mm, (b)12 mm and (c) 14 mm diameter pin

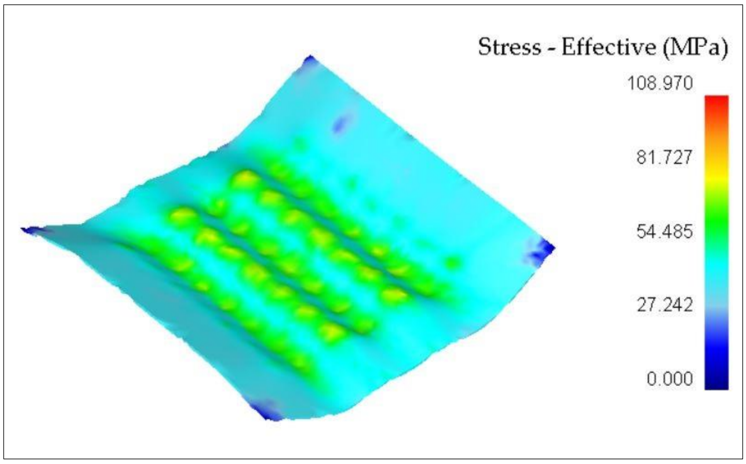

(a)

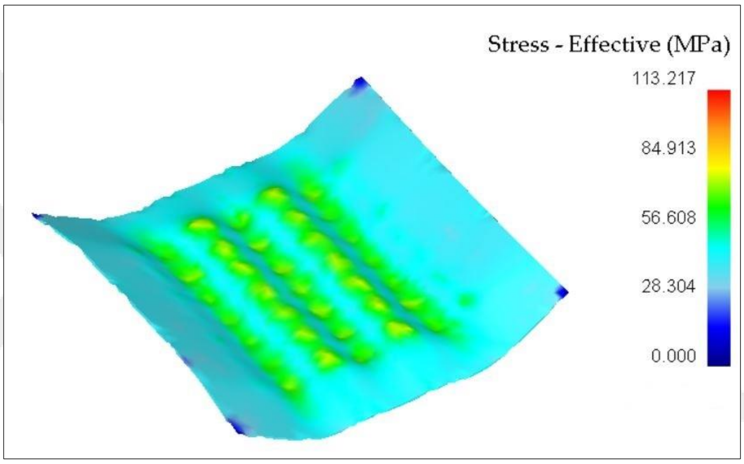

(b)

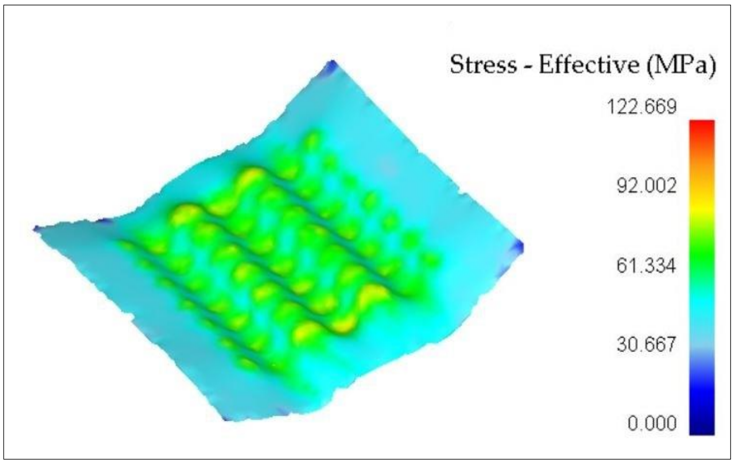

(c)

Figure 5.2 The effective stress distributions of F2 sheet metal (a) 10 mm, (b)12 mm and (c) 14 mm diameter pin

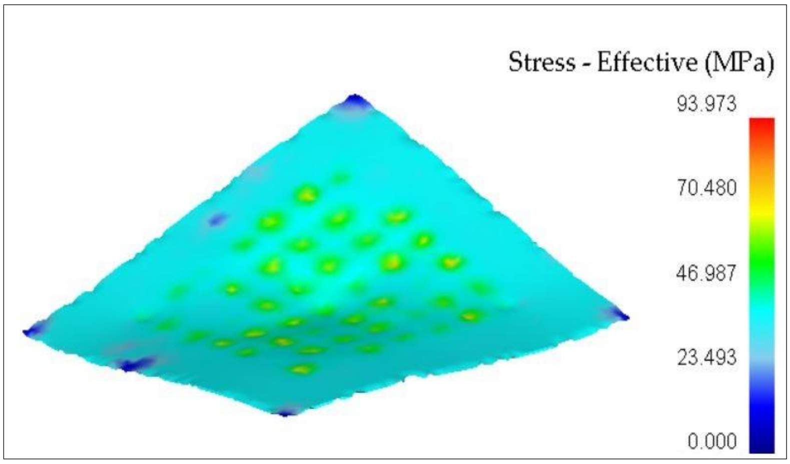

(a)

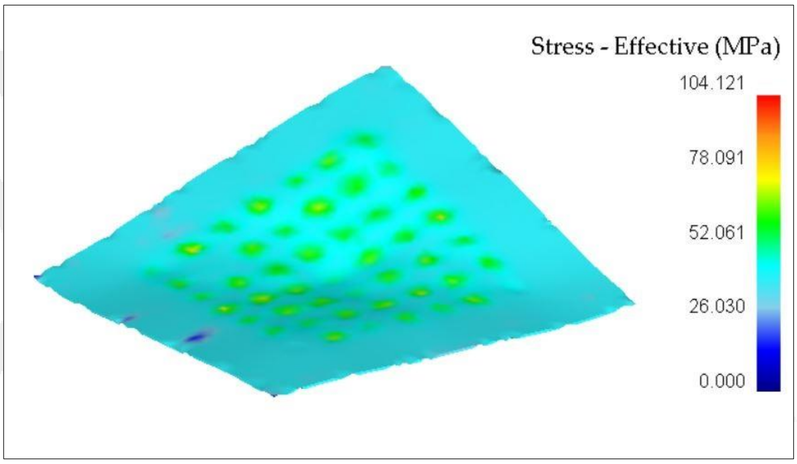

(b)

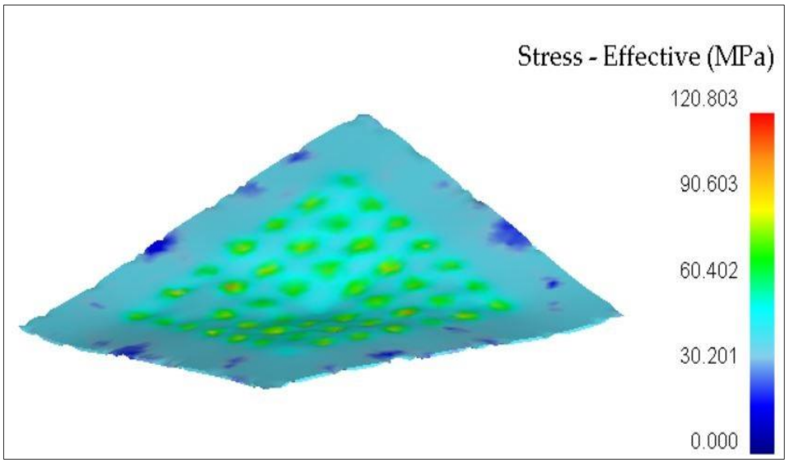

(c)

Figure 5.3 The effective stress distributions of F3 sheet metal (a) 10 mm, (b)12 mm and (c) 14 mm diameter pin

5.2.2 Effects of Pin Diameter on Damage Distribution in Relative Fixation

One issue that arises while sheet metal is being formed is tearing [63]. The sheet begins to break and creates cracks when the material's damage factor in DEFORM-3D reaches its maximum set level.

As shown in Figure 5.4, the damage factors for F1 forming with pins of 10 mm, 12 mm, and 14 mm diameter, respectively, were calculated by simulations as 0.196, 0.210, and 0.448. In 14 mm diameter pin formation, ripping occurs in comparison to the Al 1100 maximum damage factor of 0.34.

The estimated damage factors from the simulations for F2 for forming with pins of 10 mm, 12 mm, and 14 mm diameters, respectively, were derived as about 0.320, 0.340, and 0.770 as shown in Figure 5.5. Tearing of the sheet was observed in forming with employing forming the highest diameter of the pin. The damage factor value was approximately at a critical level for using the 12 mm diameter pin, but ripping did not occur.

Damage factor values for pins with small to high diameters were determined as in Figure 5.6 for the 3-D free-form shape (F3). The fracture was not detected in this form, although the 14 mm diameter pin had a damage factor that was very close to the critical threshold.

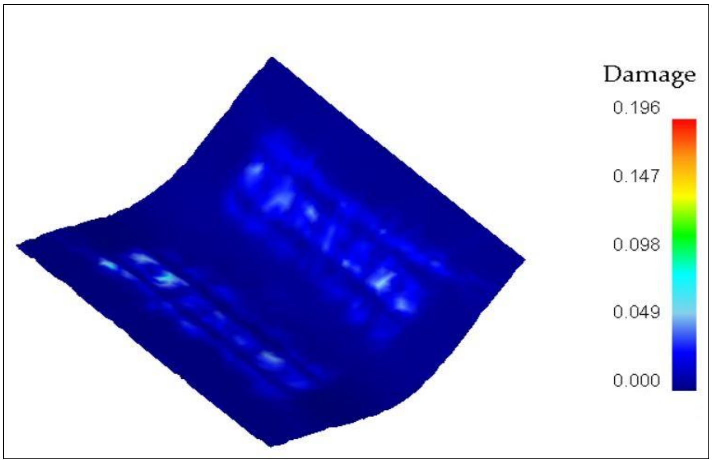

(a)

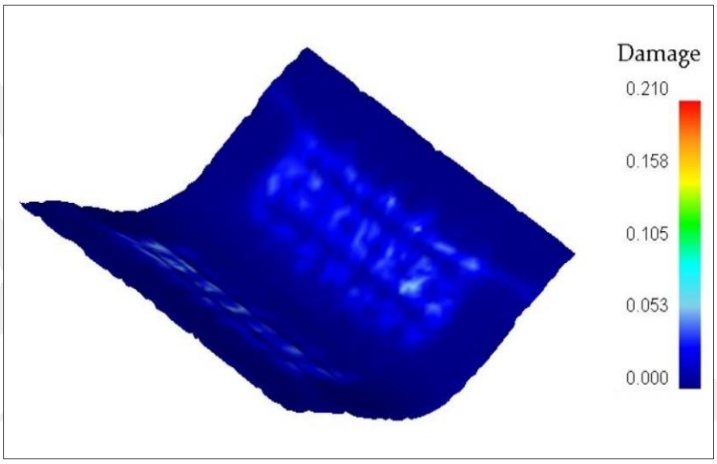

(b)

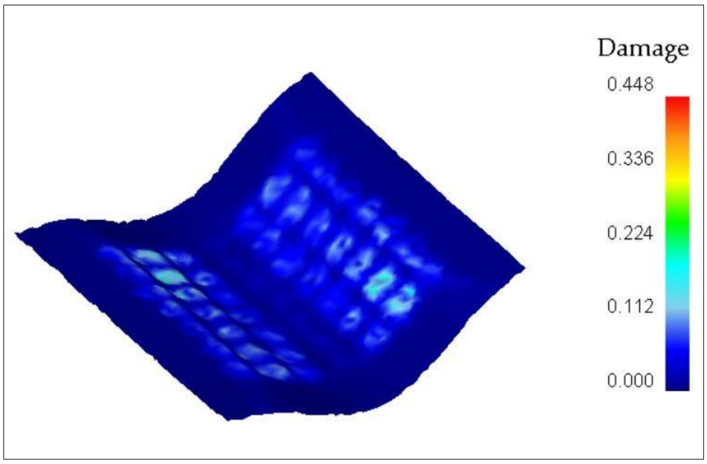

(c)

Figure 5.4 The Damage factors of F1 sheet metal (a) 10 mm, (b)12 mm and (c) 14 mm diameter pin

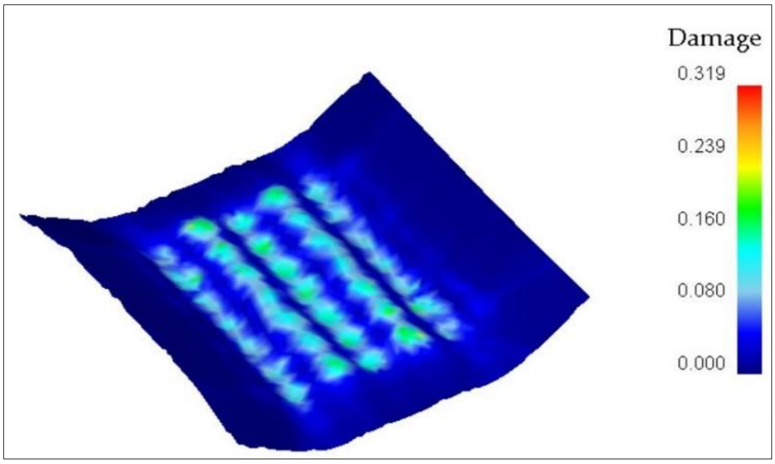

(a)

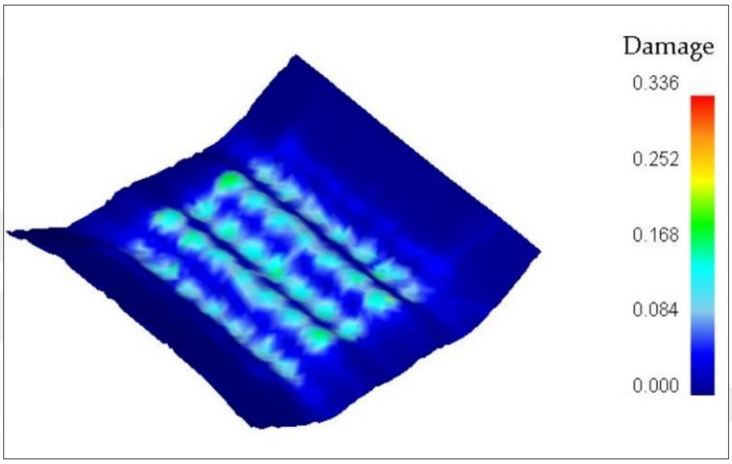

(b)

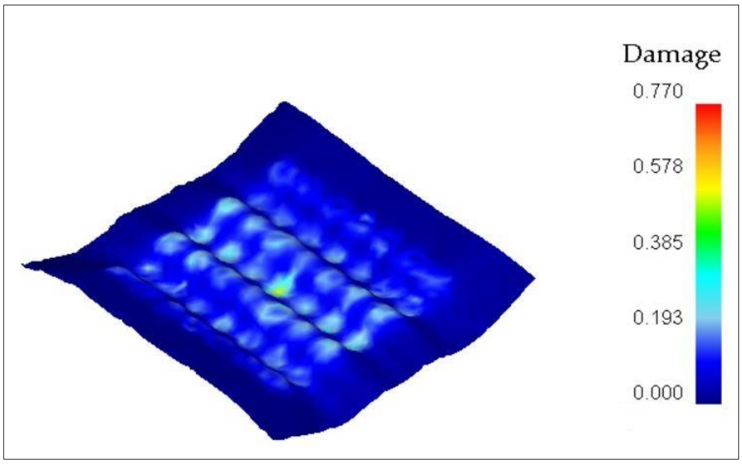

(c)

Figure 5.5 The Damage factors of F2 sheet metal (a) 10 mm, (b) 12 mm and (c) 14 mm diameter pin

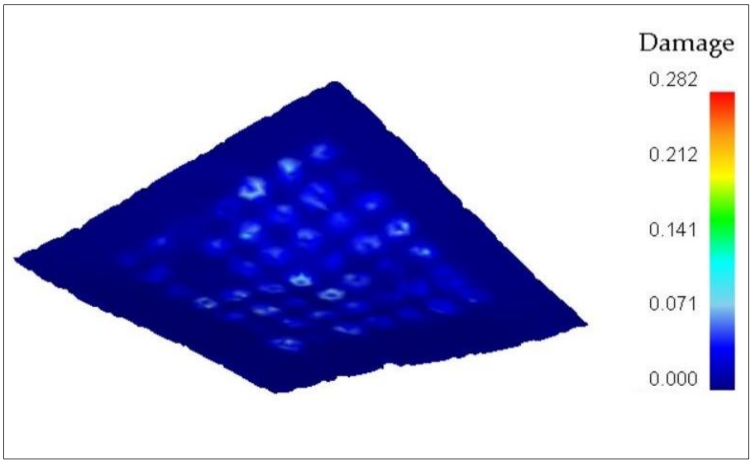

(a)

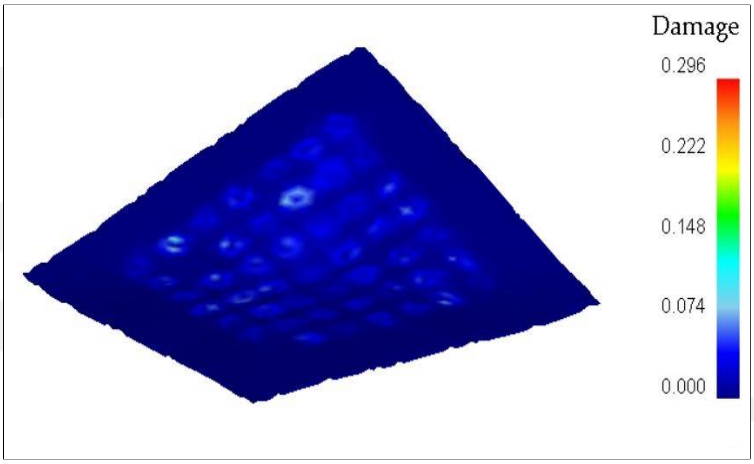

(b)

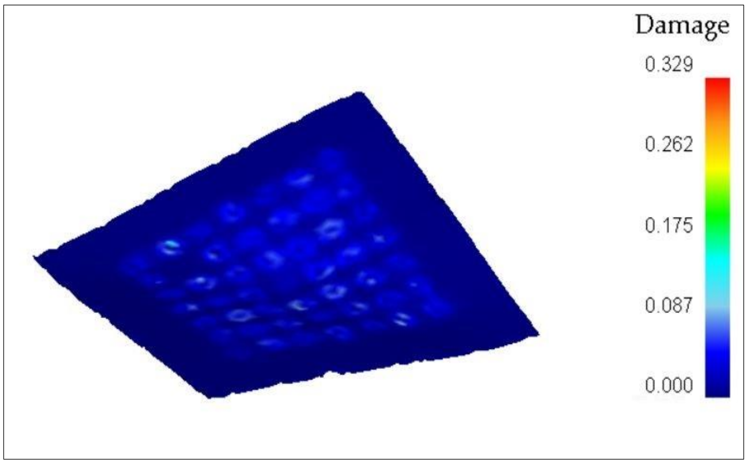

(c)

Figure 5.6 The Damage factors of F3 sheet metal (a)10 mm, (b)12 mm and (c) 14 mm pin

5.2.3 Effects of Pin Diameter on Forming Loads in Relative Fixation

Another crucial factor in forming processes is the required loading. The necessary press capacity can thus be calculated in this manner. Figure 5.7 compares the forming loads of the three forms using pins of various diameters. As can be seen from the captures, forming loads begin at rather low levels and increase progressively with the stroke until the localized forming of the sheet begins.

According to [30], when the final shape of the forming and the squeezing took place, the forces increased quickly. For F1, the highest loads measured for pins with diameters of 10 mm, 12 mm, and 14 mm were approximately 4200 N, 6300 N, and 8525 N, respectively. For F2, higher forming loads were computed because of how the effective stress distribution behaved.

With the increasing diameter of the pin, the highest loads for F2 were measured at nearly 6530 N, 8675 N, and 11200 N. For F3, the maximum loads were measured at just about 3650 N, 4640 N, and 5070 N. The maximum loads were estimated for each shape using pins with a diameter of 14 mm in accordance with the predicted effective stress distribution. As the pin diameter increases, the material flow becomes more difficult for complicated geometry components. This situation illustrated the requirement for a greater load and, thus, a press with a higher capacity.

5.2.4 Active Punch Adjustment

The second simulation series was employed using active punch adjustment. In active punch adjustment, pins moved to form sheet metal during the forming process. Pin heights and moving ranges were obtained from CAD data of shapes. After, that necessary movements were assigned to DEFORM 3D. After, forming process final forms of active punch adjustment are shown in Figure 5.8 (a), (b), and (c).

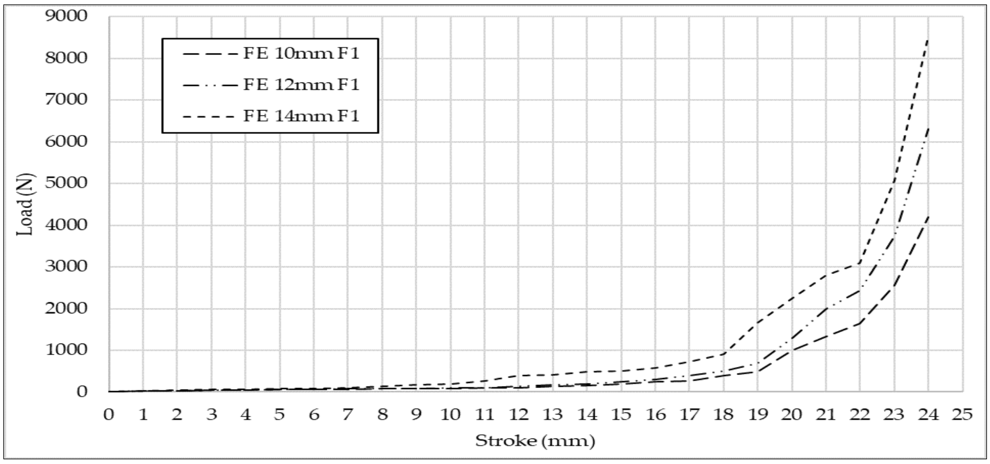

(a)

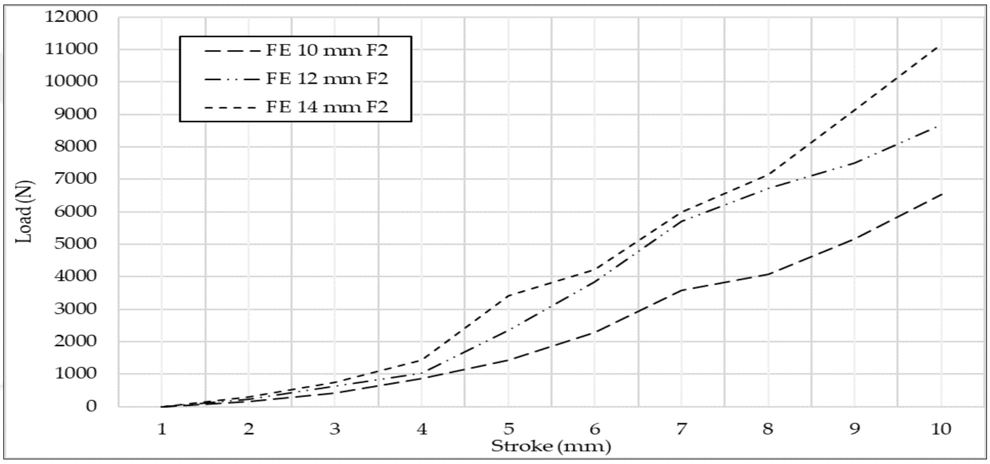

(b)

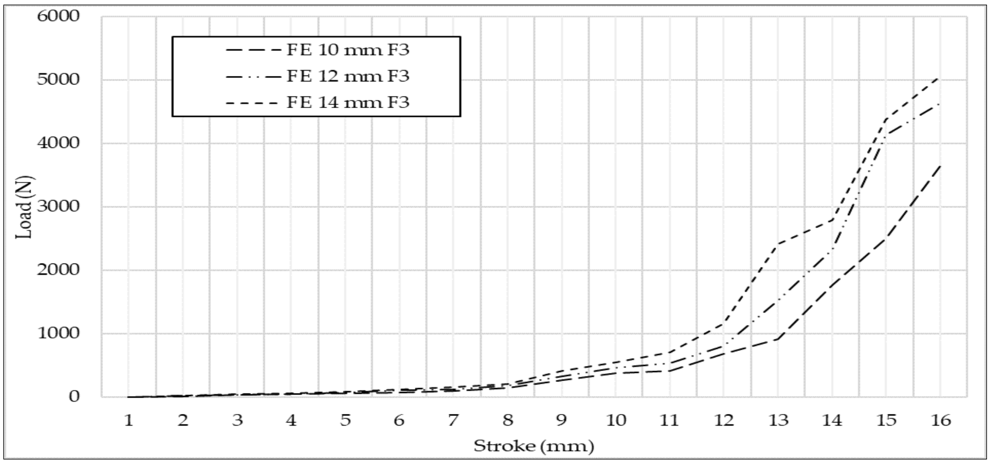

(c)

Figure 5.7 The forming loads of the three forms using pins of various diameters

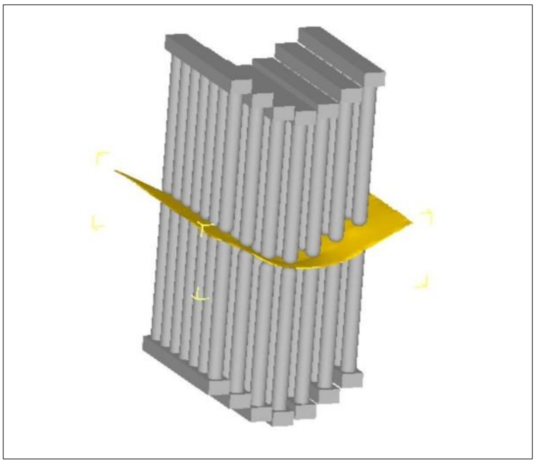

(a)

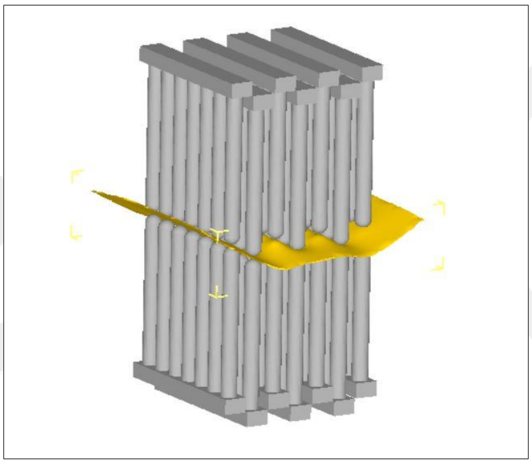

(b)

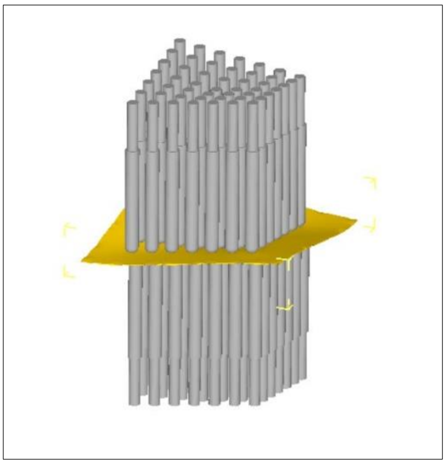

(c)

Figure 5.8 Final forms of active punch adjustment for (a) F1 10 mm, (b) F2 10 mm, and (c) F3 10 mm diameter pins.

5.2.5 Comparison between Relative Fixation and Active Punch Adjustment According to Effective Stress Distributions

After simulating active punch adjustment, some comparisons have to be made to see if there are differences between forming arrangements. Figure 5.9 shows difference in the effective stress distributions between relative fixation and active punch adjustment of F1 shape for all diameter types.

As seen in Figure 5.9, some differences were observed for effective stress distribution. For 10 mm pin forming, a 16 % variation was obtained. For 12 mm and 14 mm pin forming the differences were calculated as 13.2 % and 10.1 %, respectively. These variations of relative fixation and active punch adjustment were caused by total material flow.

In relative fixation, the flow of material occurs across the entire shape. In the active punch arrangement, on the other hand, material flow occurs according to the touch of the punches, then punch forming is finished, and the other forming process begins.

The effective stress variations are shown in Figure 5.10 for F2 for all diameter types for both arrangements. 14.1 %, 11.4 %, and 9.5 % differences were obtained between relative fixation and active adjustment.

Figure 5.11 shows the difference of arrangements for F3 for all diameters of pins. The variations were obtained as 12.7 %, 10.6 %, and 8.2 % for 10 mm, 12 mm and 14 mm pins, respectively.

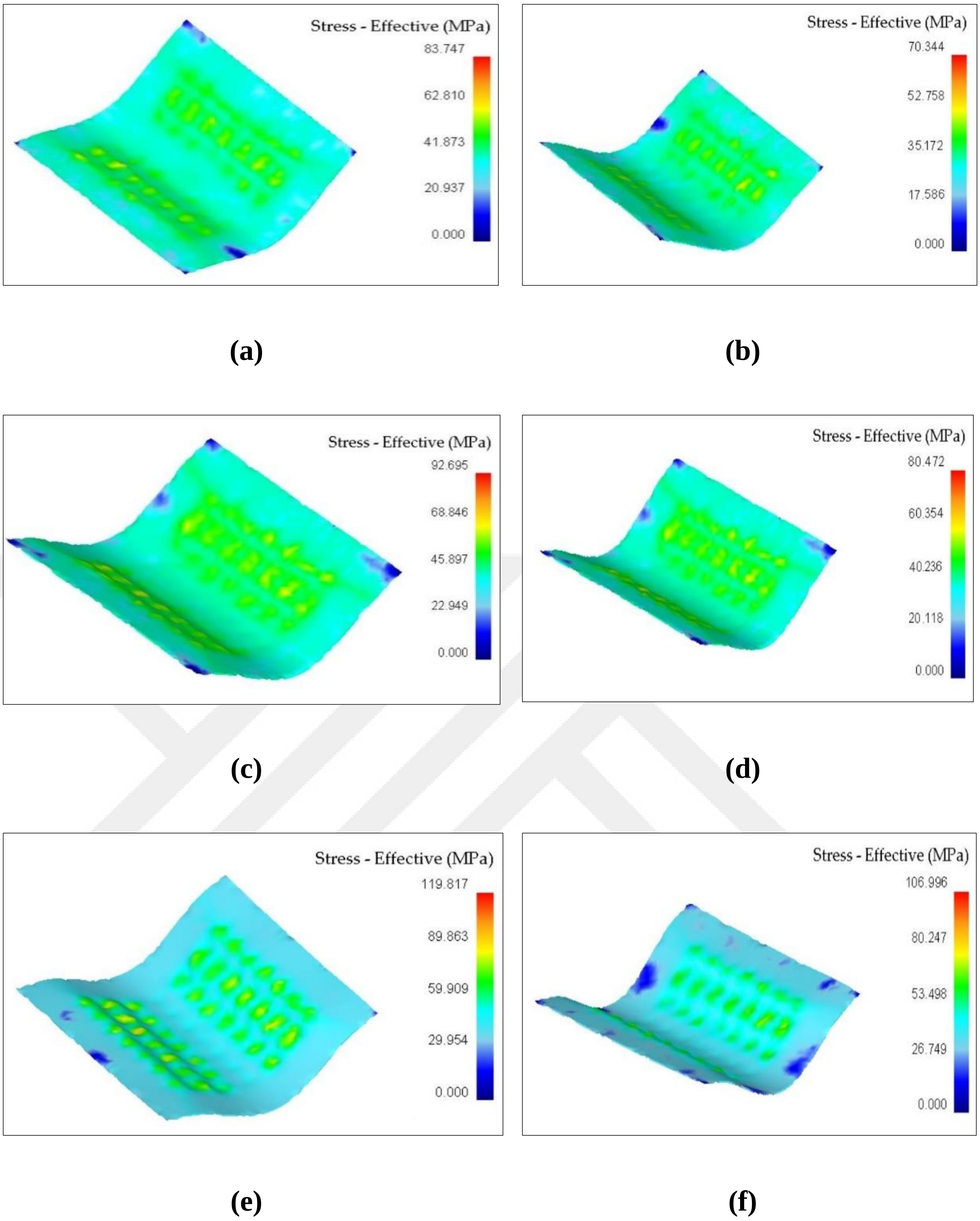

Figure 5.9 The effective stress distributions of (a) F1 RF 10 mm, (b) F1 AP 10 mm, (c) F1 RF 12 mm, (d) F1 AP 12 mm, (e) F1 RF 14 mm and (f) F1 AP 14 mm pin

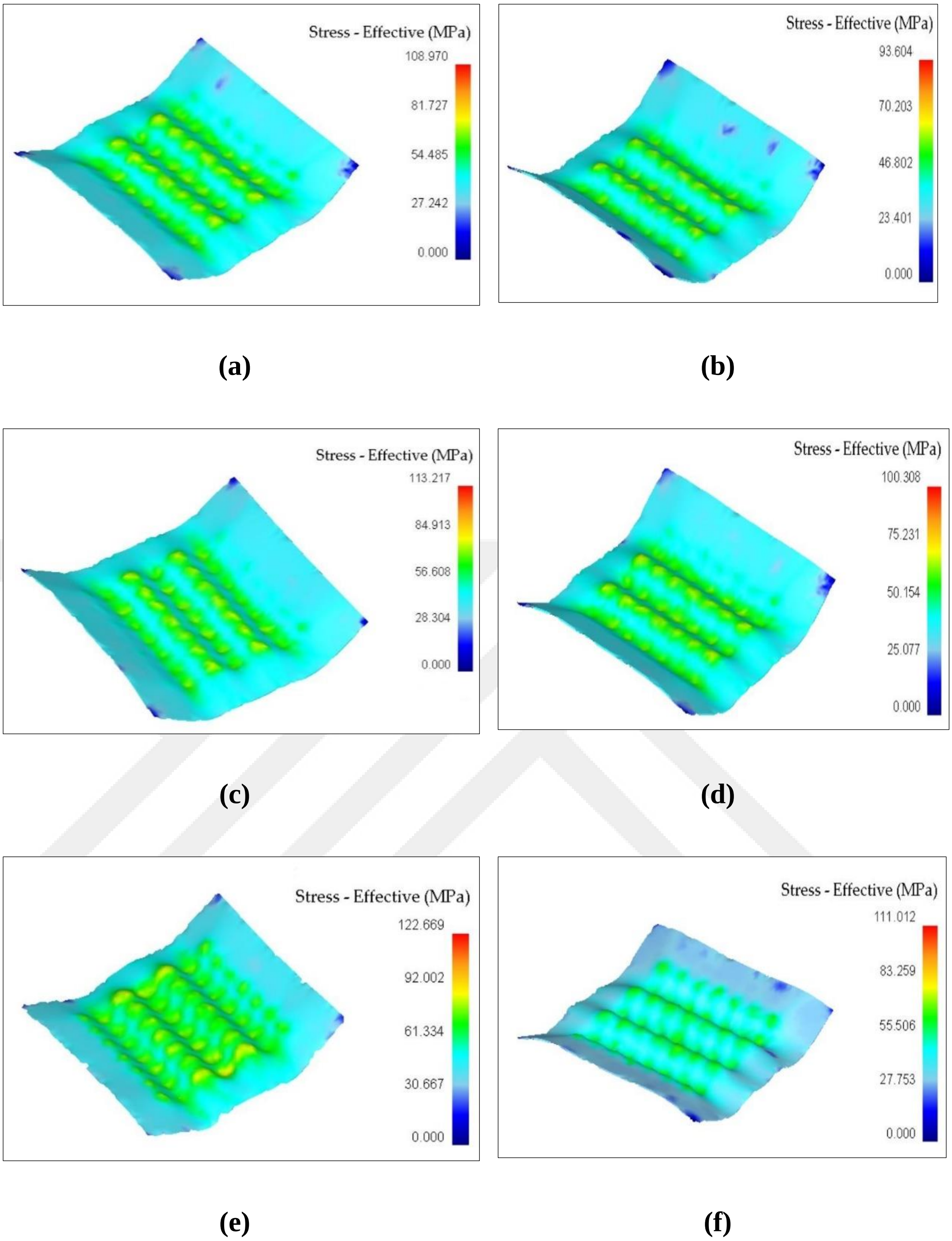

Figure 5.10 The effective stress distributions of (a) F2 RF 10 mm, (b) F2 AP 10 mm, (c) F2 RF 12 mm, (d) F2 AP 12 mm, (e) F2 RF 14 mm and (f) F2 AP 14 mm pin

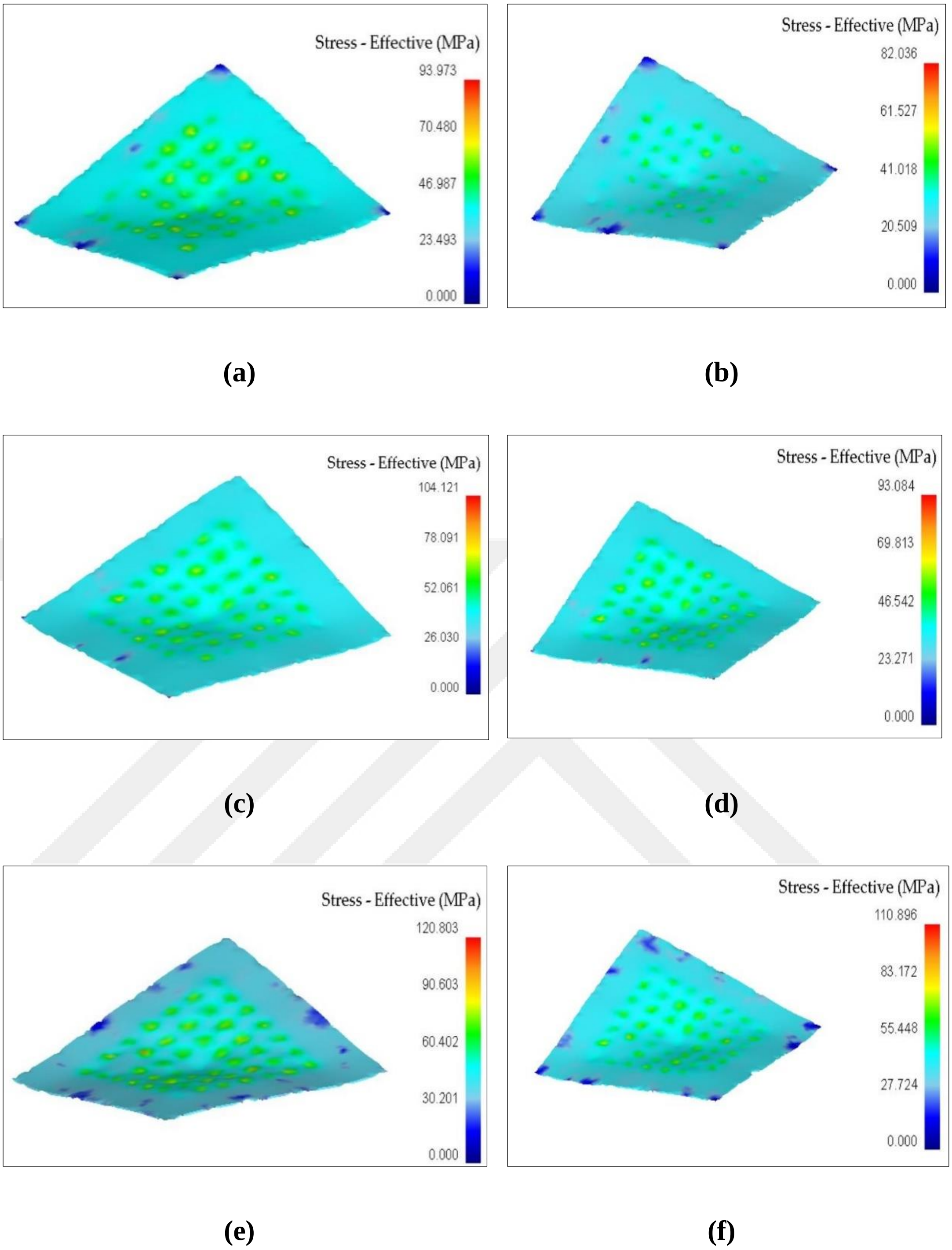

Figure 5.11 The effective stress distributions of (a) F3 RF 10 mm, (b) F3 AP 10 mm, (c) F3 RF 12 mm, (d) F3 AP 12 mm, (e) F3 RF 14 mm and (f) F3 AP 14 mm pin

5.2.6 Comparison between Relative Fixation and Active Punch Adjustment According to Damage Factors

The damage factor is also an important parameter for the metal-forming process. The effect of changing forming adjustments also affected the damage value as well as effective stress distribution. For F1, damage factor comparisons have been shown in Figure 5.12.

As a result of the comparison of damage factors similar to effective stress distributions of F1 for all pin diameters. Percentage variations were acquired as close values as effective stress comparison. In active punch adjustment, the highest damage value was reduced, but still higher than the critical value.

Figure 5.13 shows the F2 shape damage factors. Like effective stress distribution, damage factor changes are 14.7 %, 11.9 %, and 10.1 % for small to highest pins, respectively. However, the damage factor value of 12 mm pin forming nearly reached the defined value in relative fixation forming. However, with active pin adjustment this value decreased the 0.296 and this better result for forming operation.

Damage factors of F3 forming are shown in Figure 5.14. Differences in damage factor values were calculated as 13.4 % for 10 mm pin, 10.8 % for 12 mm pin, and 8.8 % for 14 pin forming. It is easily seen that active punch adjustment reduced the damage factor values in the same manner as the effective stress distribution of the F3 shape.

Forming adjustment of multi-point forming directly affects the effective stress distribution. The selection of the appropriate forming arrangement becomes more important, especially for shapes that may be critical in terms of damage factors.

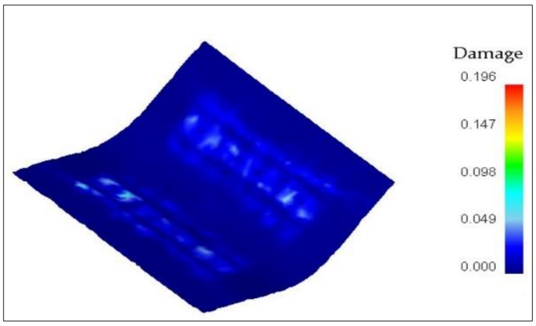

(a)

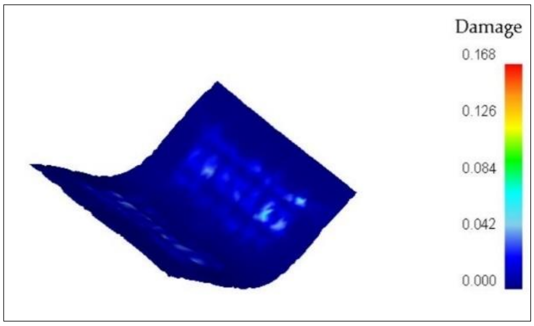

(b)

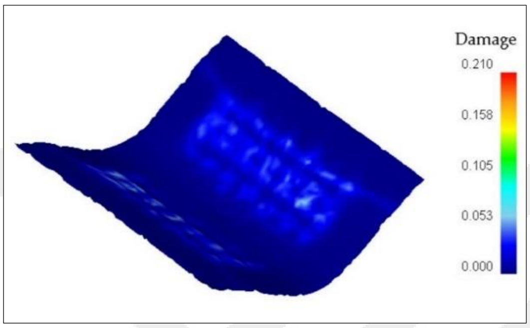

(c)

(d)

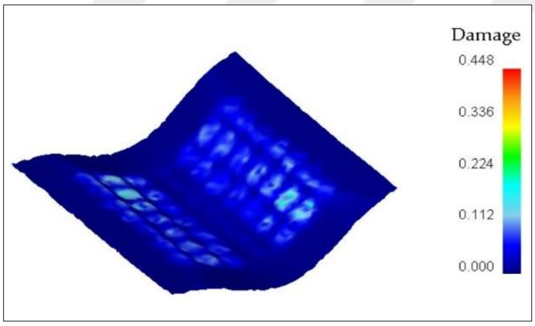

(e)

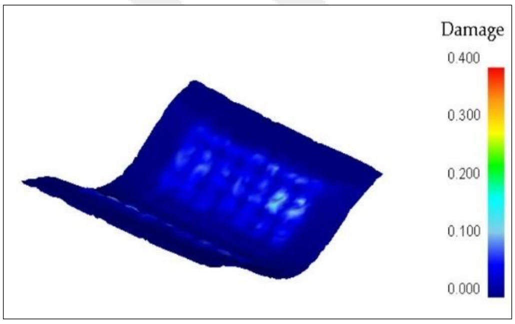

(f)

Figure 5.12 The Damage factors of (a) F1 RF 10 mm, (b) F1 AP 10 mm, (c) F1 RF 12 mm, (d) F1 AP 12 mm, (e) F1 RF 14 mm and (f) F1 AP 14 mm pin

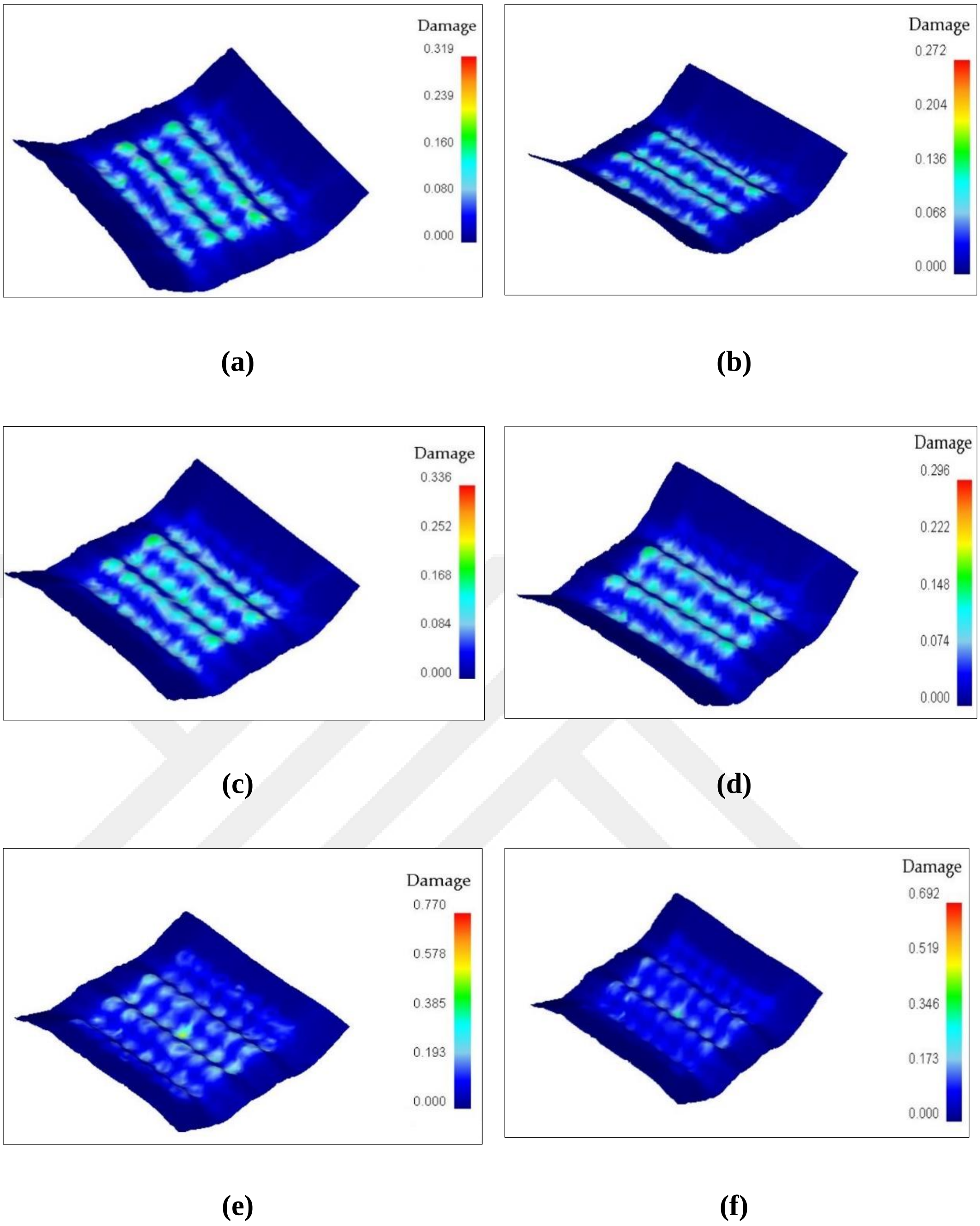

Figure 5.13 The Damage factors of (a) F2 RF 10 mm, (b) F2 AP 10 mm, (c) F2 RF 12 mm, (d) F2 AP 12 mm, (e) F2 RF 14 mm and (f) F2 AP 14 mm pin

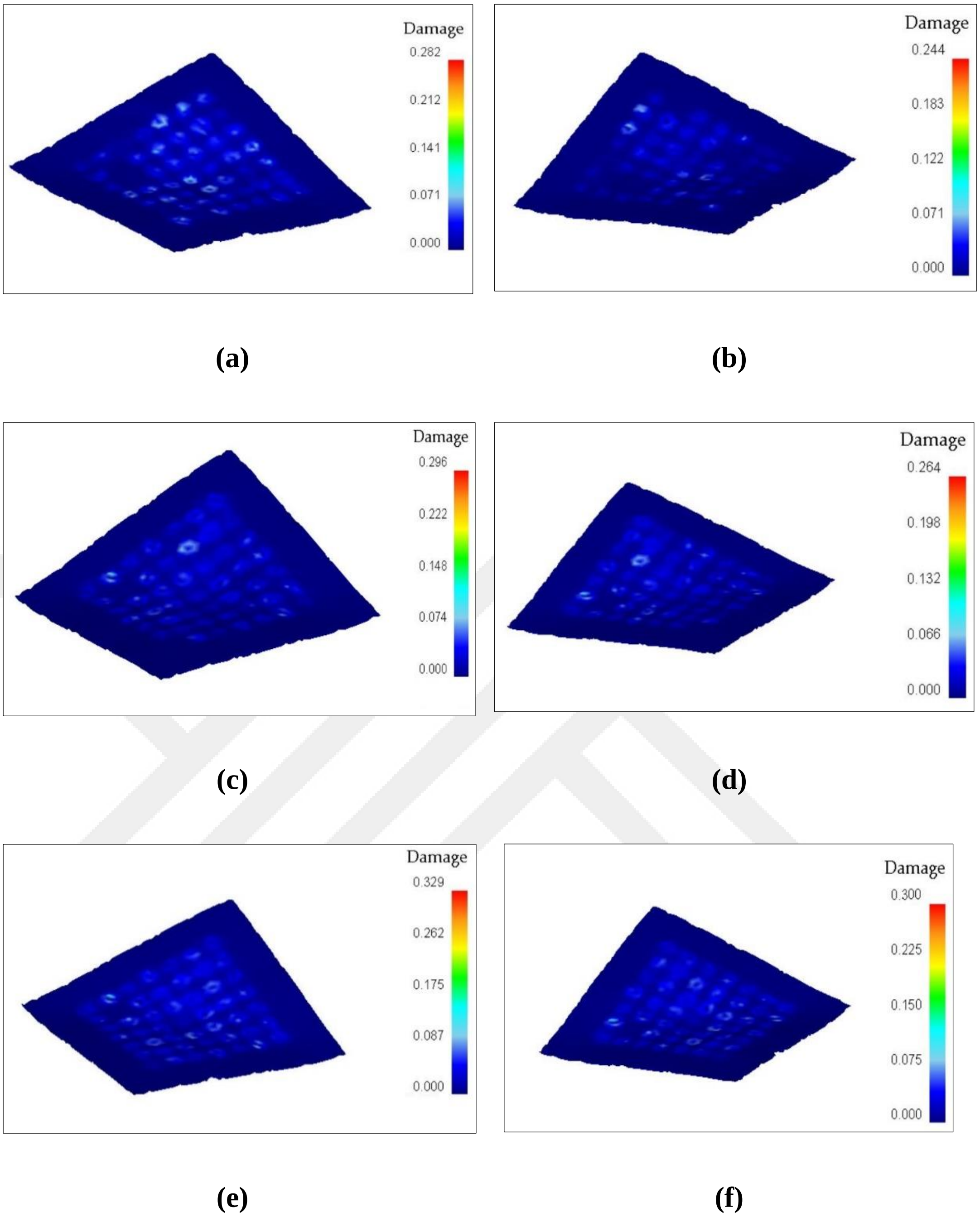

Figure 5.14 The Damage factors of (a) F3 RF 10 mm, (b) F3 AP 10 mm, (c) F3 RF 12 mm, (d) F3 AP 12 mm, (e) F3 RF 14 mm and (f) F3 AP 14 mm pin.

5.2.7 Comparison between Relative Fixation and Active Punch Adjustment According to Forming Loads

Additionally, forming loads must be compared for two forming directions. Figure 5.15 shows the load-stroke comparisons of RF and AP adjustments. As mentioned before, the same trends were obtained in the load-stroke graphs, similar to the effective stress distributions and damage factors.

The percentage differences were determined as 16 %, 13 %, and 11 % for 10 mm, 12 mm, and 14 mm pins based on the F1 shape for maximum load values, respectively. For F2 shape these values were nearly 14 %, 11.5 %, and 9.5 % from smallest to highest pin. Additionally, for 3D free-form surface shape, F3, these variations were calculated as almost 12.7 %, 10.5 %, and 8 % for 10 mm pin, 12 mm pin, and 14 mm pin forming, respectively.

So, it seems that just like effective stress and damage factor distribution, active punch adjustment is a more suitable method than relative fixation.

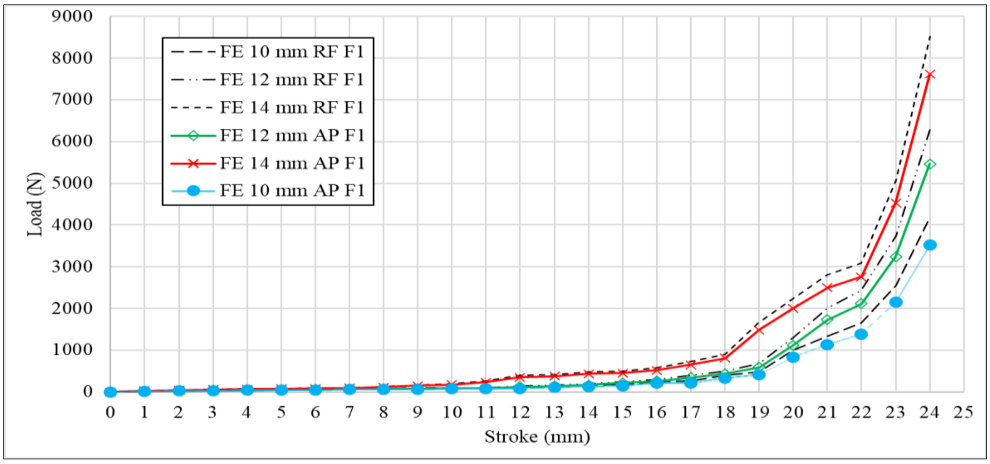

(a)

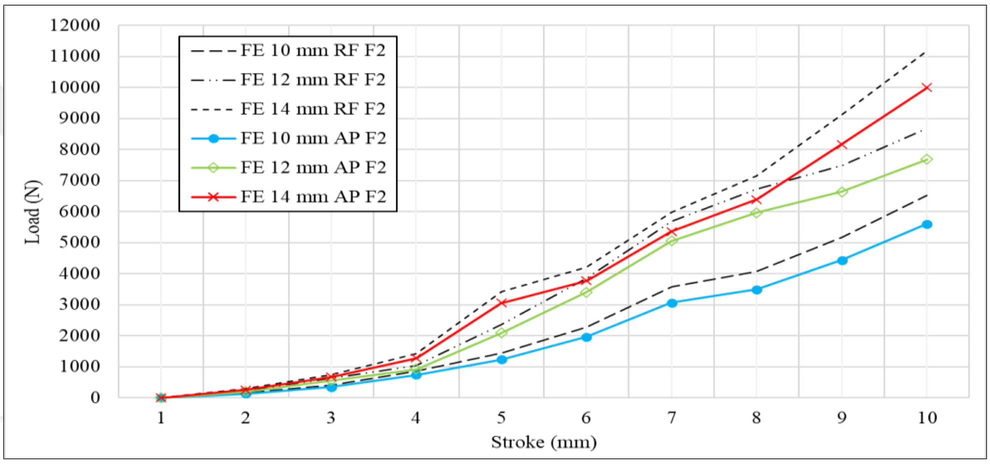

(b)

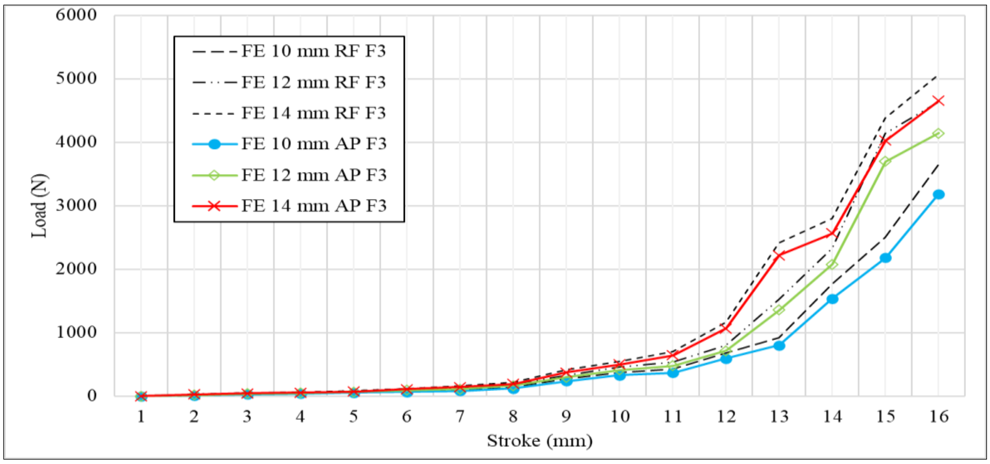

(c)

Figure 5.15 Forming load-stroke graphs of (a) F1 RF and F1 AP, (b) F2 RF and F2 AP and (c) F3 RF and F3 AP forming

5.3 Experimental Results and Discussion

Experiments were conducted with a 12 mm diameter of pin by applying the relative fixation adjustment (RF) of forming for three shapes, as mentioned before. For validation of numerical analysis thinning of contact points and load-stroke diagrams were used. Figure 5.16 depicts the final forms of the workpieces following the experimental works. The surfaces of the final workpieces have dimples that can be easily visible. In MPF, leading to the formation of dimples is caused by the area where the pin and sheet metal make contact and where the stress concentration is centered.

Interlayer elastic cushions can be used to spread these localized loads and prevent the production of dimples. By employing a polyurethane or rubber cushion, these flaws can be fixed; nevertheless, this application significantly raises the maximum load [5, 30]. Also, in this Figure 5.16 shows the contact points where thinning was measured. In the experimental and finite element analysis, the thickness of the sheets at dimple areas was also measured. The points on the lines in Figure 5.16 were measured using slicing tools in Deform 3D. A micrometre was used to gauge the degree of thinning at these sites on the final experimental workpieces.

The lines of F1 and F2 were built from left to right, and F3's line was constructed diagonally. Figure 5.17 displays the measured thickness of the experimental and FE analysis specimens of the 12 mm pin forming. Point 4, the midway of the lines, was where the maximum degree of sheet metal thinning for F1 and F2 was measured. For FE and experimental studies, the sheet metal part's thickness on F1 was determined to be nearly 0.435 mm and 0.430 mm, respectively. The thicknesses of F2 were measured as nearly 0.370 mm and 0.365 mm. Because of the geometry of the 3D free-form surface, the maximum thinning was seen on F3 at points 1, 4, and 7. Points 1 and 7 were measured to be nearly 0.415 mm and 0.405 mm thick, whereas point 4 was measured to be nearly 0.410 mm and 0.400 mm thick.

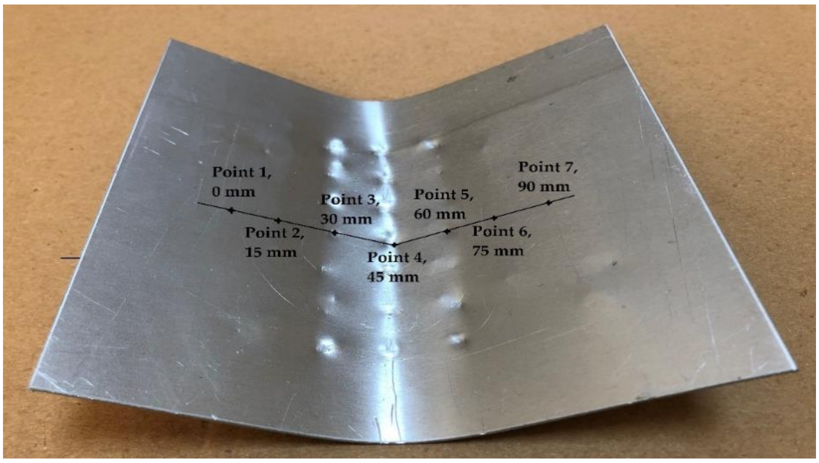

(a)

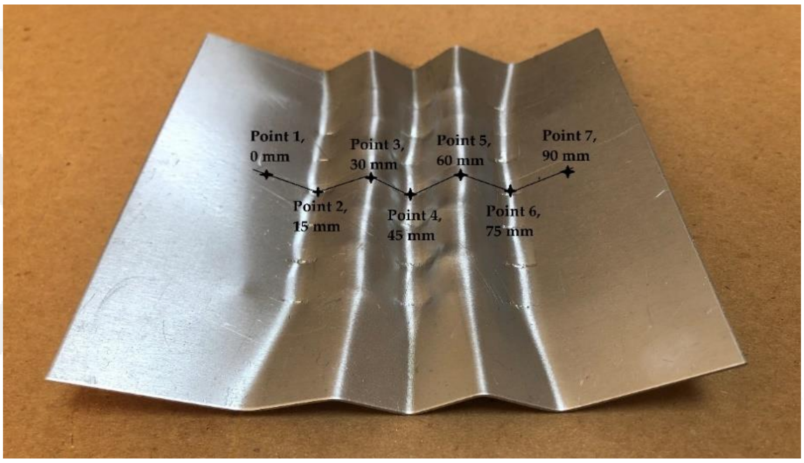

(b)

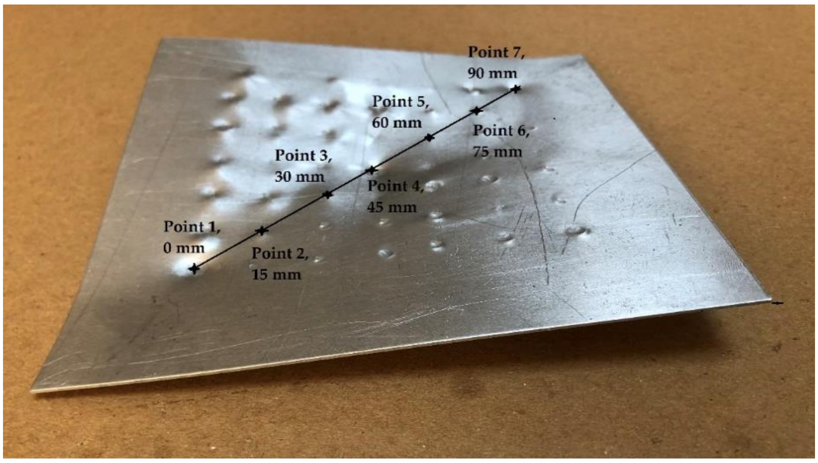

(c)

Figure 5.16 The Final forms of the workpieces after experiments (a) F1, (b) F2 and (c) F3 type forming

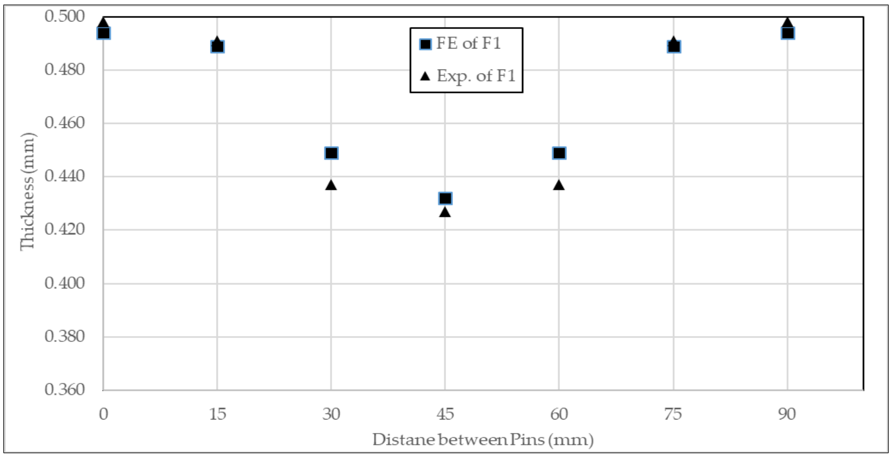

(a)

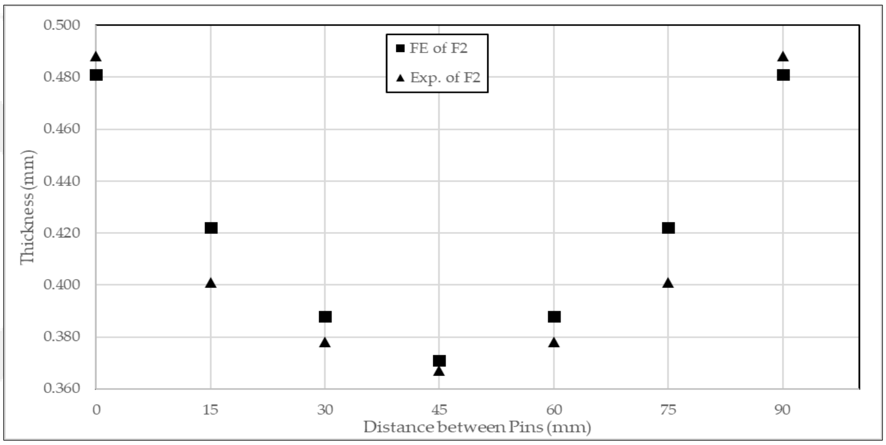

(b)

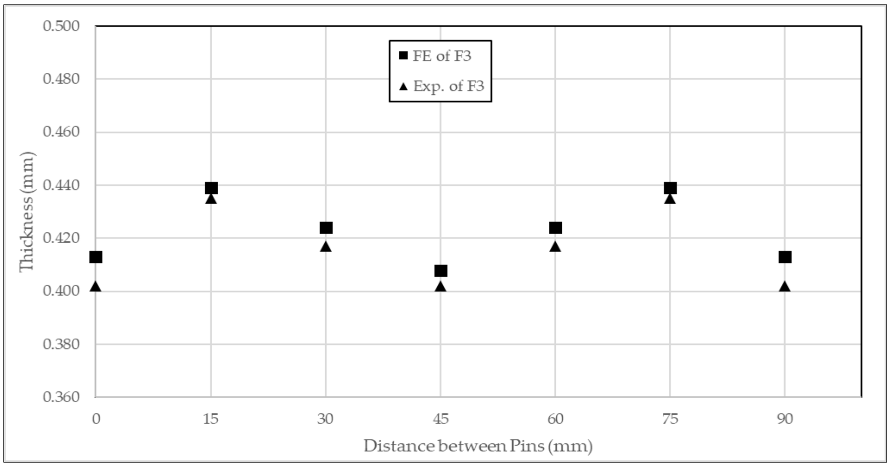

(c)

Figure 5.17 The measured thickness of the experimental and FE analysis (a) F1, (b) F2 and (c) F3 type forming

The graphs all display similar tendencies when they are analysed. The results of the analysis and modelling of FE have therefore been verified and confident. According to the research done in [31], the maximum point of F1's thinning is consistent. In that investigation, the 1060 aluminium alloy with a 2 mm thickness was subjected to MPF and multi-point forming with individually controlled force-displacement (MPF-ICFD), which produced a shape comparable to F1 in the current study. The conclusion reached was that MPF-ICFD produced less thickness fluctuation and thinning.

Figure 5.18 displays the experimental study's producing load-stoke curves as well as the findings of the matching FEA. For F1, F2, and F3, the maximum forming loads were found to be around 6800 N, 9140 N, and 4750 N, respectively. For the three forms, the percentage errors between the experimental and FEA results were computed as approximately 7.5%, 5.0%, and 2.0%, respectively. The load-stroke graphs displayed patterns resembling those in the thinning graphs. As a consequence, it was decided that the outcomes of finite element modelling and analysis appeared to be trustworthy.

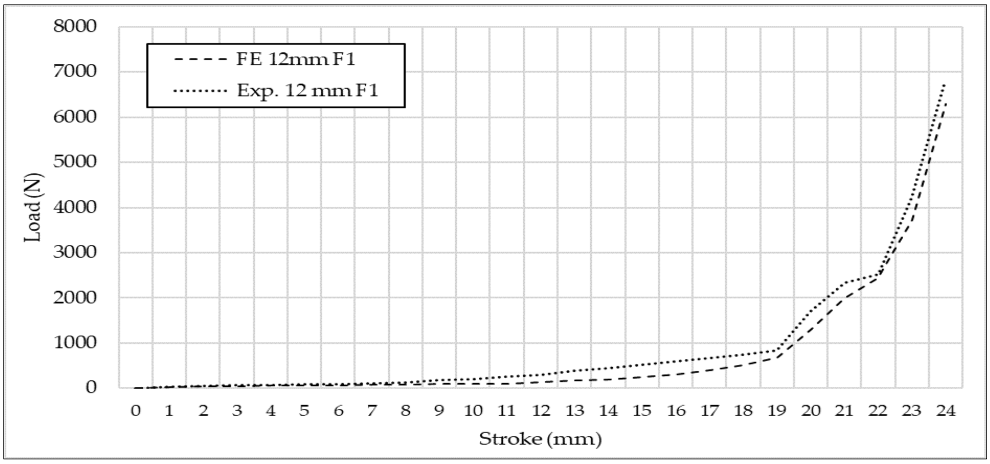

(**a**)

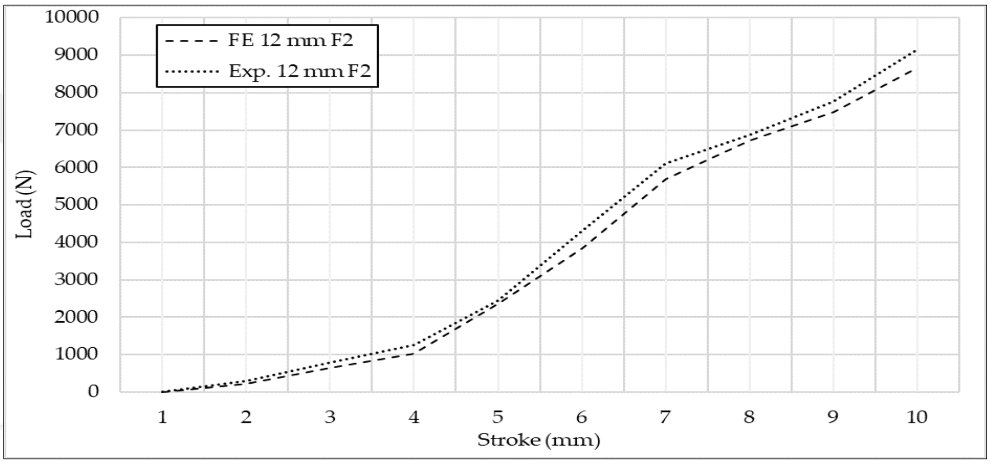

(**b**)

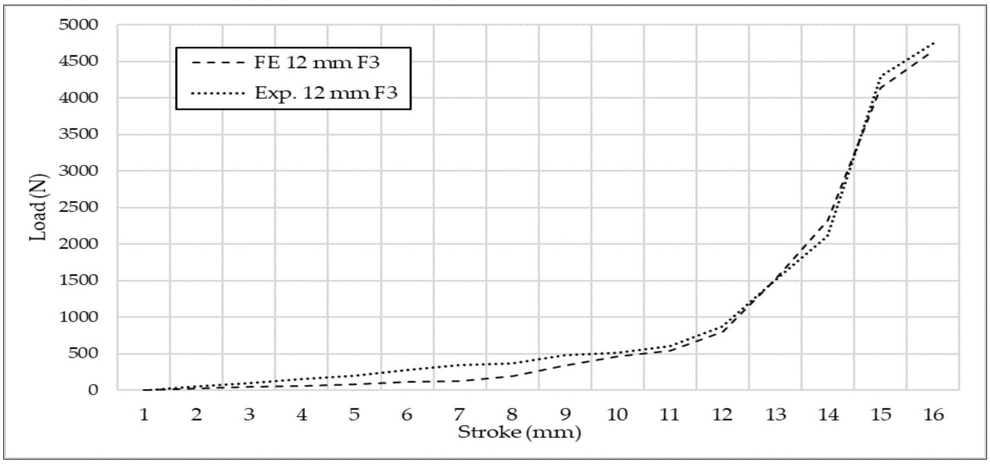

(**c**)

Figure 5.18 Experimental and FEA load-stroke comparison of (a) F1 with 12 mm, (b) F2 with 12 mm and (c) F3 with 12 mm diameter pin

CHAPTER 6
CONCLUSIONS AND FUTURE WORKS

6.1 Conclusions

The previous chapters described the finite element modelling and experimental investigations of the multi-point forming method for three different shaped parts manufactured of aluminium alloy AISI Al1100. The following conclusions may be reached after taking into account all the information presented in the thesis:

1. By adjusting the pin length in accordance with the necessary component geometry, three different parts (V-shape F1, wavy shape F2, and free-form surface F3) were manufactured in a single MPF die. This makes MPF both time and cost-effective.
2. The main contributions of this study are the evaluation of the effects of pin diameter and the difference of punch adjustments, on the multi-point forming of various parts.
3. Using the multi-point forming finite element method (FEM), forming processes may be successfully optimized. The potential of acquiring crucial data for determining essential parameters and operating timeframes is the most evident advantage of using FEM. Using the FE models and approaches suggested in this study for MPF, the final form of a produced object and any possible imperfections may be precisely anticipated.
4. The FE simulations proved that the place where the pin and sheet contact is where the higher-level stresses are located and where the thickness is reduced. On the other hand, maximum effective stress values resulted for the highest diameter pin (14 mm diameter pin), while the least stress distributions and damage factor values linked to tearing were obtained for a 10 mm diameter pin.
5. The material flow becomes more challenging in complex formed components as the pin diameter rises. This circumstance demonstrated the need for a larger load and, hence, a bigger capacity press.

6. Multi-point forming is very applicable for forming different parts. This flexible property reduces the manufacturing and set-up time, so the cost, of forming dies.
7. For the V-shape (F1), wavy shape (F2), and free-form surface (F3), the active punch adjustment method was an appropriate way compared to the relative fixation method for forming.
8. The experiments were utilized to verify the results of FE's load-stroke diagrams as well as the fracture criterion that was applied to anticipate cracks. Therefore, it can be concluded that FE simulations are a sufficiently accurate method of prediction based on multi-point forming tests that have been undertaken.

6.2 Future Works

1. By employing a larger capacity press, the experimental investigation and finite element modelling may be done using an elastic pad to prevent the formation of dimples.
2. Several forming rates and velocity profiles may be used to examine the process.
3. A system called Fibre Bragg Grating (FBG) [64] can be employed to measure the forming force on individual pins in an MPF matrix.
4. To assure more precise positioning of pin heights, to speed up the process of creating various forms, and because the MPF tools utilized in this study are compact and have a closed arrangement, digital control of MPF tool adjustment might be used. This could also enable automated correction for springback.
5. Investigations into changes in friction values or friction conditions can be examined.

REFERENCES

[1]. Groover, MP. (2007). *Fundamental of Modern Manufacturing Materials, Processes and Systems*. 3rd Edition. New Jersey, USA. John Wiley & Sons.

[2]. Walczyk, D. F., & Hardt, D. E. (1998). Design and analysis of reconfigurable discrete dies for sheet metal forming. *Journal of Manufacturing Systems*, *17*(6), 436–454. https://doi.org/10.1016/s0278-6125(99)80003-x

[3]. Li, M., Liu, Y., Su, S., & Li, G. (1999). Multi-point forming: a flexible manufacturing method for a 3-d surface sheet. *Journal of Materials Processing Technology*, *87*(1–3), 277–280. https://doi.org/10.1016/s0924-0136(98)00364-1

[4]. Cai, Z. Y., & Li, M. Z. (2002). Multi-point forming of three-dimensional sheet metal and the control of the forming process. *International Journal of Pressure Vessels and Piping*, *79*(4), 289–296. https://doi.org/10.1016/s0308-0161(02)00017-0

[5]. Li, M., Cai, Z., Sui, Z., & Yan, Q. (2002). Multi-point forming technology for sheet metal. *Journal of Materials Processing Technology*, *129*(1–3), 333–338. https://doi.org/10.1016/s0924-0136(02)00685-4

[6]. Cai, Z. Y., & Li, M. Z. (2005). Finite element simulation of multi-point sheet forming process based on implicit scheme. *Journal of Materials Processing Technology*, *161*(3), 449–455. https://doi.org/10.1016/j.jmatprotec.2004.07.082

[7]. Liu, C., Li, M., & Fu, W. (2006). Principles and apparatus of multi-point forming for sheet metal. *The International Journal of Advanced Manufacturing Technology*, *35*(11–12), 1227–1233. https://doi.org/10.1007/s00170-006-0802-1

[8]. Qian, Z., Li, M., & Tan, F. (2007). The analyse on the process of multi-point forming for dish head. *Journal of Materials Processing Technology*, *187–188*, 471–475. https://doi.org/10.1016/j.jmatprotec.2006.11.132

[9]. Karayel, D., Özkan, S.S., Nart, E., (2008). Multi-Point Flexible Forming Technology for Sheet Metal Parts and Design of Control System, *Proceedings in Steel Research International*, *12*, 788-793.

[10]. Zhang, Q., Wang, Z., & Dean, T. (2008). The mechanics of multi-point sandwich forming. International Journal of Machine Tools and Manufacture, *48*(12–13), 1495–1503. https://doi.org/10.1016/j.ijmachtools.2008.04.003

[11]. Cai, Z. Y., Wang, S. H., Xu, X. D., & Li, M. Z. (2009). Numerical simulation for the multi-point stretch forming process of sheet metal. Journal of Materials Processing Technology, *209*(1), 396–407. https://doi.org/10.1016/j.jmatprotec.2008.02.010

[12]. Quan, G. Z., Ku, T. W., & Kang, B. S. (2011). Improvement of formability for multi-point bending process of AZ31B sheet material using elastic cushion. *International Journal of Precision Engineering and Manufacturing*, *12*(6), 1023–1030. https://doi.org/10.1007/s12541-011-0136-2

[13]. Liu, Y., Li, M., & Ju, F. (2016). Research on the process of flexible blank holder in multi-point forming for spherical surface parts. *The International Journal of Advanced Manufacturing Technology*, *89*(5–8), 2315–2322. https://doi.org/10.1007/s00170-016-9198-8

[14]. Abebe, M., Lee, K., & Kang, B. S. (2015,). Surrogate-based multi-point forming process optimization for dimpling and wrinkling reduction. *The International Journal of Advanced Manufacturing Technology*, *85*(1–4), 391–403. https://doi.org/10.1007/s00170-015-7897-1

[15]. Abosaf, M., Essa, K., Alghawail, A., Tolipov, A., Su, S., & Pham, D. (2017). Optimisation of multi-point forming process parameters. *The International Journal of Advanced Manufacturing Technology*, *92*(5–8), 1849–1859. https://doi.org/10.1007/s00170-017-0155-y

[16]. Abaas, T. F., Younis, K. M., & Mansor, K. K. (2019). Die Design of Flexible Multi-Point Forming Process. *Al-Khwarizmi Engineering Journal*, *14*(2), 22–29. https://doi.org/10.22153/kej.2018.12.002

[17]. Liang, X. B., Cai, Z. Y., & Zhang, X. (2018). Forming characteristics analysis and springback prediction of bi-directional trapezoidal sandwich panels in the multi-point bend-forming. *The International Journal of Advanced Manufacturing Technology*, *98*(5–8), 1709–1720. https://doi.org/10.1007/s00170-018-2316-z

[18]. Cai, Z. Y., Zhang, X., & Liang, X. B. (2018). Multi-point forming of sandwich panels with egg-box-like cores and failure behaviours in forming process:

Analytical models, numerical and experimental investigations. *Materials & Design*, 160, 1029–1041. https://doi.org/10.1016/j.matdes.2018.10.037

[19]. Shen, W., Yan, R. J., Lin, Y., & Fu, H. Q. (2018). Residual stress analysis of hull plate in multi-point forming. *Journal of Constructional Steel Research*, *148*, 65–76. https://doi.org/10.1016/j.jcsr.2018.05.017

[20]. Zhu, L., Liang, Q., Yu, T., Yuan, P., & Hu, Y. (2019). Experimental and theoretical study of constant curvature multi-square punch forming process of strips under follower load. *International Journal of Mechanical Sciences*, *156*, 462–473. https://doi.org/10.1016/j.ijmecsci.2019.04.008

[21]. Li, Y., Shi, Z., Rong, Q., Zhou, W., & Lin, J. (2019). Effect of pin arrangement on formed shape with sparse multi-point flexible tool for creep age forming. *International Journal of Machine Tools and Manufacture*, *140*, 48–61. https://doi.org/10.1016/j.ijmachtools.2019.03.001

[22]. Erhu, Q., Mingzhe, L., & Rui, L. (2019). Study on the multi-point forming process with a swinging punch unit. *The International Journal of Advanced Manufacturing Technology*, *104*(1–4), 675–685. https://doi.org/10.1007/s00170-019-03726-x

[23]. Peng, H., Li, M., Li, Z., & Li, X. (2019). Surface quality and shape accuracy of multi-point warm press forming Corian sheets. *The International Journal of Advanced Manufacturing Technology*, *104*(9–12), 4727–4733. https://doi.org/10.1007/s00170-019-04339-0

[24]. Su, S., Jiang, Y., & Xiong, Y. (2020, April). Multi-point forming springback compensation control of two-dimensional hull plate. *Advances in Mechanical Engineering*, *12*(4), 168781402091609. https://doi.org/10.1177/1687814020916094

[25]. Moheen, M., Abdel-Wahab, A., Hassanin, H., & Essa, K. (2020, October 12). Reconfigurable Multipoint Forming Using Waffle-Type Elastic Cushion and Variable Loading Profile. *Materials*, *13*(20), 4506. https://doi.org/10.3390/ma13204506

[26]. Huang, X. Y., Zhao, J., Yu, G. C., Meng, Q. D., Mu, Z. K., & Liu, Y. J. (2021). Multi-point flexible straightening process by reciprocating bending for metal profiles. *Transactions of Nonferrous Metals Society of China*, *31*(7), 2039–2050. https://doi.org/10.1016/s1003-6326(21)65636-4

[27]. Feng, F., Li, J., Chen, R., Huang, L., Su, H., & Fan, S. (2021). Multi-point die electromagnetic incremental forming for large-sized sheet metals. *Journal of Manufacturing Processes*, *62*, 458–470. https://doi.org/10.1016/j.jmapro.2020.12.022

[28]. Wang, M. W., Cai, Z. Y., Zhang, X., Gao, J. X., & Zhang, W. G. (2022). A universal elastoplastic equivalent method for sandwich panels and its application in plastic forming. *Thin-Walled Structures*, *181*, 110114. https://doi.org/10.1016/j.tws.2022.110114

[29]. Li, X., & Hu, S. (2022). Numerical Simulation and Experimental Research on Multi-Point Forming of Aluminium Alloy Sheets Based on Ultrasonic Vibration. *Mathematical Problems in Engineering*, *2022*, 1–11. https://doi.org/10.1155/2022/7688376

[30]. Tolipov, A., Hassanin, H., El-Sayed, M. A., Eldessouky, H. M., Alsaleh, N. A., Alfozan, A. K., Essa, K., & Ahmadein, M. (2022, March 14). Multipoint Forming Using Hole-Type Rubber Punch. *Metals*, *12*(3), 491. https://doi.org/10.3390/met12030491

[31]. Jia, B. B., Chen, G., Wang, W. W., Shen, Y., & Gu, Y. (2022, October 15). Deformation characteristics and forming force limits of multi-point forming with individually controlled force–displacement. *The International Journal of Advanced Manufacturing Technology*, *123*(5–6), 1565–1576. https://doi.org/10.1007/s00170-022-10236-w

[32]. Shao, H., Wang, Y., Wan, H., Wang, H., Zhang, Z., & Fu, W. (2023). Research on springback compensation for multi-point forming of corrosion-resistant aluminium alloy hyperbolic component. *Matéria (Rio De Janeiro)*, *28*(2). https://doi.org/10.1590/1517-7076-rmat-2022-0304

[33]. Li, X., & Hu, S. (2023, January 1). Ultrasonic Vibration Theory and Its Application in Reducing Springback for Multi-point Forming. *Journal of Physics: Conference Series*, *2437*(1), 012091. https://doi.org/10.1088/1742-6596/2437/1/012091

[34]. Abebe, M., Park, J. W., & Kang, B. S. (2016). Reliability-based robust process optimization of multi-point dieless forming for product defect reduction. *The International Journal of Advanced Manufacturing Technology*, *89*(1–4), 1223–1234. https://doi.org/10.1007/s00170-016-9172-5

[35]. Nakajima, N., (1969). Research on die and electrode by steel wire bind. *Japanese Journal of Mechanical Academy*, *72*, 32-40.

[36]. Li M, Nakamura H, Watanabe S (1992) Study of the basic forming principles (1st Report: Research on multi-point forming for sheet metal). *Proc Japanese Spring Conference for Technology of Plasticity*, 519–522.

[37]. Li, M. Z.; Cai, Z. Y.; Liu, C. G., (2005). Recent Developments in Multi-Point Forming Technology, *Proceedings of the 8th International Conference on Technology of Plasticity*, 707–708.

[38]. Li, M. Z., Cai, Z. Y., & Liu, C. G. (2007, February). Flexible manufacturing of sheet metal parts based on digitized-die. *Robotics and Computer-Integrated Manufacturing*, *23*(1), 107–115. https://doi.org/10.1016/j.rcim.2005.09.005

[39]. Yaşar, M., Korkmaz, Z., & Gavas, M. (2007, January). Forming sheet metals by means of multi-point deep drawing method. *Materials & Design*, *28*(10), 2647–2653. https://doi.org/10.1016/j.matdes.2006.10.017

[40]. Obermeyer, E., & Majlessi, S. (1998). A review of recent advances in the application of blank-holder force towards improving the forming limits of sheet metal parts. *Journal of Materials Processing Technology*, *75*(1–3), 222–234. https://doi.org/10.1016/s0924-0136(97)00368-3

[41]. Jeswiet, J., Geiger, M., Engel, U., Kleiner, M., Schikorra, M., Duflou, J., Neugebauer, R., Bariani, P., & Bruschi, S. (2008). Metal forming progress since 2000. *CIRP Journal of Manufacturing Science and Technology*, *1*(1), 2–17. https://doi.org/10.1016/j.cirpj.2008.06.005

[42]. Zhang, S., Wang, Z., Wang, Z., Xu, Y., & Chen, K. (2004). Some new features in the development of metal forming technology. *Journal of Materials Processing Technology*, *151*(1–3), 39–47. https://doi.org/10.1016/j.jmatprotec.2004.04.098

[43]. Ahmetoglu, M., Broek, T., Kinzel, G., & Altan, T. (1995). Control of Blank Holder Force to Eliminate Wrinkling and Fracture in Deep-Drawing Rectangular Parts. *CIRP Annals*, *44*(1), 247–250. https://doi.org/10.1016/s0007-8506(07)62318-x

[44]. Emblom, W. J., Weinmann, K. J., & Beard, J. E. (2009). Strain Control in an Intelligent Die Based Upon Local Force Control and Blank Holder Forces. *ASME 2009 International Manufacturing Science and Engineering Conference, Volume 1*. https://doi.org/10.1115/msec2009-84283

[45]. Li, K., Carden, W., & Wagoner, R. (2002). Simulation of springback. *International Journal of Mechanical Sciences*, *44*(1), 103–122. https://doi.org/10.1016/s0020-7403(01)00083-2

[46]. Samuel, M. (2000). Experimental and numerical prediction of springback and side wall curl in U-bendings of anisotropic sheet metals. *Journal of Materials Processing Technology*, *105*(3), 382–393. https://doi.org/10.1016/s0924-0136(00)00587-2

[47]. Ling, Y., Lee, H., & Cheok, B. (2005). Finite element analysis of springback in L-bending of sheet metal. *Journal of Materials Processing Technology*, *168*(2), 296–302. https://doi.org/10.1016/j.jmatprotec.2005.02.236

[48]. Bahloul, R., dal Santo, P., Mkaddem, A., & Potiron, A. (2005). Optimisation of Springback Predicted by Experimental and Numerical Approach by Using Response Surface Methodology. *Advanced Materials Research*, *6–8*, 753–762. https://doi.org/10.4028/www.scientific.net/amr.6-8.753

[49]. Zhongyi, C., & Mingzhe, L. (2001). Optimum path forming technique for sheet metal and its realization in multi-point forming. *Journal of Materials Processing Technology*, *110*(2), 136–141. https://doi.org/10.1016/s0924-0136(00)00837-2

[50]. High-speed rail in China. https://en.wikipedia.org/wiki/High-speed_rail_in_China

[51]. Wisselink, H. H. (2005). Finite Element Simulation of the Stretch-Forming of Aircraft Skins. *AIP Conference Proceedings*. https://doi.org/10.1063/1.2011194

[52]. Li, W. D., Wan, M., Kong, Y. M., Zhang, P., Xu, C. X. (2004). Research on Digital Stretch Forming System for Aircraft Skin [C]. *In Proceedings of the 1st International Conference on New Forming Technology*, 429–434.

[53]. Gogu, G., Chedmail, P., (2003). *Technological Parameter Calculation and Stretch Forming Process Control of 3D Profile Parts [M], Recent advances in Integrated Design and Manufacturing in Mechanical Engineering*; Springer: USA.

[54]. Tan, F., Li, M., & Cai, Z. (2007, June). Research on the process of multi-point forming for the customized titanium alloy cranial prosthesis. *Journal of Materials Processing Technology*, *187–188*, 453–457. https://doi.org/10.1016/j.jmatprotec.2006.11.149

[55]. Zhou, Z. (2004). Clinical Contrast Researching to the Common Material for Cranial Prosthesis. *Chinese Journal of Nervous and Mental Diseases*. 447–448.

[56]. Chen, W. (2001). Expectations for Mending Absent Crania. Journal of Shantou University Medical College, 154–156.

[57]. Borchers, F., Clausen, B., Ehle, L. C., Eich, M., Epp, J., Frerichs, F., Hettig, M., Klink, A., Kohls, E., Lu, Y., Meyer, H., Rommes, B., Schneider, S., Strunk, R., & Zielinski, T. (2021). The Influence of Former Process Steps on Changes in

Hardness, Lattice and Microstructure of AISI 4140 Due to Manufacturing Processes. *Metals*, *11*(7), 1102. https://doi.org/10.3390/met11071102

[58]. Saeed, M. (2008). *Finite Element Analysis: Theory and Application with Ansys. 3rd Edition*. New Jersey, USA. Pearson Prentice Hall.

[59]. DEFORM 3D Version 6.1 User's Manual. https://vdocuments.mx/deform-3d-v61-manual.html

[60]. Engin, K. E., & Eyercioglu, O. (2017). The Effect of the Thickness-to-Die Diameter Ratio on the Sheet Metal Blanking Process. *Strojniški Vestnik - Journal of Mechanical Engineering*, *63*(9), 501–509. https://doi.org/10.5545/sv-jme.2016.4272

[61]. Semiatin, S.L. (1996) *Forming and Forging ASM Handbook*, 9th Ed. ASM International: Phoenix, AZ, USA, 796–814.

[62]. Smith, L., Averill, R., Lucas, J., Stoughton, T., & Matin, P. (2003). Influence of transverse normal stress on sheet metal formability. *International Journal of Plasticity*, *19*(10), 1567–1583. https://doi.org/10.1016/s0749-6419(02)00035-9

[63]. Dib, M., Ribeiro, B., & Prates, P. (2018). Model Prediction of Defects in Sheet Metal Forming Processes. *Engineering Applications of Neural Networks*, 169–180. https://doi.org/10.1007/978-3-319-98204-5_14

[64]. Jin, W., Venuvinod, P., & Wang, X. (1995). An optical fibre sensor based cutting force measuring device. *International Journal of Machine Tools and Manufacture*, *35*(6), 877–883. https://doi.org/10.1016/0890-6955(94)e0025-e

[65]. Martín, F., Martín, M., Sevilla, L., & Sebastián, M. (2015). The Ring Compression Test: Analysis of Dimensions and Canonical Geometry. *Procedia Engineering*, *132*, 326–333. https://doi.org/10.1016/j.proeng.2015.12.502

CURRICULUM VITAE

Mahmut TANDOĞAN

He completed his primary, secondary and high school education in Adıyaman. He completed his undergraduate education in Gaziantep University Mechanical Engineering Department in 2014, his Master education in Gaziantep University Institute of Science, Mechanical Engineering Department in 2017, and his Ph.D. education at the same university in 2023. He worked as a research assistant at Adıyaman University Technology Faculty between 2014-2015 and Gaziantep University Mechanical Engineering Department between 2015-2018. He is still working as a research assistant at Adıyaman University Mechanical Engineering Department since 2018. He is fluent in English. He is married and has 1 child.